AQUIFER TEST ANALYSIS

San Pedro River Basin Aquifer Test
Sierra Vista, Arizona

Prepared for
Bureau of Land Management
Building 50
Denver Federal Center
Lakewood, CO 80225

David Schafer & Associates
1 White Pine Road
North Oaks, Minnesota 55127

REPORT

August 2004

DS&A
David Schafer & Associates

Aquifer Test Analysis

San Pedro River Basin
Aquifer Test
Sierra Vista, Arizona

TABLE OF CONTENTS

TABLES

FIGURES

FIGURES, continued

FIGURES, continued

INTRODUCTION

This report describes the analysis of the constant-rate pumping and recovery test conducted for the Bureau of Land Management near the San Pedro River at Sierra Vista, Arizona. The tested well is located within the San Pedro Riparian National Conservation Area. The purpose of the pumping test was to determine aquifer properties at the site, as well as the hydrologic connection between stream flow, the shallow flood plain aquifer, and the deep aquifer in the San Pedro River Valley near Sierra Vista. The information gained from the pumping test was intended to enhance the understanding of the effect of future aquifer pumping in the area on vegetation within the Conservation Area.

The pumping test was conducted on an existing irrigation well about a third of a mile west of the San Pedro River. The well was pumped at a constant rate for nearly 3 days (4205 minutes), followed by nearly 6 days of recovery. Water levels were measured in the pumped well and 20 observations wells in the area, as well as in the San Pedro River.

This report presents the data measured during the pumping test, along with an analysis and interpretation of the data.

SITE LOCATION

Figure 1 shows the Sierra Vista area and the pumping test location along the San Pedro River, east of Sierra Vista. Figure 2 shows the well layout and location of the stream gauge on the San Pedro River. In addition to the wells shown on Figure 2, an existing irrigation well (North Well) 4240 feet north-northwest of the pumped well was monitored during the test. Also, during the second day of the pumping test, another irrigation well (South Well) was discovered 2320 feet south of the pumped well. Following its discovery, water level data were recorded from it as well.

PUMPED WELL

The pumped well (BLM-PUMP) was an existing 16-inch irrigation well with a diameter reduction to 8 inches at 405 feet below land surface. The well is mills knife perforated from 103 to 403 feet and 629 to 661 feet. In addition,

there is open hole from 661 to 835 feet. The well log indicates that the well was originally drilled to 908 feet, so apparently the bottom portion has filled in with sediment over time. The perforated/open intervals for the pumped well are summarized in Table 1.

A velocity survey was conducted on the pumped well to determine which horizons contributed flow to the well. The survey showed no indication of production from 100 to 200 feet, modest production from 200 feet to 400 feet, and good production from 629 feet to the bottom of the well.

Note that because the pumped well was essentially fully penetrating from 103 feet to total depth, the test data did not support a determination of the degree of interconnection among formations below 103 feet. The zone from 103 feet to total depth had to be treated as a "bulk aquifer" with respect to the data obtained from the test. The data only allowed inferences of the degree of interconnection of the "bulk aquifer" to the shallower sediments, i.e., above 103 feet.

OBSERVATION WELLS

Eighteen of the 20 observation wells that were monitored during the test are shown on Figure 2. Seven of these were pre-existing observation wells that are monitored on a continual basis. Table 1 summarizes the screened intervals in each of these wells. In general, the static water level in the deeper wells (say below 40 feet) are near land surface, while the levels in the shallower wells are well below land surface, consistent with a strong upward gradient in the area.

Eleven new observation wells were drilled in anticipation of conducting the pumping test. Ten of these were so-called shallow/deep well pairs at five locations – 20 feet, 50 feet and 200 feet south of the pumped well, and 50 feet and 200 feet east of the pumped well. As indicated in Table 1, the shallow wells penetrated to depths around 20 feet, while the deep wells were completed to around 60 feet deep. In addition to these 10 wells, a new well (SUMMERS-SHALLOW) was drilled adjacent to the existing Summers well (COT-SUMMERS). Note that although this well has "SHALLOW" in its name, its depth (57 feet) actually correlates most closely to the deep wells of the shallow/deep well pairs.

An additional existing irrigation well 4240 feet north northwest of the pumping test site was included as an observation well. This is a 16-inch well with mills knife perforations from 20 to 461 feet and open hole from 461 to 503 feet. There may be additional open hole below 503 feet, but during a camera survey of the well, the camera could not pass bridging material at that depth.

An additional irrigation well (South Well) 2320 feet south of the site was discovered during the second day of the pumping test. The available log for this well showed a depth of 940 feet. There was no information on the perforated interval, however. Because a starting static water level was not measured for the South Well, it was necessary to infer it. This was done by assuming that its residual drawdown after 6 days of recovery was the same as that observed in the pumped well – a reasonable assumption.

TEST EXECUTION

Pumping began at 9:00 am on November 11, 2003 and continued for 4205 minutes until 7:05 am on November 14. The discharge rate started at around 620 gallons per minute (gpm), declining to less than 600 gpm within a few hours. Throughout the balance of the test, there was a minor additional decline in pumping rate. Overall, the average test rate was 591 gpm. Following shutdown, recovery data were recorded until the morning of November 20, thus providing a 6-day recovery record.

Water levels were recorded electronically using down-hole pressure transducers. In addition, backup water levels were recorded manually throughout the pumping period and the first 24 hours of recovery. The manual data confirmed that valid electronic data had been obtained from all wells except BLM-South-20S. For this well, there was a discrepancy between the electronic and manual data. Therefore, the manually recorded data were used in the analysis.

During the test, the pumped water was discharged on the land surface about 1800 feet northeast of the pumped well. A portion of the water soaked into the ground, although much of it ponded on the surface. By the end of the test, the pond covered an area approximately 50 feet wide and nearly half a mile long.

Rainfall occurred twice during the test. The first incident was early on November 12 and included two hours of hard rain. It also rained later that evening and into the morning of November 13.

BACKGROUND DATA

Background water level data were collected to see what water level fluctuations occurred naturally and help distinguish between water level changes caused by conducting the pumping test and changes associated with other causes.

Background water level fluctuations have several causes, among them barometric pressure changes, operation of other wells in the aquifer, earth tides, daily transpiration of shallow groundwater by plants, and long-term trends related to weather patterns.

Along with water level data, barometric pressure data were recorded during the pumping and recovery test to see if a correlation existed between groundwater levels and barometric pressure data. By comparing barometric pressure data and background water levels, it is possible to correct the measured groundwater levels for changes in barometric pressure prior to data analysis.

The background data showed that there was negligible fluctuation in the water levels in most of the observation wells. Figure 3 shows several representative hydrographs. Only the hydrographs for COT-UCD and COT-BLM, near the San Pedro River, showed significant fluctuation. Well COT-LD, also near the river, showed only minor fluctuations. The other two curves (South-200-Deep and South-200-Shallow) were typical of all of the other observation wells in that they showed negligible background effects.

The two hydrographs that showed significant response (COT-UCD and COT-BLM) were compared to the barometric pressure to see if a correlation existed. Figures 4 and 5 show comparisons of the COT-UCD hydrograph and barometric pressure, emphasizing early and late data, respectively. The hydrograph shows an overall drop in water level attributable to the pumping test, but the correlation of early and late data to barometric pressure changes is apparent.

Examination of figures 4 and 5 revealed a very odd response. The magnitude of the hydrograph response was approximately equal to that of the barometric pressure change. Normally, this would suggest a 100 percent barometrically efficient well. However, as seen on Figures 4 and 5, an *increase* in barometric pressure corresponded to a *rise* in the water level in the well, opposite to the expected response.

A possible explanation of the observed data is that the transducer used to measure the water level data was non-vented. If this were the case, an increase in barometric pressure would cause an increase in the measured pressure in the well, making it appear that the water level had risen, even though it had not. A barometrically *inefficient* well monitored with a non-vented transducer would produce the patterns shown on Figures 4 and 5. An alternate explanation of the observed response is that a vented transducer was used but that the vent tube within the transducer cable was kinked or damaged, causing the transducer to respond much like a non-vented one. Such damage could occur if the cable were driven over by a vehicle or folded too tightly over the edge of the well casing.

If one of these explanations of the observed response is correct, it would imply that the actual water level change in response to barometric pressure change was negligible.

Figure 6 shows a comparison of the COT-BLM hydrograph and barometric pressure. There is no correlation evident in the two signals. Further, there is no apparent explanation of the rather erratic response of the COT-BLM hydrograph.

SURFACE WATER DATA

Figure 7 shows a comparison of hydrographs for the San Pedro River and adjacent alluvial well COT-LD. There is an apparent correlation, especially evident in the early data shown on an expanded scale on Figure 8. Both the river levels and groundwater levels showed daily fluctuations of a couple of hundredths of a foot. A careful comparison of the curves on Figure 8 showed that the surface water level changes lagged those in the observation well by a couple of hours, on average. That is, the fluctuations occurred in the aquifer first and the river levels responded later, apparently being affected by the adjacent groundwater levels. The observed response implies a hydraulic connection between the San Pedro River and its adjacent alluvium. The underlying cause of the minor groundwater level changes could be either

barometric pressure changes or transpiration of groundwater by vegetation along the river.

Note that the river levels showed a general declining trend, while the groundwater levels showed a rising trend. These effects are presumed to be in response to antecedent weather patterns in the area.

ANALYTICAL METHODS APPLICABLE TO THE PUMPED AQUIFER

Following is a description of some of the analytical analysis methods applied to data from wells completed in the pumped aquifer (North Well, South Well, COT-SUMMERS, pumped well).

Drawdown

For wells completed within the pumped aquifer, the Theis Equation (1935) provides a good estimate of response to pumping. The Theis equation describes drawdown around a well as follows:

$$s = \frac{114.6Q}{T} W(u)$$

where,

$$W(u) = \int_u^\infty \frac{e^{-x}}{x} dx$$

and

$$u = \frac{1.87 r^2 S}{Tt}$$

and where,

s = drawdown, in feet
Q = discharge rate, in gpm
T = transmissivity, in gallons per day per foot (gpd/ft)
S = storage coefficient (dimensionless)
t = pumping time, in days
r = distance from center of pumpage, in feet

To use the Theis method to analyze drawdown data, the time-drawdown data are plotted on log-log graph paper. Then, Theis curve matching is performed using the Theis type curve – a plot of the Theis well function $W(u)$ versus $1/u$. Curve matching is accomplished by overlaying the type curve on the data plot and, while keeping the coordinate axes of the two plots parallel, shifting the data plot to align with the type curve, effecting a match position. An arbitrary point, referred to as the match point, is selected from the overlapping parts of the plots. Match point coordinates are recorded from the two graphs, yielding four values – $W(u)$, $1/u$, s and t. Using these match point values, standard formulas are used to compute the aquifer parameters as follows:

$$T = \frac{114.6Q}{s} W(u)$$

$$S = \frac{Ttu}{1.87r^2}$$

where,

s = match point drawdown, in feet
Q = discharge rate, in gpm
T = transmissivity, in gpd/ft
t = match point pumping time, in days
r = distance from center of pumpage, in feet
S = storage coefficient (dimensionless)
$W(u)$ = match point value
u = match point value

The equation for storage coefficient is valid only for observation well data.

An alternative solution method applicable to time-drawdown data is the Cooper-Jacob method (1946), a simplification of the Theis equation that is mathematically equivalent to the Theis equation for small distances from the pumped well and/or large pumping times. The Cooper-Jacob equation describes drawdown around a pumping well as follows:

$$s = \frac{264Q}{T}\log\frac{0.3Tt}{r^2S}$$

where,

s = drawdown, in feet
Q = discharge rate, in gpm
T = transmissivity, in gpd/ft
t = pumping time, in days
r = distance from center of pumpage, in feet
S = storage coefficient (dimensionless)

The Cooper-Jacob equation is a simplified approximation of the Theis equation and is valid whenever the u value is less than about 0.05.

For small radius values (e.g., corresponding to borehole radii), u is less than 0.05 at very early pumping times and, therefore, is less than 0.05 for nearly all measured drawdown values. Thus, for pumped wells, the Cooper-Jacob equation can be considered a valid approximation of the Theis equation.

For observation wells, a longer time is required before the u-value criterion is satisfied and the greater the distance from the pumped well, the longer the time required. For distant observation wells, the Cooper-Jacob method is often invalid and only the Theis method may be used.

According to the Cooper-Jacob method, the time-drawdown data are plotted on a semilog graph, with time plotted on the logarithmic scale. Then a straight line of best fit is constructed through the data points and transmissivity is calculated using:

$$T = \frac{264Q}{\Delta s}$$

where,

T = transmissivity, in gpd/ft
Q = discharge rate, in gpm
Δs = change in head over one log cycle of the graph, in feet

For the initial pumping (or recovery) response, casing storage effects dominate the early data, invalidating the Theis and Cooper-Jacob methods of analysis.

The duration of casing storage effects can be estimated using the following equation (Schafer, 1978).

$$t_c = \frac{0.6\left(D^2 - d^2\right)}{\frac{Q}{s}}$$

where,

t_c = duration of casing storage effect, in minutes
D = inside diameter of well casing, in inches
d = outside diameter of column pipe, in inches
Q = discharge rate, in gpm
s = drawdown observed in pumped well at time t_c, in feet

The casing storage affected data must be excluded from any analysis performed on the pumping test data.

Recovery

During recovery, the remaining drawdown (residual drawdown) around a pumped well after it has been shut off can be described by superimposing the pumped well, which runs indefinitely, and an imaginary injection well, which begins injecting an equal volume of water into the aquifer at the time of pump shutoff. The corresponding Theis description of residual drawdown is as follows:

$$s' = \frac{114.6Q}{T}\left[W(u) - W(u')\right]$$

Where u is the u value calculated for time since pumping started, t, and u' is the u value calculated for the time since pumping stopped, t'.

In this equation, for large distances from the pumped well and for early recovery times, s' actually continues increasing temporarily after pump shutoff, before it begins decreasing. This is because the continuing effect of having pumped the well causes greater additional drawdown than the initial recovery affect associated with shutting down the pumped well. That is, $W(u)$ increases faster than $W(u')$, initially.

When the pump is shut off, the ongoing rate of drawdown increase, R_d, caused by the pumping event is greater than the rate of recovery, R_r, associated with shut down where:

$$R_d = \frac{\partial}{\partial t'}\left[\frac{114.6Q}{T}W(u)\right]$$

$$R_r = \frac{\partial}{\partial t'}\left[\frac{114.6Q}{T}W(u')\right]$$

After pump shutdown, R_d steadily decreases while R_r increases. Drawdown reaches a maximum value when the two terms are equal, and then begins to decline. This occurs when:

$$\frac{\partial}{\partial t'}\left[\frac{114.6Q}{T}W(u)\right] = \frac{\partial}{\partial t'}\left[\frac{114.6Q}{T}W(u')\right]$$

Taking the derivatives of these expressions and simplifying, it can be shown the drawdown reaches a maximum when:

$$\frac{\exp\left(\frac{1.87r^2S}{Tt'}\right)}{t'} = \frac{\exp\left(\frac{1.87r^2S}{T(P+t')}\right)}{P+t'}$$

Aquifer diffusivity (transmissivity divided by storage coefficient) can be estimated by observing the recovery time, t', at which drawdown begins decreasing and solving the above equation for the ratio T/S.

Recovery data were analyzed by two methods – the Theis recovery method applied to residual drawdown data, and Theis curve matching applied to *calculated recovery* data described below.

The Theis recovery method is a semi-log analysis method analogous to the Cooper-Jacob procedure. In this method, residual drawdown is plotted on a semi-log graph versus the ratio t/t', where t is the time since pumping began

and t' is the time since pumping stopped. A straight line of best fit is constructed through the data points and T is calculated from the slope of the line as follows:

$$T = \frac{264Q}{\Delta s}$$

The recovery data are particularly useful compared to time-drawdown data. Because the pump is not running, spurious data responses associated with dynamic discharge rate fluctuations are eliminated. The result is that the data set is generally "smoother" and easier to analyze.

The Theis recovery method is valid only when sufficient recovery time has passed that the u value criterion is satisfied, i.e., $u' < 0.05$. For earlier recovery times, Theis curve matching must be performed by plotting recovery time, t', versus *calculated recovery*, s_c, where:

$$s_c = s_e - s'$$

where,

s_c = calculated recovery
s_e = extrapolated drawdown
s' = residual drawdown

The extrapolated drawdown, s_e, is the drawdown that would have been observed had the pump continued to run. The values of s_e must be determined by extrapolating the original drawdown graph, either graphically or by analytical calculation. The calculated recovery values obtained from the above equation are plotted on log-log graph paper and analyzed using the Theis curve matching described earlier.

Because the calculated recovery values are obtained by extrapolating the time-drawdown data, the resulting values of the aquifer parameters from this recovery data approach are not new, independent values. Instead, they depend to a significant extent on the original drawdown data.

Distance-Drawdown Methods

Distance-drawdown data can be analyzed by constructing either semi-log or log-log plots of drawdown data recorded at a specific pumping time. Use of

the semi-log approach requires that the *u* value condition be satisfied of all of the observation wells. Because this condition often is not satisfied of the most distant wells, it is preferable to use the log-log plot and Theis curve matching.

In this method, drawdown, *s*, is plotted against the reciprocal of the distance squared, $1/r^2$, on log-log graph paper. Theis curve matching is performed as described earlier, yielding four match point values – $W(u)$, $1/u$, s, and $1/r^2$. Using these match point values, aquifer parameters are computed as follows:

$$T = \frac{114.6Q}{s} W(u)$$

$$S = \frac{Ttu}{1.87} \cdot \frac{1}{r^2}$$

ANALYTICAL METHODS APPLICABLE TO OVERLYING AQUIFERS

The equations that describe the response of one or more overlying aquifers to pumping the main aquifer are extremely complex. The combination of the great complexity of even the most idealized governing equations and the real-world departure of the subsurface materials from the idealized assumptions usually make application of analytical approaches for multiple aquifers impractical or impossible. Such data are best analyzed by using computer modeling or by approximating the horizontally layered system as a single, homogeneous, anisotropic aquifer. This latter approach is presented later in this report. In addition, it is possible to glean information on the inter-relationship of the various strata simply by observing the major features and trends of the hydraulic response.

ANALYSIS OF WELLS IN THE PUMPED AQUIFER

This section presents detailed analyses of pumping and recovery data from wells completed within the pumped aquifer – the pumped well, North Well, South Well, COT-SUMMERS.

Pumped Well

Figure 9 shows the drawdown data from the pumped well. The total drawdown reached 128.3 feet by the end of the three-day pumping test.

A straight line could not be fitted to all of the drawdown data. Casing storage phenomena affected the early data, causing the data points to fall above the straight line shown on the graph. The casing storage calculation produced an estimated casing storage time, t_c, of approximately 17 minutes. This means that the drawdown data from the first 17 minutes of the pumping test can be expected to describe a line steeper than the desired straight line of best fit.

Even after 17 minutes, however, the data trace continued to flatten, rather than stabilizing as expected. One possible cause of this response is the gradually declining pumping rate during the early stages of the pumping test. This also could be explained by a gradually increasing formation transmissivity away from the well.

The straight line of best fit on Figure 9 produced an estimated formation transmissivity of 8800 gpd/ft. The slope of the drawdown trace did not stabilize at this level, however, but continued to flatten at late pumping time. It is possible that water contributed to the pumped aquifer from overlying strata resulted in a gradually increasing storage coefficient, producing the observed late time flattening. The ongoing flattening slope also could have been caused by infiltration of rainwater or re-infiltration of a portion of the pumped water.

Figure 10 shows the recovery data from the pumped well, plotted as residual drawdown, s', versus t/t'. The straight line of best fit produced a transmissivity value of 11,100 gpd/ft.

The casing storage duration of 17 minutes corresponded to a t/t' value of about 250. In most pumping tests, the casing storage time is associated with a distinct transition from an earlier, steep slope to a later, flat slope, with the calculated casing storage time, t_c, showing the end of the transition section, i.e., marking the start of the flat slope. However, the pumped well recovery data did not show this classic response. Instead, the data showed a continuous, gradual flattening, with no remarkable changes in slope at time t_c. This response, observed on both the time-drawdown and recovery graphs, was very unusual and not readily explained.

The observed casing storage effect appeared to last longer than predicted theoretically. This is the kind of response that would occur in a much larger diameter well than the pumped well. One possible cause of such a response would be a void outside the well casing in the interval of water-level change (upper 100 feet or so). There was no information indicating the existence of such a void, however. Suffice it to say that the observed casing storage response was highly unusual compared to that generally observed in pumping tests.

South Well

Figure 11 shows time-drawdown data from the South Well. Most of the data from this well were recorded at late time, because the well was not discovered until the second day of the test and was not prepared and outfitted with data logging equipment until the third day.

The late data corresponded to the flattened slope observed in the pumped well at late time, possibly being affected by increasing effective storage coefficient or recharge of rainfall or discharge water. Thus the calculated transmissivity of 15,300 gpd/ft shown on Figure 11 probably represents an overestimate.

Figure 12 shows a semi-log plot of the South Well recovery data. Note that recovery time increases from right to left, as t/t' decreases. The continuous curvature observed, as opposed to a straight line, results from the u value being greater than 0.05 for most of the recovery period. The later recovery data were used to compute transmissivity, yielding a value of 10,300 gpd/ft.

Figure 13 shows an expanded-scale view of the early recovery data from the South Well. It is evident from the graph that as recovery time increased (right to left on the graph) the drawdown continued to increase for a time before finally beginning to rebound. The initial rebound began approximately 115 minutes into recovery.

To estimate the aquifer diffusivity, the expressions derived from the derivative of the drawdown (presented earlier) were evaluated for numerous values of diffusivity. Evaluations were made for the drawdown caused by ongoing pumping and the recovery caused by pump shutoff and are shown graphically on Figure 14. Recall from the earlier discussion that these parameters should be equal at the time of the onset of water level rebound.

According to Figure 14, the derivative expressions were equal for a diffusivity of approximately 3.4 x 10^7 gpd/ft. As described later, this value was corroborated by subsequent analysis.

An attempt was made to analyze calculated recovery plotted against recovery time, as shown on Figure 15. The resulting transmissivity calculation of 18,000 gpd/ft likely represents an overestimate, because the data trace was dependent on extrapolating the late drawdown trend which was known to yield an overestimate of T (because of flattening of the drawdown curve at late time).

North Well

Figure 16 shows a log-log plot of the time-drawdown data from the North Well. Note that an offset in the data trace occurred after about one day of pumping, possibly attributable to movement of the transducer cable.

The T value obtained from the North Well data was several times larger than other values obtained from the test. This may be attributable to heterogeneous aquifer properties, the effects of increasing effective storage coefficient with time, or recharge of rainfall or discharge water.

Figure 17 shows the recovery data from the North Well. This graph was not analyzed, because the u-value criterion was not satisfied. A calculated recovery graph was not prepared because results from it would not have provided new, independent information.

Figure 18 shows an expanded-scale view of the early recovery data from the North Well. As shown on the graph, drawdown continued to increase until about 700 minutes after pump shutoff, when water levels finally began to rebound.

To estimate diffusivity, the two derivative expressions described earlier were evaluated for numerous values of diffusivity and a recovery time of 700 minutes. The results, plotted on Figure 19, show that the two expressions were equal for a diffusivity of approximately 3.1 x 10^7 gpd/ft. This result agreed well with that obtained from the South Well.

COT-SUMMERS Well

Figure 20 shows time-drawdown data of the SUMMERS well pair, COT-SUMMERS and SUMMERS-SHALLOW. SUMMERS-SHALLOW shows muted response, clearly showing that it is located in an overlying zone separated from the pumped aquifer by an aquitard.

COT-SUMMERS, on the other hand, showed dramatic response and was judged to be well connected to the pumped aquifer. It is inferred, however, that the well is probably completed within tight sediments. The response to pumping was rather sluggish, taking hundreds of minutes to show measurable drawdown. The time-drawdown curve could not be analyzed because of the sluggish response. It was concluded from the response that COT-SUMMERS was completed in an aquitard within, or hydraulically connected to, the pumped aquifer. This conclusion also was supported by observed reverse water level fluctuations, described next.

Reverse Water Level Fluctuations

Figure 21 shows an expanded-scale view of the early time-drawdown data from the SUMMERS well pair. As indicated, both wells showed a water level rise for several hours after pumping began, before water levels finally began declining. Such water level responses are called reverse water level fluctuations, also referred to as the Noordbergum Effect (Wolff, 1970; Rodrigues, 1983; Hsieh, 1996). They are occasionally seen in observation wells completed within aquitards or aquifers adjacent to the pumped aquifer and separated from it by an aquitard.

Reverse water level fluctuations are brought about by poroelastic effects and corresponding pore pressure changes. When the main aquifer is pumped, it undergoes elastic distortion in response to the change in pore water pressures, as well as the down thrust on the land surface at the wellhead associated with operating the pump. When the main aquifer becomes distorted, adjacent layers of aquitards and aquifers also are distorted. This creates transient pore pressure changes within these units. At some locations, the pressures decline, while at other locations they rise. As time goes on, these pressure changes are relieved as water moves from high pressure areas to low pressure areas.

Clearly, pressures rose at the SUMMERS well pair due to poroelastic effects. After several hours, movement of water out of the high pressure zones

relieved the pressure and the wells eventually registered the expected drawdown.

Figure 22 shows recovery data from the SUMMERS well pair. As before, the sluggish response in COT-SUMMERS, precluded analysis.

Both wells showed reverse water level fluctuations during recovery, consistent with what was observed during pumping. Figure 23 shows an expanded-scale view of the early recovery from COT-SUMMERS. It is evident that when the pump was turned off, water levels declined rapidly and substantially at first, before showing signs of the expected recovery.

Distance-Drawdown Analysis

The drawdown data were analyzed using distance-drawdown techniques to obtain estimates of transmissivity and storage coefficient. Figure 24 shows Theis curve matching results of drawdown data recorded at the end of the pumping test. The analysis produced a transmissivity of 8900 gpd/ft and a storage coefficient of 9.5×10^{4}. The *T* value was in good agreement with the values obtained from time-drawdown and recovery analysis of the pumped well data.

The distance-drawdown data were plotted on a larger scale, shown on Figure 25, so that the pumped well could be included. The type curve passed remarkably close to the plotted drawdown value for the pumped well. Normally, the pumped well data point plots above the curve, that is, the pumped well has more drawdown than predicted theoretically. This is because pumped wells are usually somewhat inefficient and have a pumping water level that is lower than the position of the cone of depression in the aquifer, just outside the well. According to Figure 25, the efficiency of the pumped well in this test is quite high. It is possible that the nature of the well design (part open hole and part perforated with large slots) permitted enough sand removal early in the life of the well to enhance its efficiency.

Distance-drawdown data were plotted for an earlier pumping time of 700 minutes for comparison purposes as shown on Figure 26. The sluggish response of COT-SUMMERS precluded using data from it at such early pumping time, so only data from the North and South Wells were used. The analysis produced a transmissivity of 9400 gpd/ft, similar to the previous value, but a much lower storage coefficient of 2.8×10^{-4}. It is possible that this value is more representative of the storage coefficient of the main aquifer,

and that the larger value, calculated above, included significant storage contribution from the overlying aquifers and aquitards, or simply reflected recharge of rainfall and/or discharge water from the test.

The aquifer diffusivity (T/S) was computed from the distance-drawdown parameter values determined on Figure 26, yielding a value of approximately 3.4×10^7 gpd/ft. This is an excellent agreement with the values obtained from the drawdown derivative analyses for the North and South Wells – 3.1×10^7 gpd/ft and 3.4×10^7 gpd/ft, respectively.

Summary of Aquifer Properties

It appears that the best estimate of aquifer properties includes a transmissivity of about 9400 gpd/ft and a short-term storage coefficient of 2.8×10^{-4}. It is possible that the long-term storage coefficient is closer to 10^{-3}, or perhaps higher, because of storage contribution from the overlying sediments. It is also possible that the larger observed storage coefficient was an artifact of recharge during the pumping test.

HYDRAULIC RESPONSE OF OVERLYING FORMATIONS

The response of the observation wells located in sediments above the pumped aquifer was reviewed to assess subjectively the nature of the response and hydraulic relationships among the various units. Recall that several wells were installed in the upper 20 feet or so of sediments ("shallow" wells or "20-foot zone") and a number of wells were installed to depths around 50 to 70 feet or so ("deep" wells or "60-foot zone" [including the well named SUMMERS-SHALLOW, which was actually 57 feet deep]).

All of the deeper wells showed significant response to pumping, though substantially less than that observed in the pumped aquifer. This implies that a significant aquitard separates the 60-foot zone from the pumped aquifer, but that the two likely are hydraulically connected.

The response in the 20-foot zone was about an order of magnitude less than that observed in the 60-foot zone. This implies that a significant aquitard separates these two zones, yet the presence of a measurable response shows that they are hydraulically connected.

Only those shallow wells 200 feet from the pumped well and closer showed a clear cut response to pumping. Those located 960 feet and farther from the pumped well did not show a discernable response. There were no wells completed in the 20-foot zone between 200 feet and 960 feet from the pumped well. Time-drawdown and recovery graphs are presented below for those wells that responded to the pumping test.

South-20 Well Pair

Figures 27 and 28 show drawdown and recovery, respectively, for the South-20 well pair located 20 feet south of the pumped well. Note on Figure 27 that the drawdown at the end of the pumping test for the deeper well (completed in the 60-foot zone) is around 19 feet. This is much less than the nearly 70 feet of drawdown interpolated for the pumped aquifer at a distance of 20 feet, using the distance-drawdown graph shown on Figure 26. The dramatically reduced drawdown in the 60-foot zone shows that there is a tight aquitard separating the 60-foot zone from the pumped aquifer.
Similarly, the drawdown in the shallow well (completed in the 20-foot zone) is only about 2 feet, approximately an order of magnitude less than that in the deeper obsevation well. This implies that very low permeability material separates the 20-foot zone from the 60-foot zone.

Because aquitards separate these two zones from the main aquifer, it was not possible to apply conventional time-drawdown and recovery analysis methods to the test data from the South-20 well pair, or any of the other observation wells in the 20-foot and 60-foot zones. Nevertheless, the drawdown and recovery graphs are presented for all responding observation wells.

South-50 Well Pair

Figure 29 shows time-drawdown data for the South-50 well pair. Figure 30 shows an expanded-scale plot of the same data illustrating the presence of reverse water level fluctuations in the deeper well, but none in the shallow well.

Figure 31 shows recovery data from these wells, while Figure 32 shows an expanded-scale plot of the reverse water level fluctuations associated with the recovery response of the deeper well.

South-200 Well Pair

Figure 33 shows time-drawdown data for the South-200 well pair. The expanded scale on Figure 34 clearly shows reverse water level fluctuations in the deeper well.

Figure 35 shows recovery data for both wells, while Figure 36 shows an expanded-scale plot illustrating the reverse water level fluctuations for the deeper well.

East-50 Well Pair

Figure 37 shows time-drawdown data for the East-50 well pair. The expanded scale on Figure 38 clearly shows reverse water level fluctuations in the deeper well.

Figure 39 shows recovery data for both wells, while Figure 40 shows an expanded-scale plot illustrating the reverse water level fluctuations for the deeper well.

East-200 Well Pair

Figure 41 shows time-drawdown data for the East-200 well pair. The expanded scale on Figure 42 clearly shows reverse water level fluctuations in the deeper well.

Figure 43 shows recovery data for both wells, while Figure 44 shows an expanded-scale plot illustrating the reverse water level fluctuations for the deeper well.

Distant Observation Wells

Figures 45 and 46 show drawdown and recovery data for 60-foot zone wells COT-UWD and COT-UCD, respectively. The graphs show that it took several days following pump shutoff before water levels stopped declining and began recovering. This effect is analogous to the delayed recovery response in the pumped aquifer wells discussed earlier.

The data from the first day of pumping in COT-UWD (Figure 45) showed a slight water level rise. This effect is likely a result of ongoing recovery from

antecedent step-drawdown test pumping, but could include poroelastic effects as well.

It is of note that none of the four distant shallow observation wells (20-foot zone wells) showed discernable response to pumping, suggesting that exceedingly tight sediments separate them from underlying formations.

Distance-Drawdown Analysis

An attempt was made to analyze the observation well data using distance-drawdown methods, even though most of the observation wells were not completed in the pumped aquifer. This was done by applying partial penetration analysis to account for the different screen intervals in the pumped well and observation wells. A method presented by Schafer (1998, 2001) based on the Hantush Equation (1961a, 1961b) for partially penetrating wells was used. In this method, drawdowns observed in the observation wells are corrected for partial penetration effects to equivalent drawdowns that would have been observed in fully penetrating wells. These drawdown values are then analyzed using distance-drawdown methods. The objective of the analysis was to estimate the vertical resistance of the aquitards separating the pumped aquifer from the 60-foot zone, and the 60-foot zone from the 20-foot zone.

In a strict sense, the method is only applicable to homogeneous, anisotropic conditions, whereas the actual site is vertically heterogeneous. Therefore, the method was considered to provide only approximate results. The procedure was used to provide rough estimates of the effective vertical resistance to flow, based on the homogeneous, anisotropic model. Then, a simplifying assumption was made that the aquitards accounted for essentially all of the vertical resistance to flow. The aquitard resistance was then calculated based on this assumption.

For homogeneous, anisotropic conditions, Hantush modified the Theis equation for partially penetrating wells as follows:

$$s = \frac{Q}{4\pi T}\left(W(u) + f_s\right)$$

where all terms are expressed in consistent units, and f_s represents the increase or decrease in drawdown measured in an observation well caused by partial penetration. According to Hantush, at late pumping times when $t > b^2S/(2TA)$, f_s can be expressed as follows:

$$f_s = \frac{4b^2}{\pi^2 (l-d)(l'-d')} \sum_{n=1}^{\infty} \left(\frac{1}{n^2}\right) K_0 \left(\frac{n\pi r \sqrt{K_z / K}}{b}\right)$$
$$\left[\sin\left(\frac{n\pi l}{b}\right) - \sin\left(\frac{n\pi d}{b}\right)\right]\left[\sin\left(\frac{n\pi l'}{b}\right) - \sin\left(\frac{n\pi d'}{b}\right)\right]$$

where,

f_s = incremental dimensionless drawdown component
b = aquifer thickness
d = distance from top of aquifer to top of screened interval of pumped well
d' = distance from top of aquifer to top of screened interval of observation well
l = distance from top of aquifer to bottom of screened interval of pumped well
l' = distance from top of aquifer to bottom of screened interval of observation well
K_0 = modified Bessel function of the second kind and of zero order
K = horizontal hydraulic conductivity
K_V = vertical hydraulic conductivity
r = distance from pumped well to observation well

For each observation well, a correction factor C_f is introduced which, when multiplied by the actual drawdown, will produce the drawdown that would have been observed in a fully penetrating well. Combining the Theis and Hantush equations, it can be shown that C_f can be expressed as follows:

$$C_f = \frac{W(u)}{W(u) + f_s}$$

C_f depends on duration of pumping (t), distance to the observation well (r), transmissivity and storage coefficient (T, S), anisotropy (A, equal to K_V/K), position of the screened interval in pumped and observation wells (d, l, d', l') and aquifer thickness (b).

The measured drawdown for each observation well can be corrected to the fully penetrating equivalent drawdown by multiplying by the correction factor:

$$s_f = C_f s$$

The drawdown values corresponding to the fully penetrating case can then be analyzed by conventional straight-line or curve-matching distance-drawdown methods to compute transmissivity and storage coefficient.

In typical analyses, the correction factors are a function of both transmissivity and storage coefficient, which are among the parameters being sought. Because of this, an iterative procedure generally is applied in which initial estimates of T and S are made and from which the initial correction factors can be computed. Using these correction factors, fully penetrating drawdown values are computed and analyzed using distance-drawdown methods to determine revised values for T and S. The revised T and S values are used to compute revised correction factors, C_f, and corrected drawdowns, s_f. This process is repeated until the calculated T and S values change only slightly from those obtained in the previous iteration.

The correction factors are also a function of the anisotropy ratio. Therefore, the calculations must be performed for several different estimated anisotropy ratios. The estimated anisotropy value which leads to the best solution, i.e., best straight-line fit or best curve-match, is deemed to be the actual anisotropy ratio.

For the Sierra Vista pumping tests analysis, because T and S had already been determined, they were held fixed at 9,400 gpd/ft and 9.5×10^{-4}, respectively, and only the vertical anisotropy ratio was varied to arrive at a solution.

Table 2 shows input parameter values used in the partial penetration analysis. Note that because the spinner log for the pumped well showed no production above 200 feet, the producing interval used in the calculations was assumed to

be below 200 feet. Also, as a simplification, a static water level (top of aquifer) of 4 feet below land surface was applied to all wells.

Figure 47 shows distance-drawdown data for the 60-foot zone observation wells corrected for partial penetration for isotropic conditions ($A = 1.0$). (The main aquifer wells are also shown on the graph for comparison purposes.) It is clear that the observation wells did not fit the expected distance-drawdown type curve. Therefore, the effective vertical anisotropy ratio had to be adjusted, as part of the solution process, to obtain a better fit.

It turned out that it was not possible to obtain a good curve match for all of the 60-foot zone observation wells for a single value of A. Figures 48 and 49 show distance-drawdown data corrected for vertical anisotropy ratios of 0.03 and 0.0066, respectively. The corrected drawdown values are listed in Table 3.

Figure 48 shows that the 60-foot zone observation wells close to the pumped well (right side of the graph) fit the type curve reasonably well for $A = 0.03$, while Figure 49 shows that the distant observation wells (left side of the graph) fit the type curve for $A = 0.0066$. These anisotropy values were used to calculate resistance values for the aquitard separating the 60-foot zone from the main aquifer.

For the purpose of this analysis, the producing zone of the pumped well was assumed to extend from 200 feet to 835 feet below land surface, as indicated by the Spinner survey conducted on the pumped well. (The Spinner survey showed little or no production from above 200 feet.) The transmissivity of 9400 gpd/ft, or 1260 square feet per day, was divided by the production zone thickness of 635 feet, yielding an average horizontal hydraulic conductivity of 1.98 feet per day.

The effective vertical anisotropy ratio for the nearby observation wells (Figure 48) of 0.03 was considered to cover the interval from the center of the producing zone, 517.5 feet below land surface, to 60 feet, a distance of 457.5 feet. The effective vertical hydraulic conductivity, K_V, was computed as K_V = 1.98 x 0.03 = 0.059 feet per day. The total vertical resistance can be computed as the ratio of the sediment thickness to K_V: 457.5/0.059 = 7750 days. As a first order approximation, this can be taken as the aquitard resistance separating the 60-foot zone from the pumped aquifer in the vicinity of the pumped well.

Similarly, the vertical anisotropy ratio of 0.0066 for the distant observation wells (Figure 49) led to a K_V value of 1.98 x 0.0066 = 0.013 feet per day. The corresponding aquitard resistance was estimated as 457.5/0.013 = 35,200 days for the broad area around the test site. This larger resistance value would be more representative of global conditions.

The substantial difference in computed resistance near the well (7750 days) and away from the well (35200 days) could reflect geologic differences. On the other hand, it is possible that the differences could be attributable to lack of conformance of the actual setting to the assumptions that were made. For example, vertical conduits or washouts along the upper blank portion of the well casing in the pumped well could have allowed modest leakage of 60-foot zone water into the well during the test, thereby exaggerating the observed drawdown response in the nearby wells. It was not possible to determine from the existing data whether or not such a scenario occurred, but this idea is discussed in greater detail below.

The shallow observation wells (20-foot zone) were used to estimate the resistance of the geologic materials between the 20-foot zone and 60-foot zone. Figure 50 shows distance-drawdown data from the 20-foot zone wells corrected for partial penetration, but assuming isotropic conditions (A = 1.0). It is clear that the fit to the type curve is not good and that the vertical anisotropy ratio must be adjusted. Figure 51 shows the best match, obtained for a vertical anisotropy ratio of, coincidentally, 0.0066. There is substantial scatter among the data points, implying substantial geologic heterogeneity.

The effective vertical hydraulic conductivity, K_V, was computed as 1.98 x 0.0066 = 0.013 feet per day. The corresponding resistance between the 20-foot zone and the center of the pumped well producing zone (separated by 497.5 feet) was computed as 497.5/0.013 = 38,270 days. The resistance separating the 20-foot zone from the 60-foot zone near the pumped well was calculated as the difference between this value and the resistance between the 60-foot zone and the aquifer (7750 days): 38,270 – 7750 = 30,520 days.

By comparison, the resistance between the 20-foot zone and 60-foot zone over a broad area farther from the well is inferred to be far greater than this because of the lack of discernable response of the distant shallow wells to pumping. In theory, zero drawdown response would indicate infinite aquitard resistance. Of course, there may have been some drawdown response, but too little to discern above the background noise. Nevertheless, the negligible observable

drawdown implies a very large resistance between the 20-foot and 60-foot zones.

As stated above, the substantial difference in resistance near the well (30520 days) and away from the well (unknown, but extremely large) could reflect actual geologic differences, but could also signify leakage of shallow zone water directly into the well bore. It was not possible to determine which was the actual case from the available data.

Possible Drainage of Shallow Water Directly Into the Pumped Well

In examining Figures 48 and 49 (drawdown corrections for 60-foot zone wells), it can be seen that the drawdown effect in the nearest well (right side of the graph) is the greatest above the level predicted by the type curve, and diminishes steadily with increasing distance (left side of the graph). This kind of response is consistent with what would be expected if well production water was being obtained directly from the 60-foot zone.

To test this hypothesis, drawdown data from the 60-foot zone were analyzed using distance-drawdown methods, assuming that no leakage had occurred and that water from the 60-foot zone drained directly into the pumped well. This could occur, for example, if a washout existed around the outside of the 16-inch well casing, allowing entry of shallow groundwater into the annulus around the well.

Figure 52 shows the resulting log-log distance-drawdown plot for a pumping time of 700 minutes. The data fit on this graph is remarkably good – better than that obtained from the drawdown data corrected for vertical anisotropy and partial penetration. The pumping rate was not known, because it was not possible to know what the hypothesized drainage rate of water from the 60-foot zone into the pumped well would have been.

If the hypothesized drainage rate is identified as Q_{700}, the analysis showed that the resulting T value was equal to 42 Q_{700} and the storage coefficient was 7 x 10^{-5} Q_{700}. For example, suppose that 2 gpm flowed from the 60-foot zone and into the production well. The corresponding T and S values then are calculated to be 84 gpd/ft and 1.4 x 10^{-4}, respectively, both plausible values.

Figure 53 shows distance-drawdown data from the 60-foot zone plotted for a pumping time of 4205 minutes, corresponding to the end of the pumping test. Again, the fit of the data to the type curve is quite good.

As shown on the graph, the T value is 49 Q_{4205}, where Q_{4205} is the drainage rate from the 60-foot zone at the end of the test. A comparison of this equation to the equation for 700 minutes of pumping time implies that Q_{4205} must be less than Q_{700} to produce the same transmissivity. This is exactly what would be expected when a shallow aquifer is drained by gravity, analogous to pumping a well at constant drawdown. Under these conditions, the pumping rate would be expected to decline over time as the cone of depression expanded.

A comparison of the storage coefficient equations on Figures 52 and 53 shows that if Q_{4205} is less than Q_{700}, then the storage coefficient calculation for 4205 minutes must be less than that computed for a pumping time of 700 minutes. This apparent inconsistency could be related to the inexact nature of the curve-matching procedure. On the other hand, it is possible that even if 60-foot zone water had drained directly into the pumped well, some additional 60-foot zone water could also have leaked through the aquitard separating the 60-foot zone from the pumped aquifer. If this occurred, increased pumped-aquifer drawdown over time would increase the leakage rate across the aquitard, artificially increasing the size of the cone of depression within the 60-foot zone and resulting in a lower computed storage coefficient value over time.
If the annulus around the 16-inch pumped well casing is open and allowing drainage of 60-foot zone and 20-foot zone water directly into the well, most of the drawdown response observed in these zones could be attributable to the direct drainage rater than leakage across the various intervening aquitards. If this is the case, the resistance of the aquitards could be orders of magnitude greater than the values determined from the partial penetration analysis.

Unfortunately, the condition of the annular space around the pumped well casing was not known. Also, there was no way to sort out from the data, with certainty, the cause of the observed well drawdown – leakage versus direct drainage. However, it was significant that the partial penetration analysis led to marginal-quality data fits, as shown on Figures 48 and 49, and inconsistent results, as indicated by the two different anisotropy ratio values (0.03 and 0.0066) for the aquitard separating the 60-foot zone from the pumped aquifer. On the other hand, the assumption of direct drainage into the well produced good data fits (Figures 52 and 53) and reasonable results, including declining drainage rate over time, which would be expected, and decreasing apparent storage coefficient, which would be consistent with some leakage contribution across the aquitard.

The aquitard resistance values determined from the partial penetration analysis are likely lower-bound values. If water was draining directly into the pumped well from the 20-foot and 60-foot zones, it could be concluded that the actual aquitard resistances are possibly orders of magnitude greater than the calculated values. To improve on the estimates of aquitard leakance would require utilizing a pumped well with known construction characteristics, and an effective grout seal around the blank casing.

SUMMARY

Data were analyzed from the constant-rate pumping and recovery test conducted for the Bureau of Land Management near the San Pedro River in the San Pedro Riparian National Conservation Area. The data covered a 3-day pumping period at a rate of 591 gpm and a 6-day recovery period. Water level measurements were recorded in the pumped well and 20 observation wells during the test. Three of the observation wells were completed in the producing aquifer, while the rest were completed shallower, in either a 20-foot zone or 60-foot zone.

Pumping and recovery data were analyzed by a variety of analytical methods resulting in the following observations and conclusions:

1. The casing storage response was highly unusual, consistent with what would be seen in a much larger diameter well.
2. Barometric pressure changes had negligible effect on water levels. There was only one incidence of an apparent effect. However, this was consistent with water levels having been measured using a non-vented transducer or a vented transducer with a damaged cable, thus providing a false apparent response.
3. There was a correlation between shallow groundwater levels adjacent to the San Pedro River and the river levels.
4. The transmissivity was estimated to be about 9,400 gpd/ft.
5. The storage coefficient of the pumped aquifer was estimated to be 2.8×10^{-4}. Late-time data led to a calculated storage coefficient of 9.5×10^{-4}. This could reflect additional storage contribution from the shallow sediments and/or possibly infiltration of either rainfall or discharge water.

6. Recovery data suggested an aquifer diffusivity of 3.1 to 3.4 x 10^7 gpd/ft, consistent with the transmissivity and storage coefficient estimates above.
7. Reverse water level fluctuations were observed in all 60-foot zone wells between 50 feet and 480 feet from the pumped well, as well as COT-SUMMERS completed near the top of the production zone.
8. Response of the 20-foot zone and 60-foot zone wells to pumping could have been attributable to either of two causes – leakage through intervening aquitards or direct drainage into the pumped well. It was not possible to know which was the actual case, although the direct drainage scenario led to better data fits and more consistent results.
9. Partial penetration analysis incorporating vertical anisotropy (based on the aquitard leakage scenario) predicted aquitard resistances of 7750 days near the pumped well and 35,200 days away from the pumped well for the aquitard separating the 60-foot zone from the pumped aquifer, and 30,520 days near the pumped well and a far greater unknown value away from the pumped well for the aquitard separating the 20-foot zone from the 60-foot zone. If direct drainage occurred during the pumping test, the actual aquitard resistances could be orders of magnitude greater than these values.

REFERENCES

ASTM, 2001. Standard Test Method for (Analytical Procedure) Determining Transmissivity, Storage Coefficient, and Anisotropy Ratio from a Network of Partially Penetrating Wells, Annual Book of ASTM Standards, Volume 04.09.

Cooper, H. H., Jr. and Jacob, C. E., 1946. A Generalized Graphic Method for Evaluating Formation Constants and Summarizing Well Field History, Transactions. Am. Geophys. Union, v. 27, No. 4, pp. 526-534.

Hantush, M. S., 1961a. Drawdown Around a Partially Penetrating Well, Journal of the Hyd. Div., Proceedings of the American Society of Civil Engineers, vol. 87, no. HY5, pp. 83-98.

Hantush, M. S., 1961b. Aquifer Tests on Partially Penetrating Wells, Journal of the Hyd. Div., Proceedings of the American Society of Civil Engineers, vol. 87, no. HY5, pp. 171-194.

Hsieh, P. A., 1996. Deformation-Induced Changes in Hydraulic Head During Ground-Water Withdrawal, Ground Water, vol. 34, no. 6, pp. 1082-1089.

Rodrigues, J. D., 1983. The Noordbergum Effect and the Characterization of Aquitards at the Rio Maion Mining Project, Ground Water, vol. 21, no. 2, pp. 200-207.

Schafer, David C., 1978. Casing Storage Can Affect Pumping Test Data, Johnson Drillers' Journal, Jan/Feb, Johnson Division, UOP Inc., St. Paul, Minnesota.

Schafer, David C., 1998. Determining Vertical Anisotropy Ratio Using a Graphical, Iterative Procedure Based on the Hantush Equation, Ground Water, Vol. 36, No. 2, March/April 1998.

Theis, C. V., 1935. The Relation Between the Lowering of the Piezometric Surface and the Rate and Duration of Discharge of a Well Using Groundwater Storage, Transactions. Am. Geophys. Union, v. 16, pp. 519-524.

Wolff, Roger G., 1970. Relationship Between Horizontal Strain Near a Well and Reverse Water Level Fluctuation. Water Resources Research, vol. 6, no. 6, pp. 1721-1728.

DS&A
David Schafer & Associates

Table 1. Screened Intervals in Pumped Well and Observation Wells
San Pedro River Basin Aquifer Test
Sierra Vista, Arizona

Well	Screened Interval (feet below land surface)	Distance From Pumped Well (feet)	Static Water Level (feet)	Drawdown at 4205 Minutes (feet)
BLM-PUMP	103-403 629-661 661-835 open hole*		4.03	128.33
North Irrigation Well	20-461 461-503 open hole*	4240	8.00	0.79
South Irrigation Well	??-940	2320	5.37 Estimated	6.83
Pre-existing Observation Wells:				
COT-SUMMERS	193.5-198.5	480	2.36	24.76
COT-UWS	14-19	960	14.44	negligible
COT-UWD	58-63	960	4.55	1.19
COT-BLM	17-20	1580	17.95	negligible
COT-UCD	48-53	1580	2.58**	0.38
COT-LS	7.5-8.5	1660	7.50***	negligible
COT-LD	11.75-12.75	1660	8.00***	negligible
New Observation Wells:				
BLM-South-20Shallow	14.5-19.5	20	14.23	1.82
BLM-South-20Deep	53.5-63.5	20	8.23	19.21
BLM-South-50Shallow	14.5-19.5	50	15.12	0.74
BLM-South-50Deep	50-60	50	9.35	12.20
BLM-East-50Shallow	18.5-23.5	50	13.90	2.21
BLM-East-50Deep	59-69	50	7.91	15.12
BLM-South-200Shallow	17.5-22.5	200	14.62	1.37
BLM-South-200Deep	55-65	200	9.90	7.47
BLM-East-200Shallow	14.5-19.5	200	14.57	0.23
BLM-East-200Deep	57-67	200	8.91	7.77
SUMMERS-SHALLOW	47-57	480	12.73	2.05

*fill below depth indicated **transducer was moved; actual static around 4.20 feet
***measuring point elevation about 10 feet lower than nearby wells

DS&A
David Schafer & Associates

Table 2. Input Parameters For Partial Penetration Analysis
San Pedro River Basin Aquifer Test
Sierra Vista, Arizona

Well	Screened Interval (feet)	Distance From Pumped Well (feet)	Observed Drawdown (feet)	Assigned Distance From Top of Aquifer to Top of Screen (feet)	Assigned Distance From Top of Aquifer to Bottom of Screen
Main Aquifer Wells					
Pumped Well	103-835		128.3	196	831
COT-SUMMERS	193.5-198.5	480	24.76	189.5	194.5
South Well	?-940	2320	6.83	0	936
North Well	20-503	4240	0.79	16	499
20-Foot Zone Wells					
BLM-South-20Shallow	14.5-19.5	20	1.82	10.5	15.5
BLM-South-50Shallow	14.5-19.5	50	0.74	10.5	15.5
BLM-East-50Shallow	18.5-23.5	50	2.21	14.5	19.5
BLM-South-200Shallow	17.5-22.5	200	1.37	13.5	18.5
BLM-East-200Shallow	14.5-19.5	200	0.23	10.5	15.5
60-Foot Zone Wells					
BLM-South-20Deep	53.5-63.5	20	19.21	49.5	59.5
BLM-South-50Deep	50-60	50	12.20	46	56
BLM-East-50Deep	59-69	50	15.12	55	65
BLM-South-200Deep	55-65	200	7.47	51.000	61
BLM-East-200Deep	57-67	200	7.77	53	63
SUMMERS-SHALLOW	47-57	480	2.05	43	53
COT-UWD	58-63	960	1.19	54	59
COT-UCD	48-53	1580	0.31 adjusted	44	49

DS&A
David Schafer & Associates

Table 3. Results of Partial Penetration Calculations
San Pedro River Basin Aquifer Test
Sierra Vista, Arizona

Well	Screened Interval (feet)	Distance From Pumped Well (feet)	Observed Drawdown (feet)	Corrected Drawdown For A = 1 (feet)	Corrected Drawdown For A = 0.006	Corrected Drawdown For A = 0.03
Main Aquifer Wells						
Pumped Well	103-835		128.3			
COT-SUMMERS	193.5-198.5	480	24.76	25.35	38.26	31.91
South Well	?-940	2320	6.83	6.83	6.83	6.83
North Well	20-503	4240	0.79	0.79	1.63	0.89
20-Foot Zone Wells						
BLM-South-20Shallow	14.5-19.5	20	1.82	3.52	119.20	
BLM-South-50Shallow	14.5-19.5	50	0.74	1.18	40.60	
BLM-East-50Shallow	18.5-23.5	50	2.21	3.52	122.25	
BLM-South-200Shallow	17.5-22.5	200	1.37	1.60	49.83	
BLM-East-200Shallow	14.5-19.5	200	0.23	0.27	8.55	
60-Foot Zone Wells						
BLM-South-20Deep	53.5-63.5	20	19.21	36.41	779.54	108.58
BLM-South-50Deep	50-60	50	12.20	19.10	411.23	56.69
BLM-East-50Deep	59-69	50	15.12	23.51	437.71	68.68
BLM-South-200Deep	55-65	200	7.47	8.65	154.82	22.95
BLM-East-200Deep	57-67	200	7.77	8.99	155.52	23.75
SUMMERS-SHALLOW	47-57	480	2.05	2.13	35.35	4.62
COT-UWD	58-63	960	1.19	1.20	14.43	2.03
COT-UCD	48-53	1580	0.31 adjusted	0.31	5.69	0.45

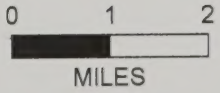

DS&A
David Schafer & Associates

FIGURE
1

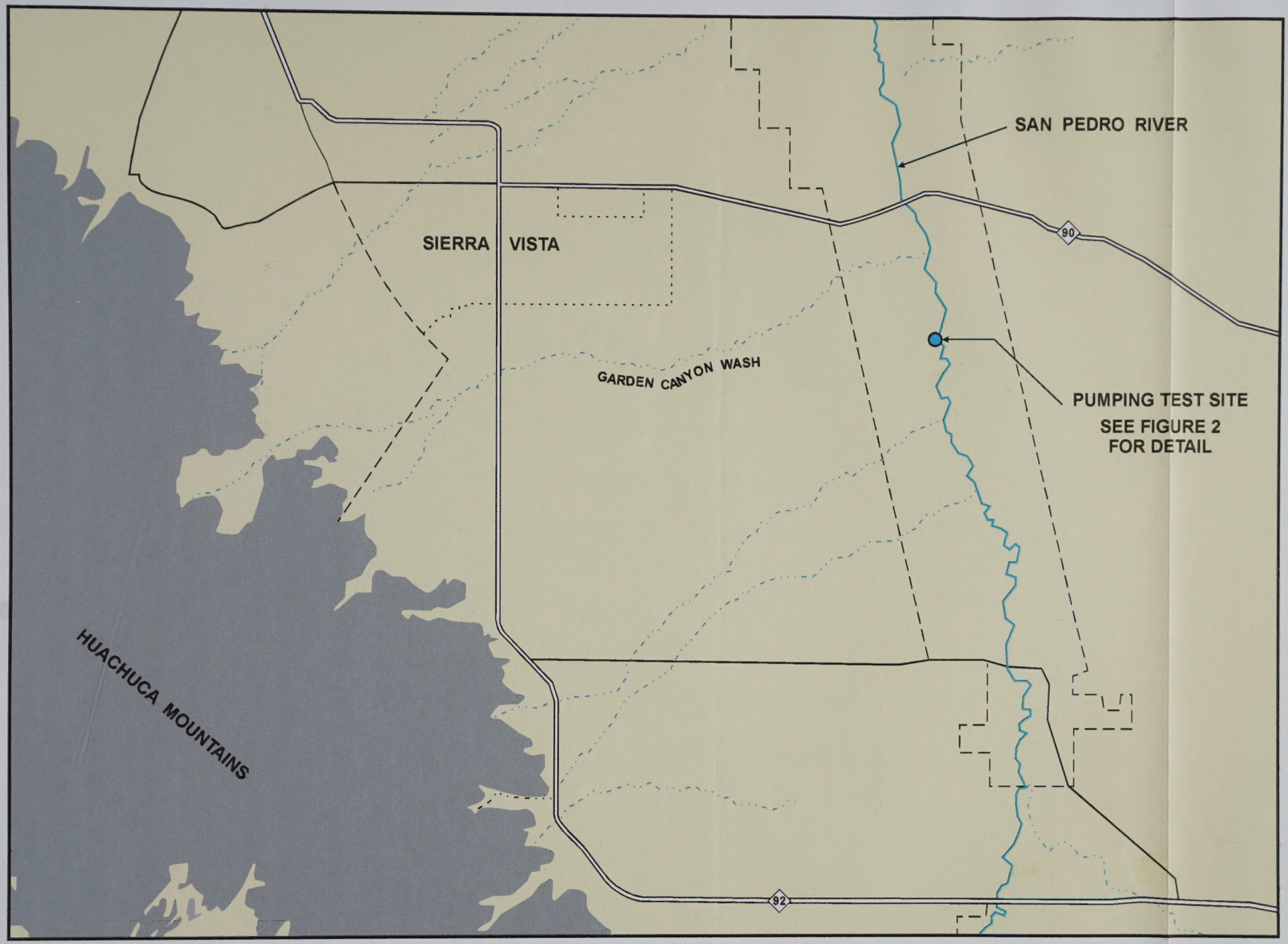

DS&A
David Schafer & Associates

AREA MAP

SAN PEDRO RIVER BASIN AQUIFER TEST
SIERRA VISTA, ARIZONA

FIGURE
1

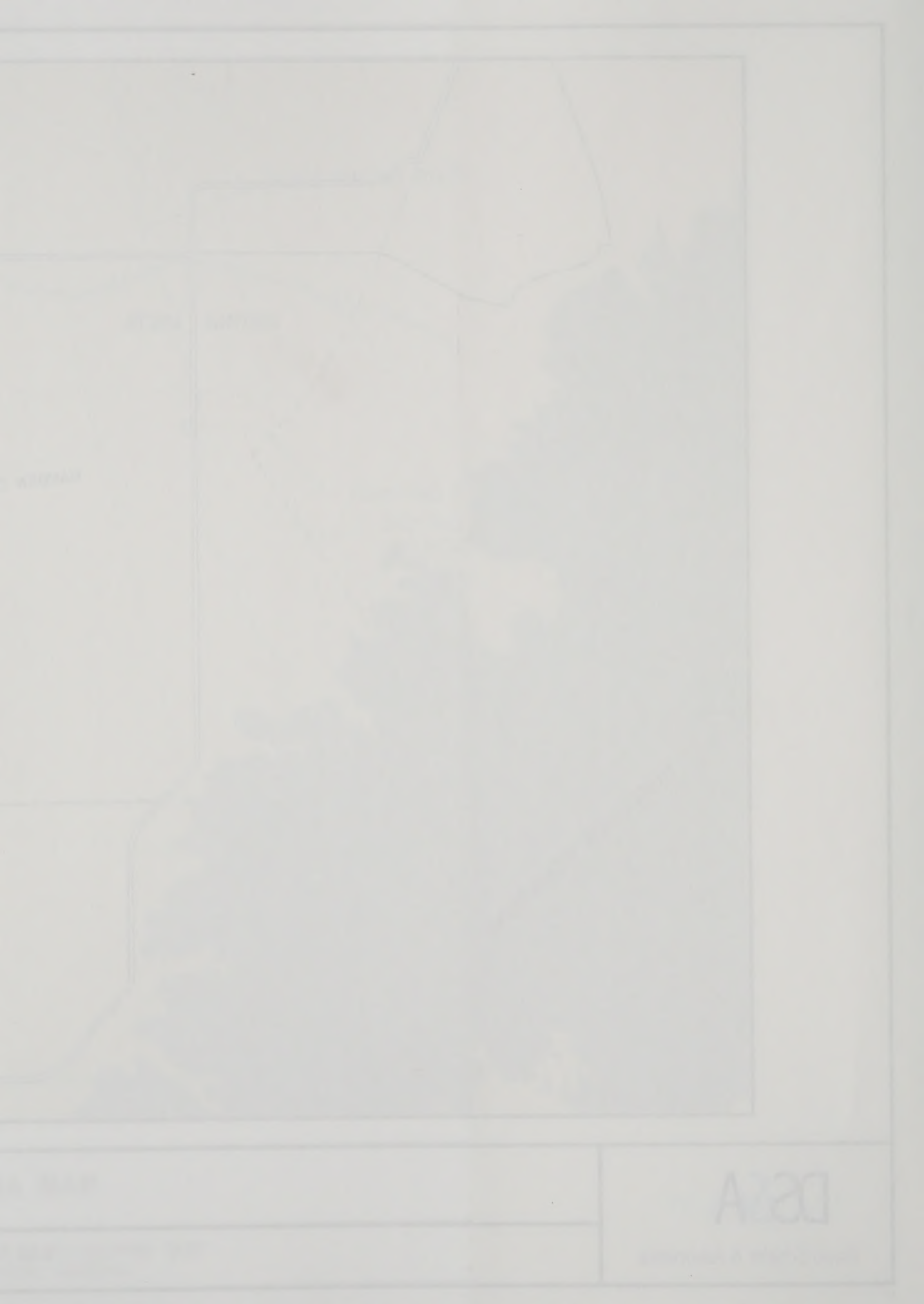

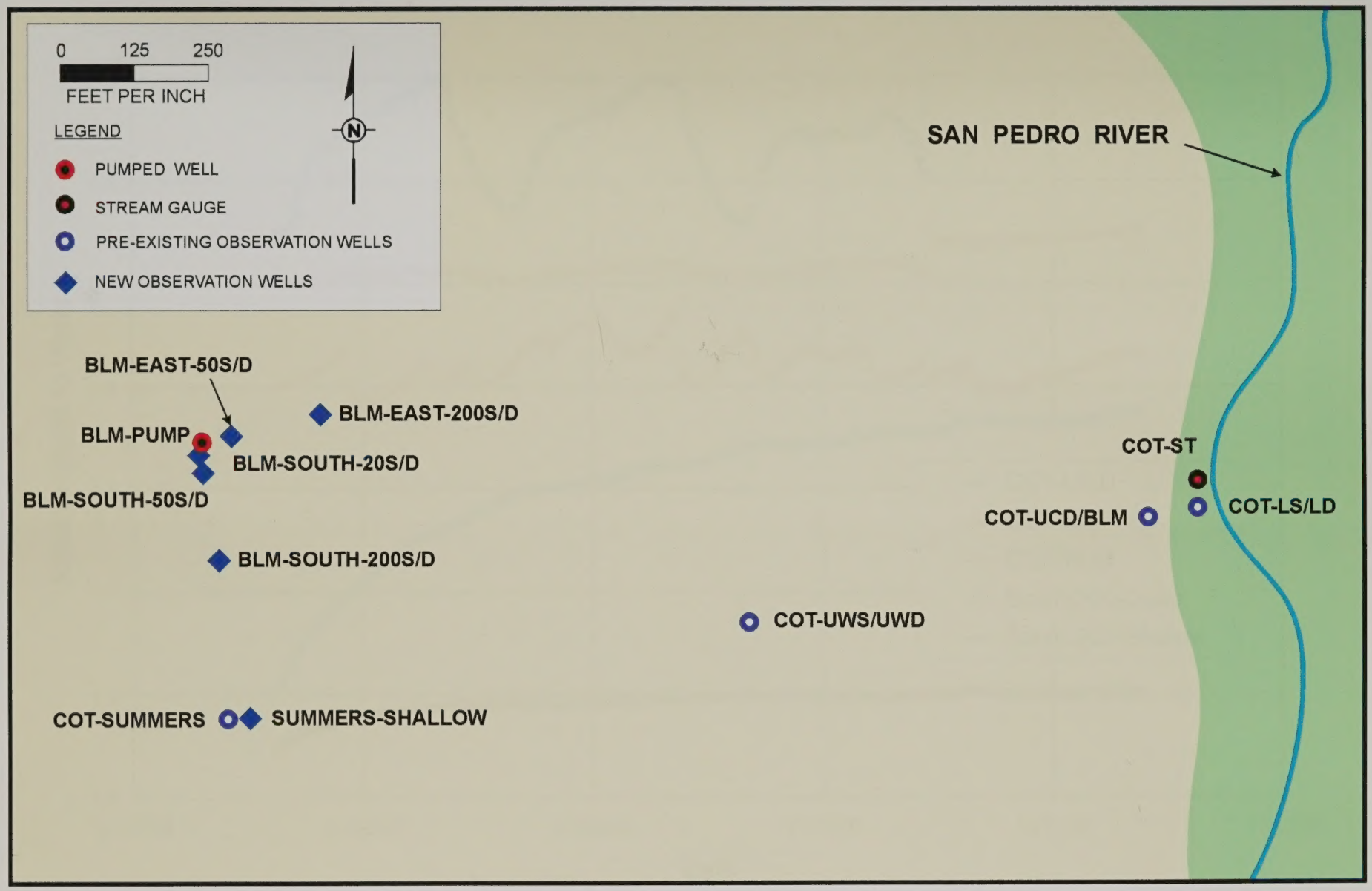

David Schafer & Associates

PUMPING TEST SITE

SAN PEDRO RIVER BASIN AQUIFER TEST
SIERRA VISTA, ARIZONA

FIGURE
2

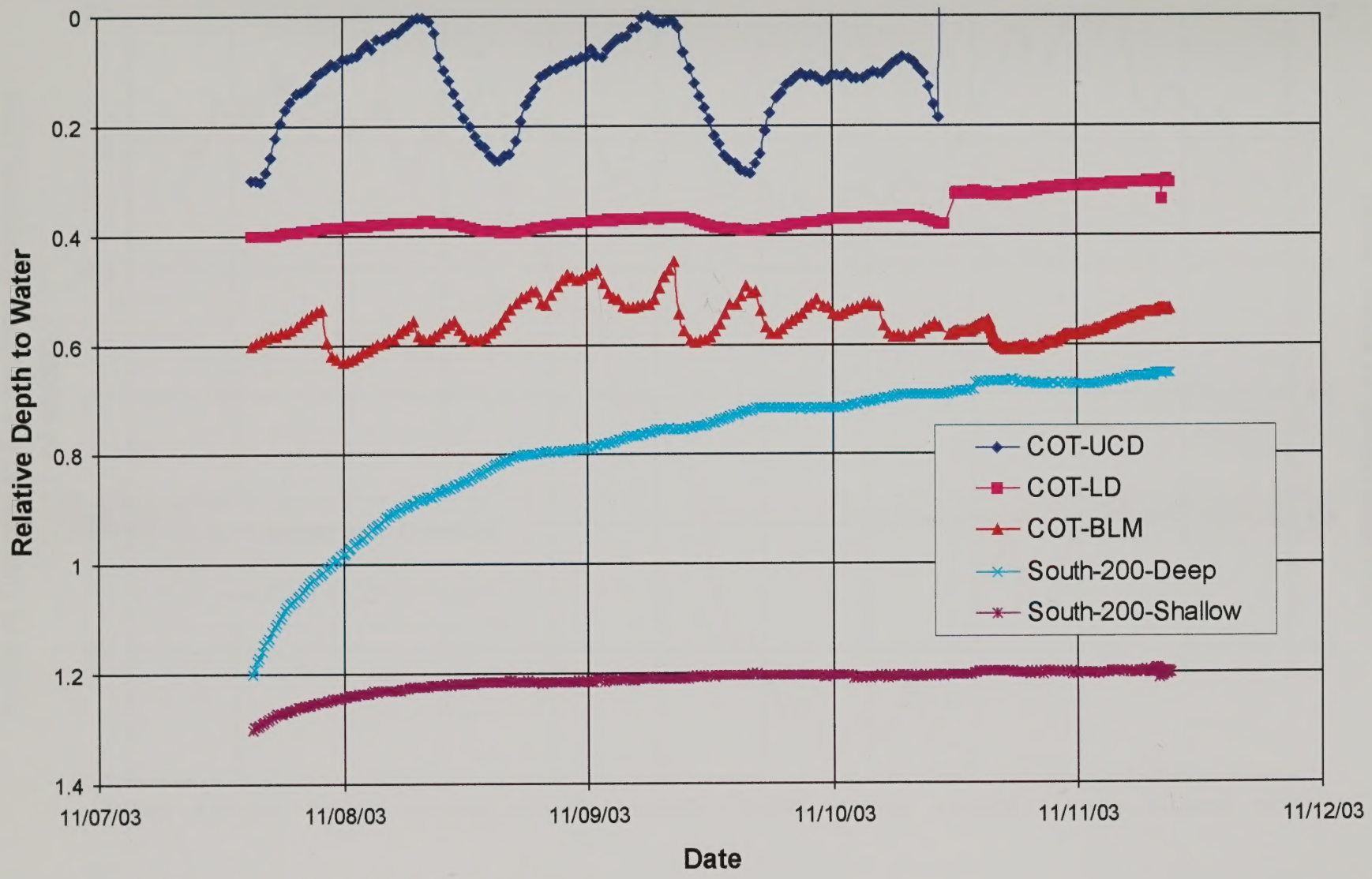

DS&A
David Schafer & Associates

BACKGROUND HYDROGRAPHS PRIOR TO PUMPING TEST

SAN PEDRO RIVER BASIN AQUIFER TEST
SIERRA VISTA, ARIZONA

FIGURE
3

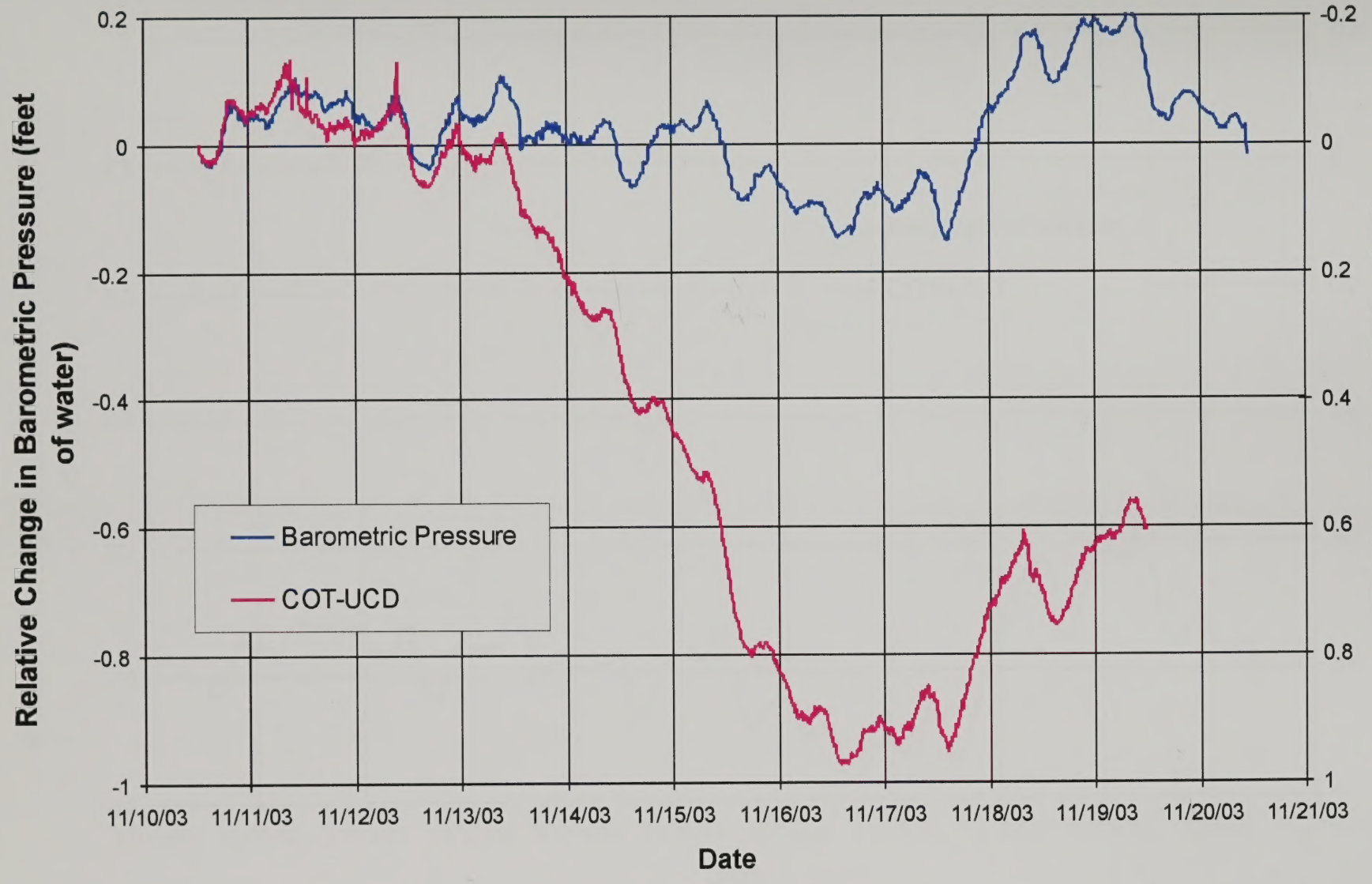

David Schafer & Associates

COMPARISON OF BAROMETRIC PRESSURE AND COT-UDC HYDROGRAPH - EARLY DATA

SAN PEDRO RIVER BASIN AQUIFER TEST
SIERRA VISTA, ARIZONA

FIGURE
4

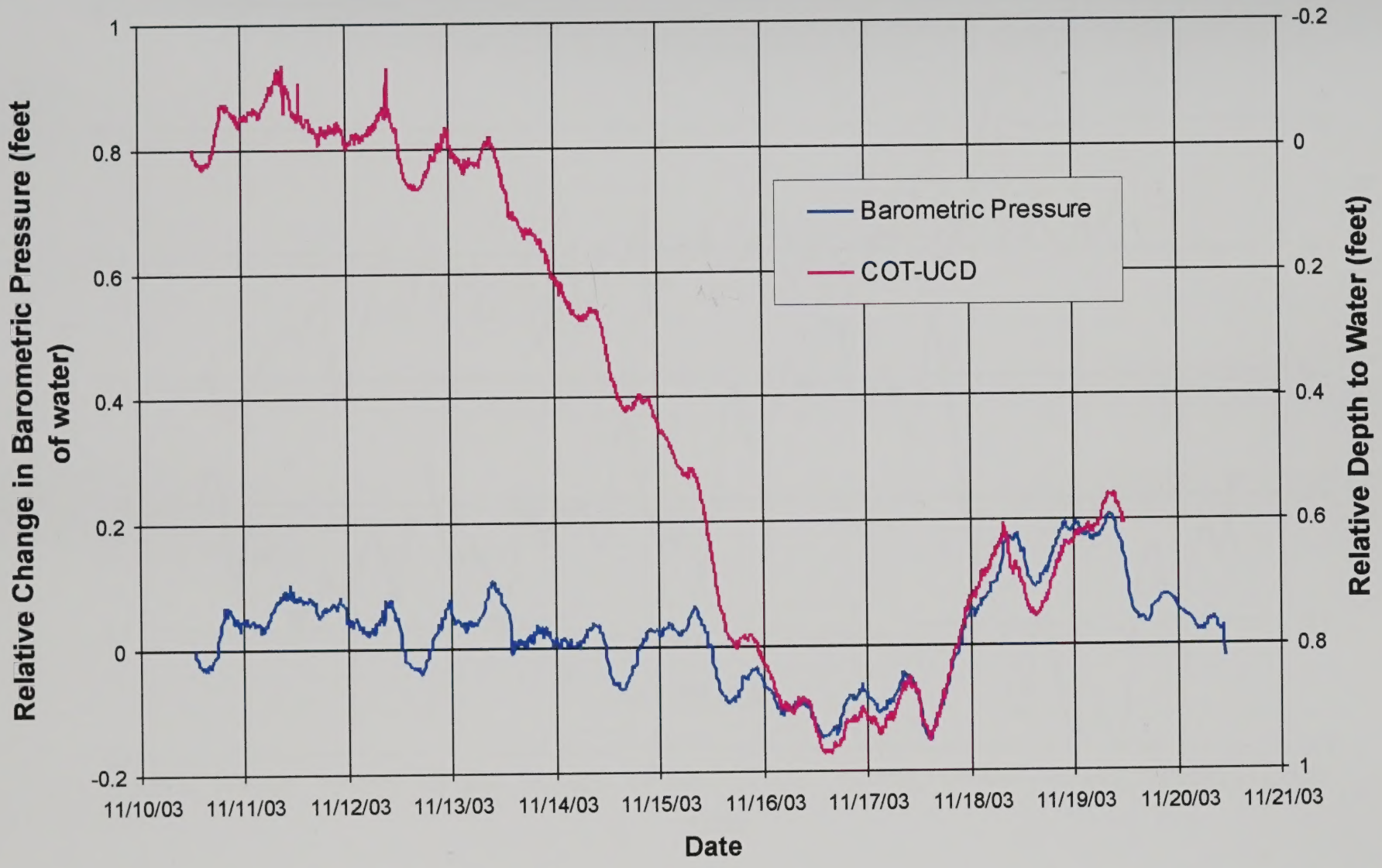

DS&A
David Schafer & Associates

COMPARISON OF BAROMETRIC PRESSURE AND COT-UDC HYDROGRAPH - LATE DATA

SAN PEDRO RIVER BASIN AQUIFER TEST
SIERRA VISTA, ARIZONA

FIGURE
5

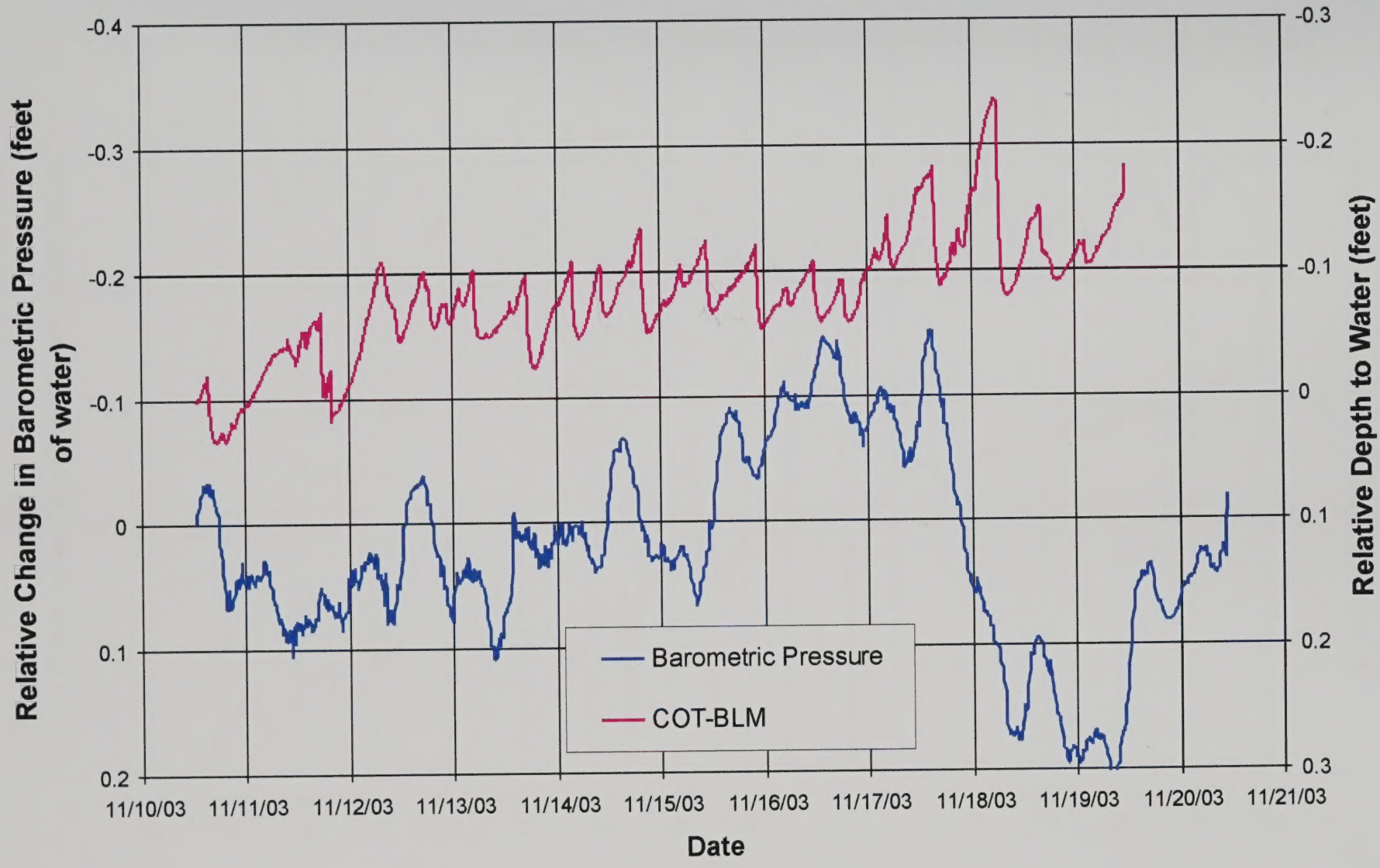

David Schafer & Associates

COMPARISON OF BAROMETRIC PRESSURE AND COT-BLM HYDROGRAPH

SAN PEDRO RIVER BASIN AQUIFER TEST
SIERRA VISTA, ARIZONA

FIGURE
6

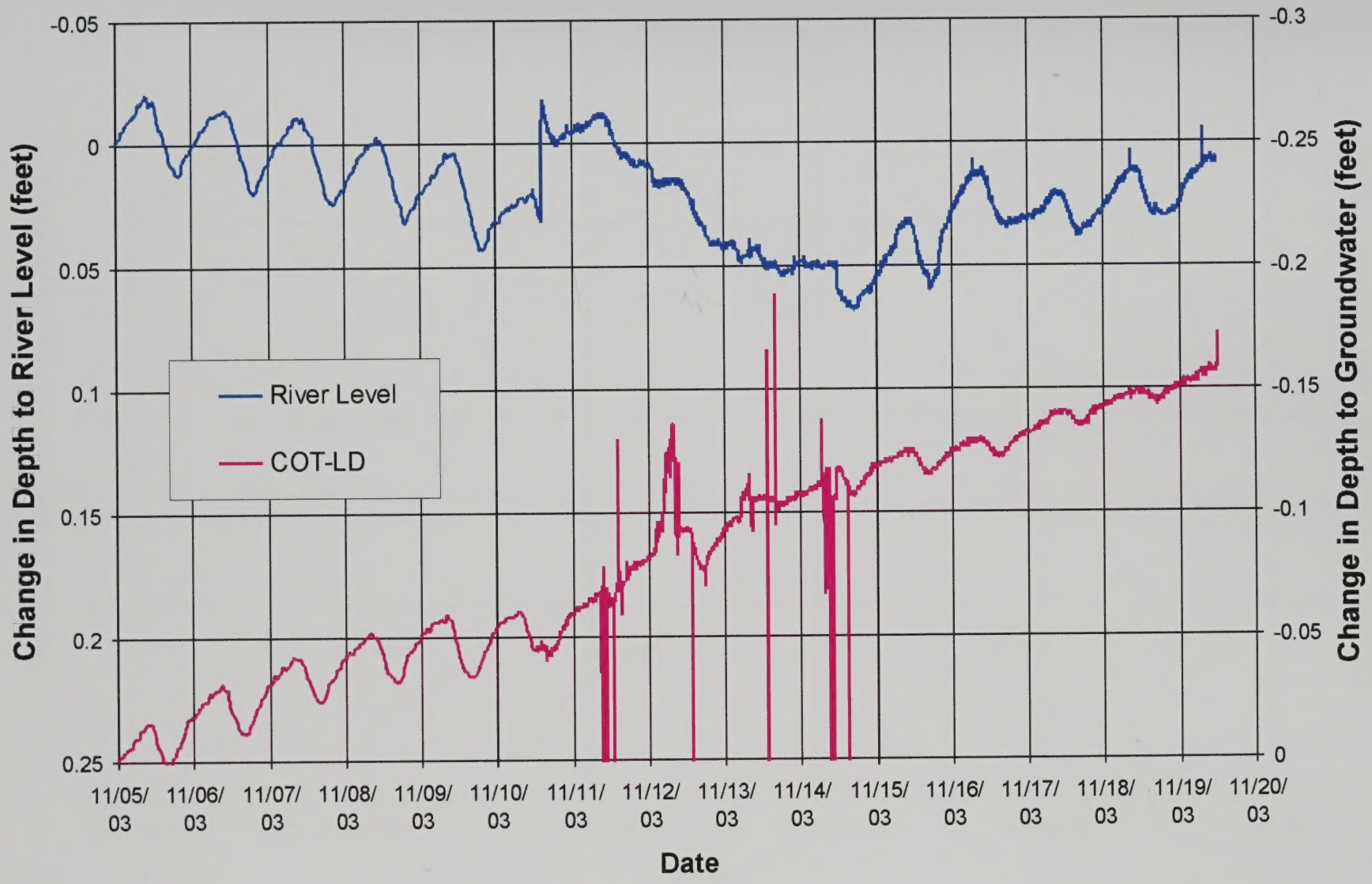

DS&A
David Schafer & Associates

COMPARISON OF CHANGES IN SAN PEDRO RIVER LEVELS AND COT-LD HYDROGRAPH

SAN PEDRO RIVER BASIN AQUIFER TEST
SIERRA VISTA, ARIZONA

FIGURE
7

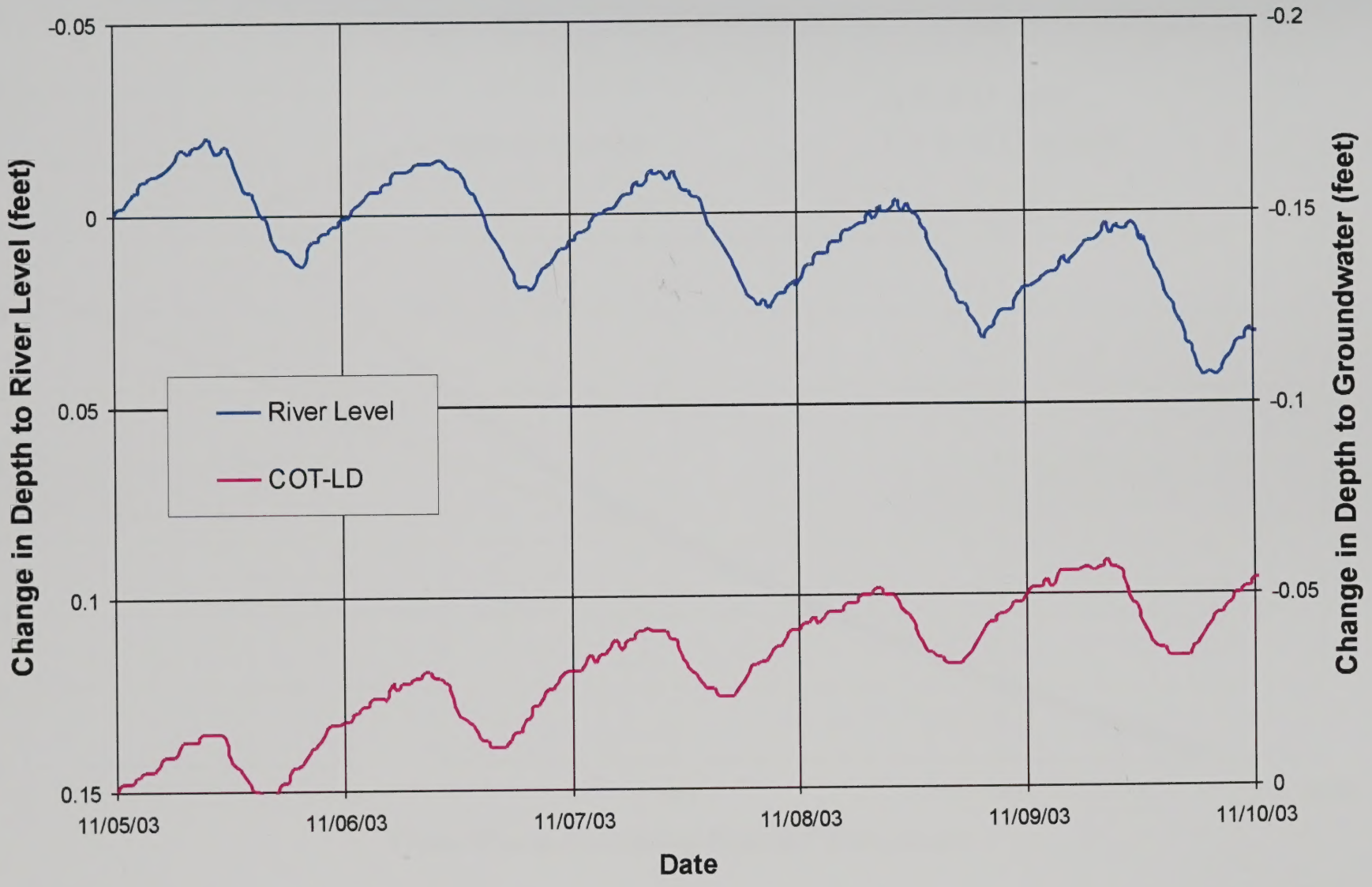

DS&A
David Schafer & Associates

COMPARISON OF CHANGES IN SAN PEDRO RIVER LEVELS AND COT-LD HYDROGRAPH - EXPANDED VIEW

SAN PEDRO RIVER BASIN AQUIFER TEST
SIERRA VISTA, ARIZONA

FIGURE
8

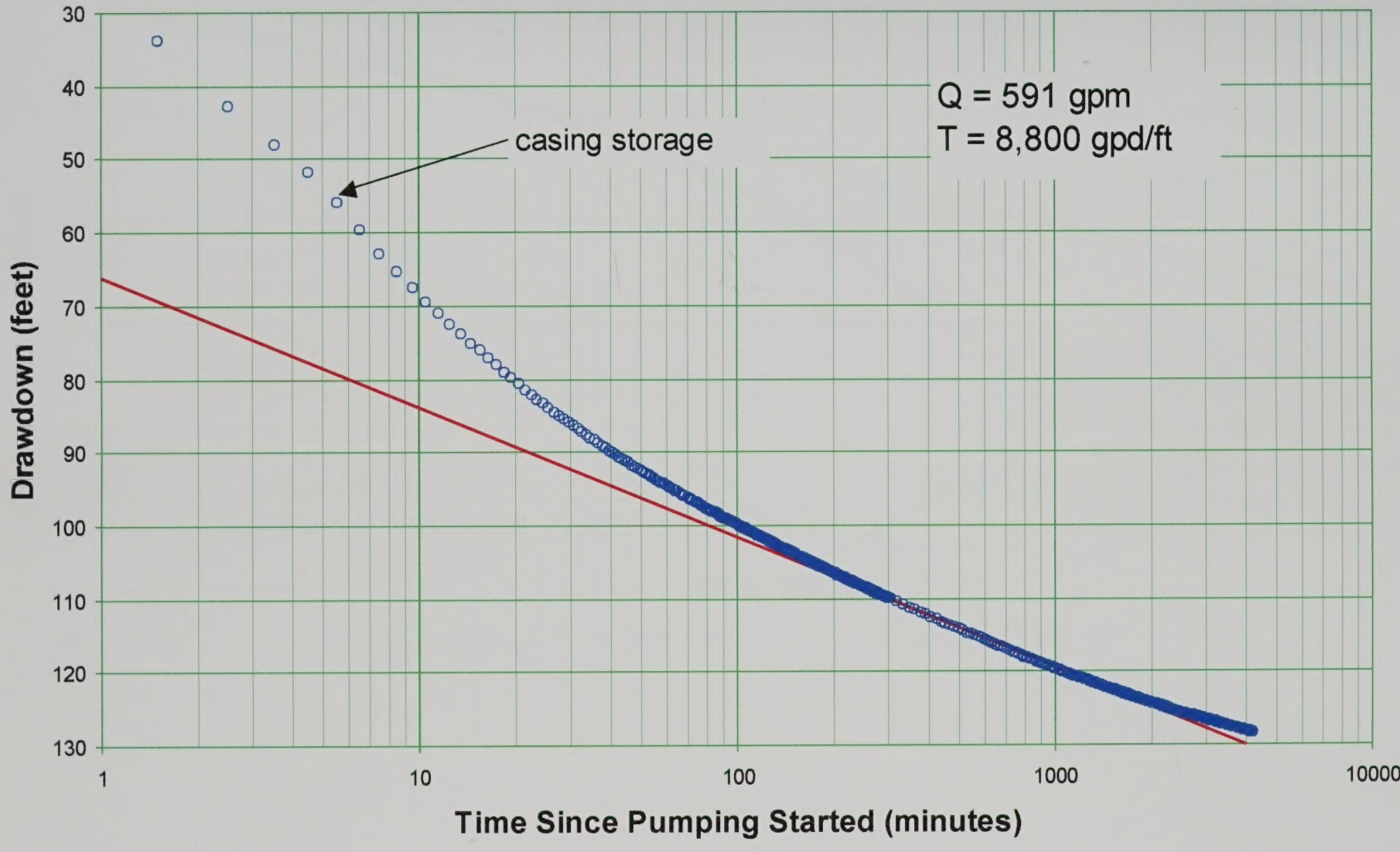

David Schafer & Associates

PUMPED WELL DRAWDOWN DATA

SAN PEDRO RIVER BASIN AQUIFER TEST
SIERRA VISTA, ARIZONA

FIGURE
9

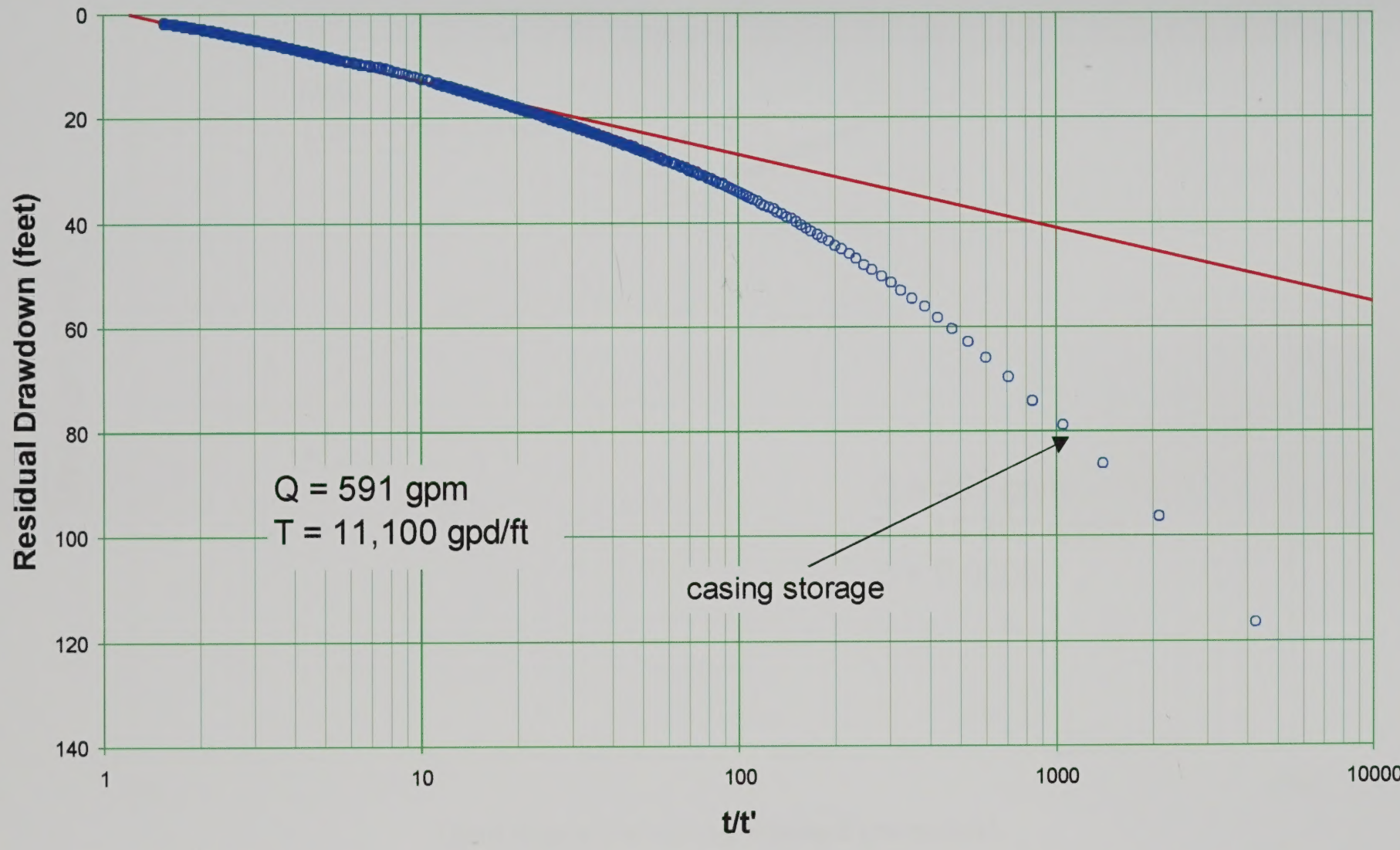

DS&A
David Schafer & Associates

PUMPED WELL RECOVERY

SAN PEDRO RIVER BASIN AQUIFER TEST
SIERRA VISTA, ARIZONA

FIGURE
10

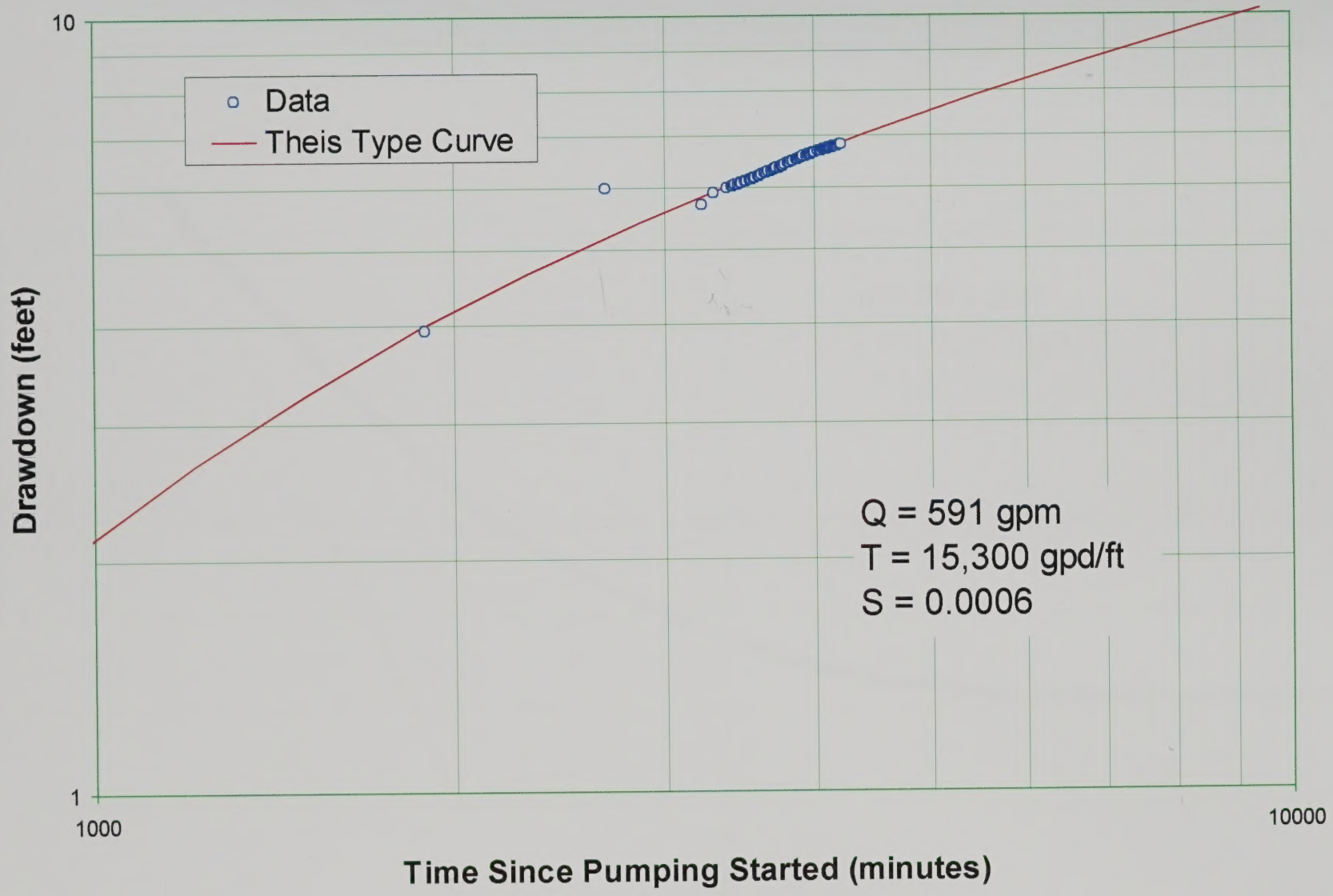

DS&A
David Schafer & Associates

LOG-LOG PLOT OF SOUTH WELL DRAWDOWN

SAN PEDRO RIVER BASIN AQUIFER TEST
SIERRA VISTA, ARIZONA

FIGURE
11

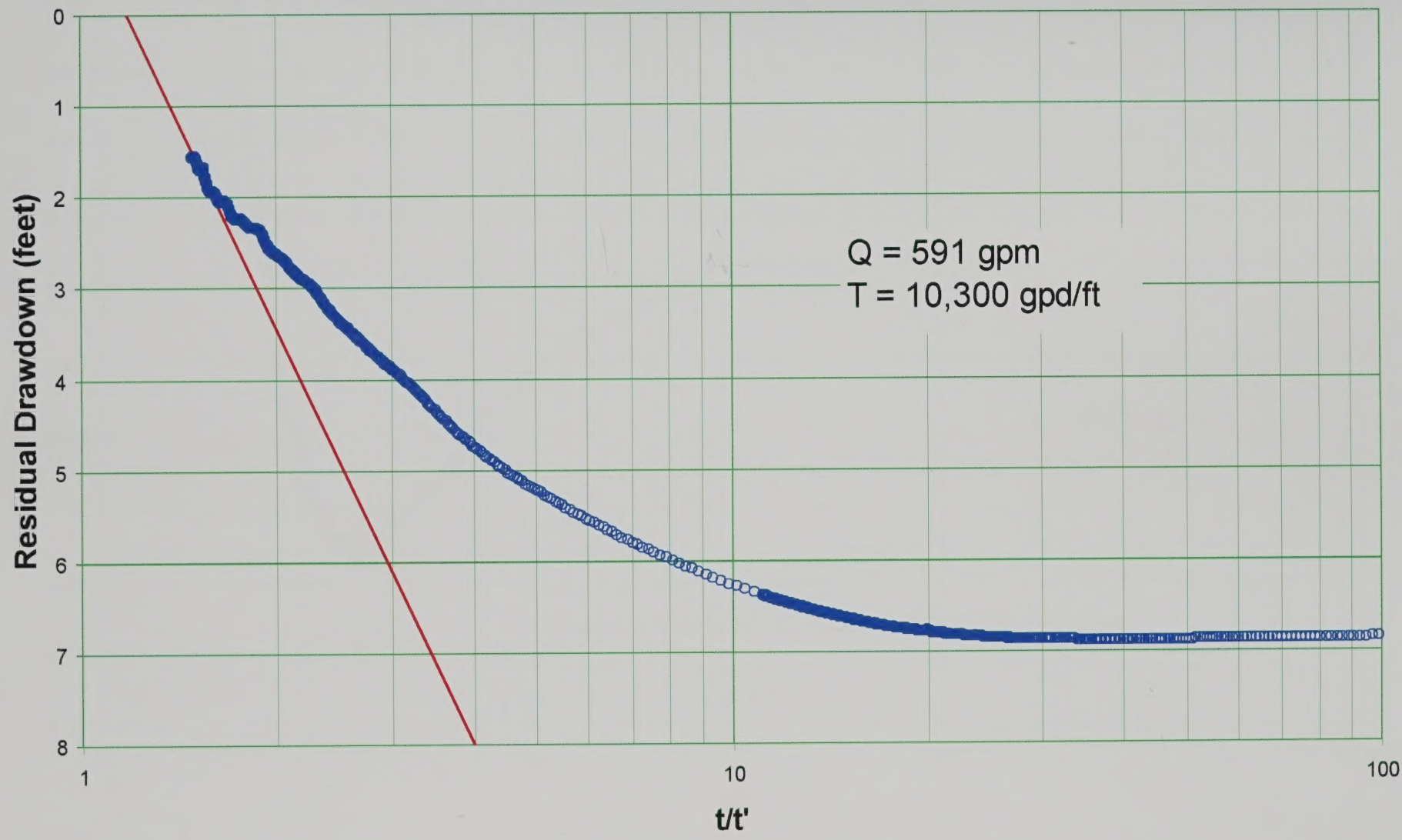

DS&A
David Schafer & Associates

SOUTH WELL RESIDUAL DRAWDOWN

SAN PEDRO RIVER BASIN AQUIFER TEST
SIERRA VISTA, ARIZONA

FIGURE
12

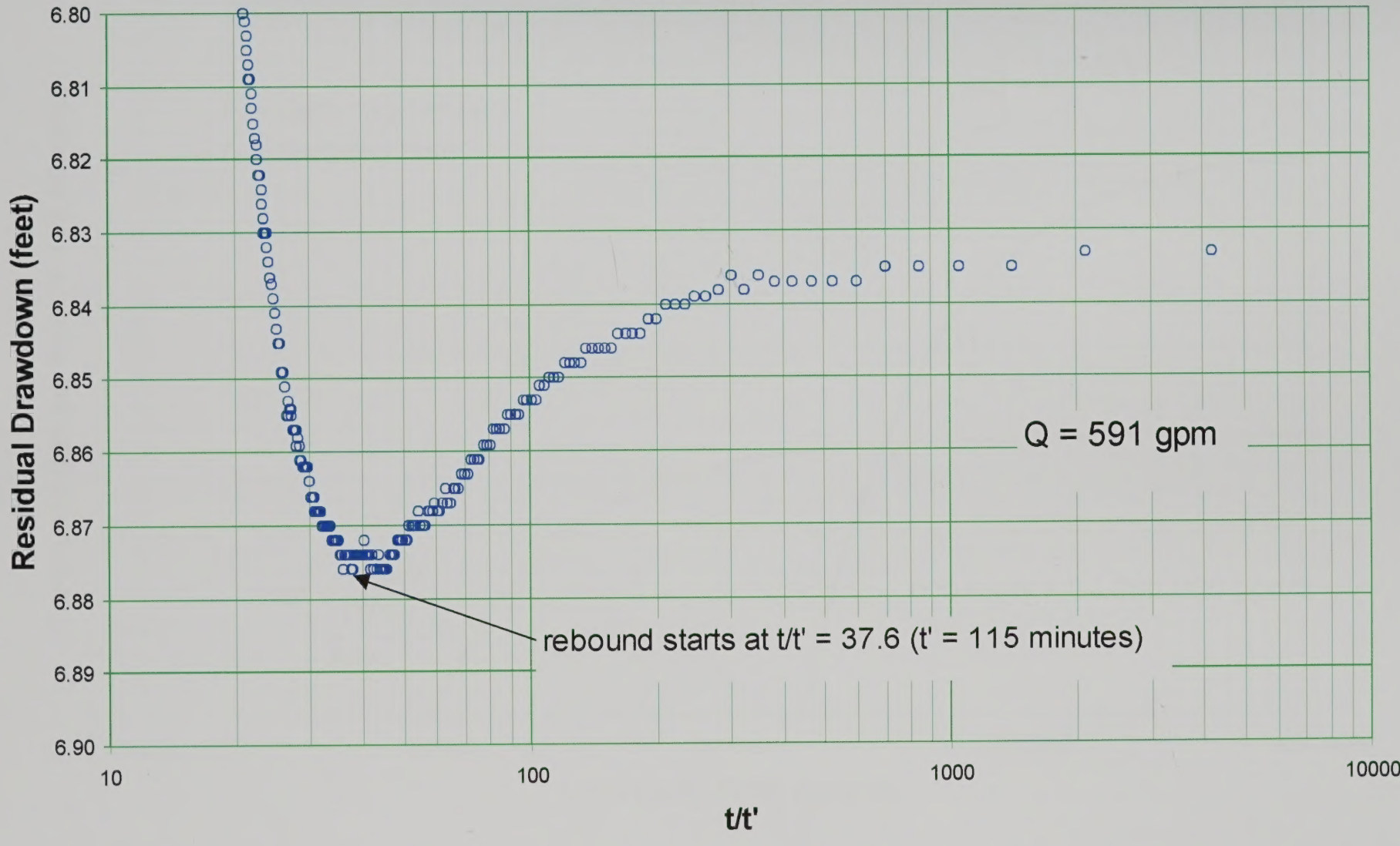

DS&A
David Schafer & Associates

SOUTH WELL RESIDUAL DRAWDOWN - EXPANDED VIEW

SAN PEDRO RIVER BASIN AQUIFER TEST
SIERRA VISTA, ARIZONA

FIGURE
13

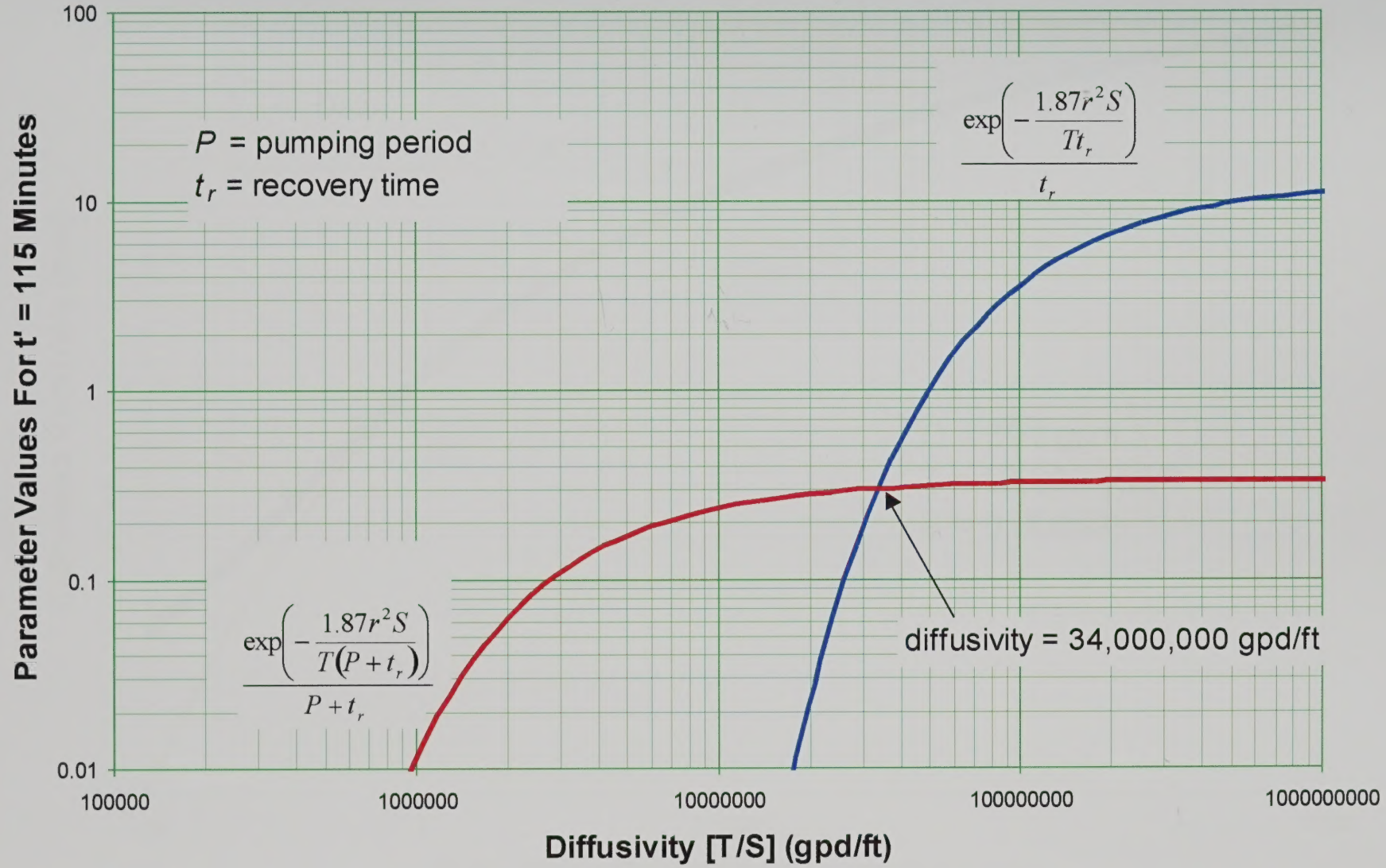

DS&A
David Schafer & Associates

DRAWDOWN DERIVATIVES FOR SOUTH WELL

SAN PEDRO RIVER BASIN AQUIFER TEST
SIERRA VISTA, ARIZONA

FIGURE
14

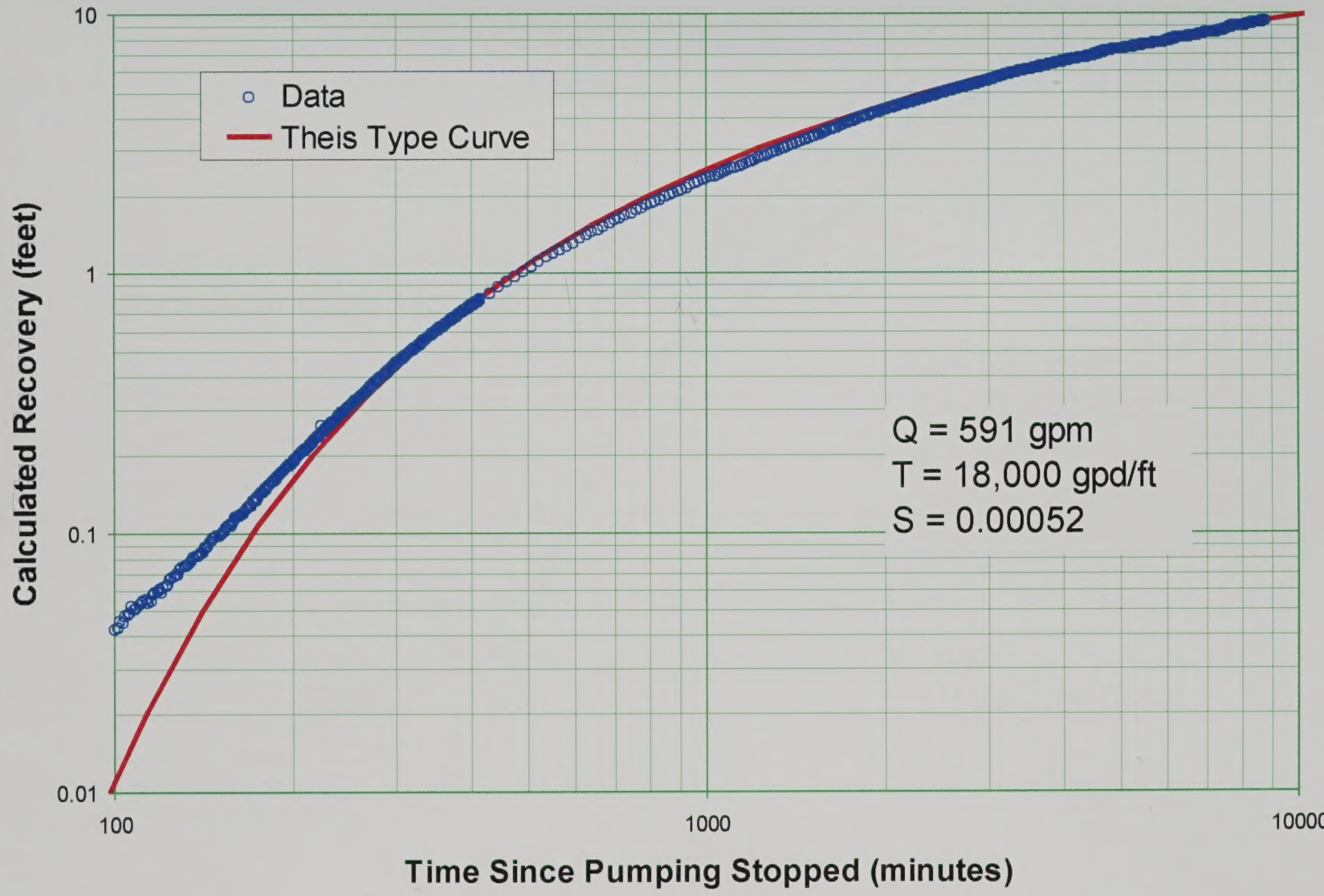

DS&A
David Schafer & Associates

SOUTH WELL CALCULATED RECOVERY

SAN PEDRO RIVER BASIN AQUIFER TEST
SIERRA VISTA, ARIZONA

FIGURE
15

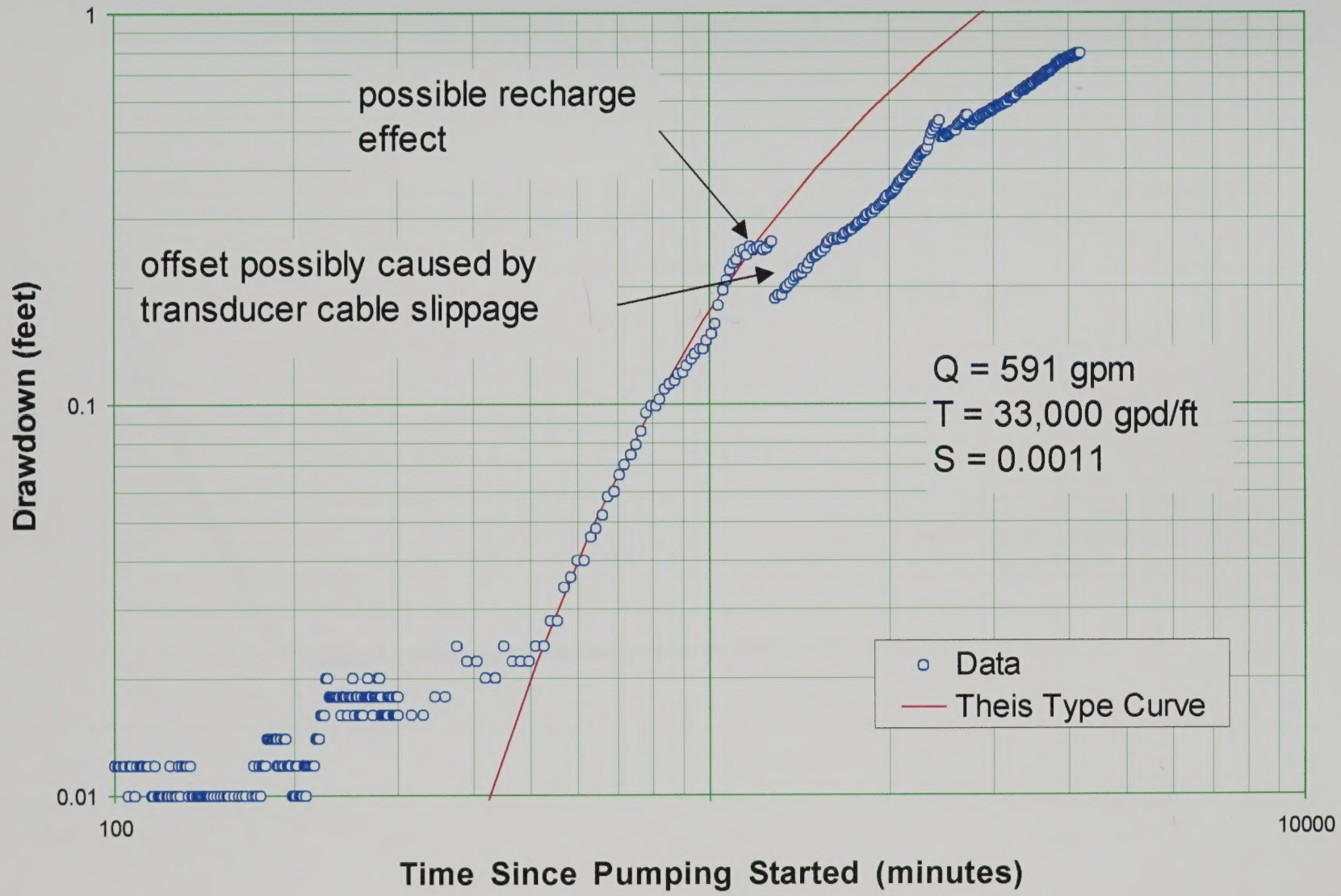

David Schafer & Associates

LOG-LOG PLOT OF NORTH WELL DRAWDOWN

SAN PEDRO RIVER BASIN AQUIFER TEST
SIERRA VISTA, ARIZONA

FIGURE
16

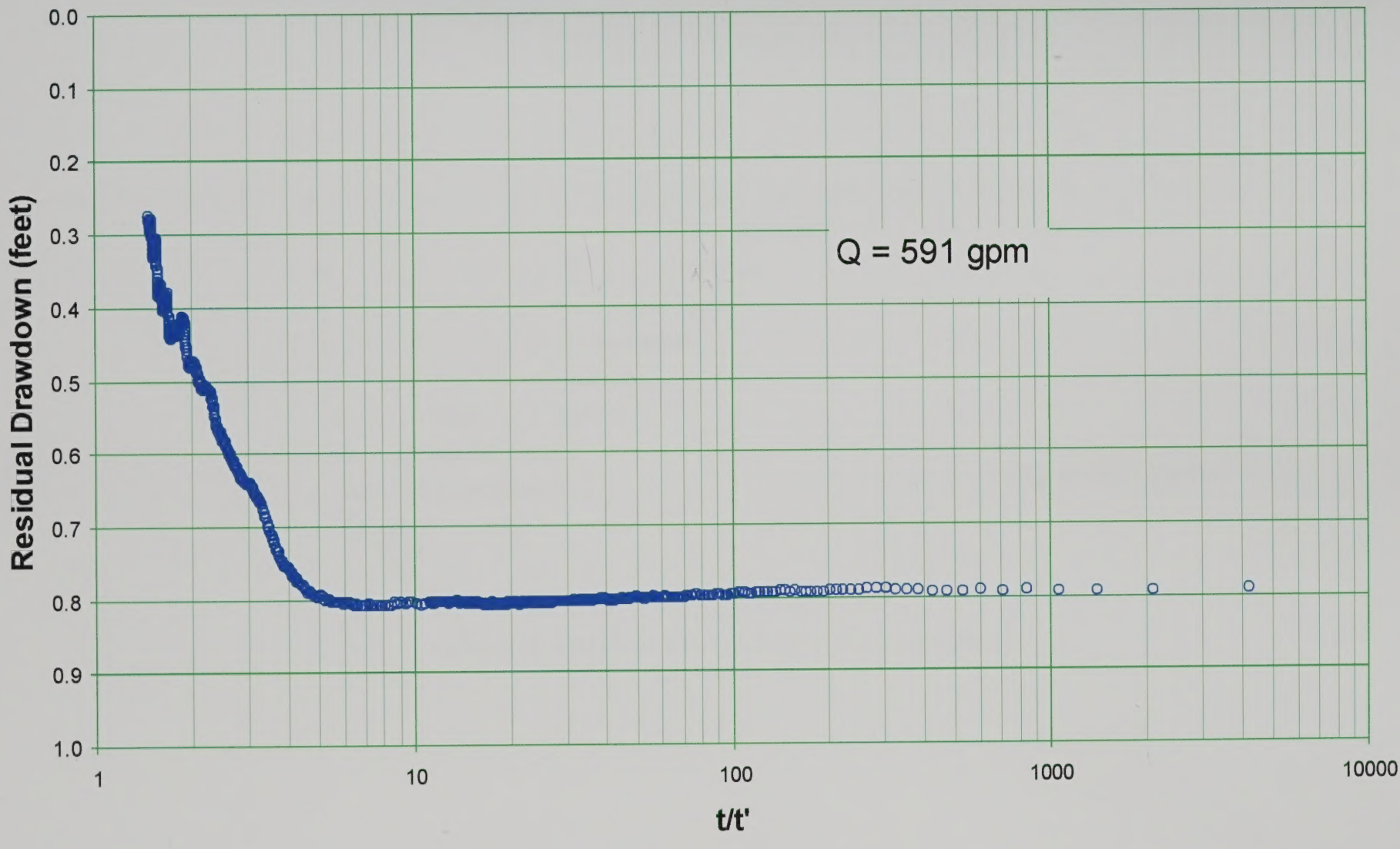

DS&A
David Schafer & Associates

NORTH WELL RESIDUAL DRAWDOWN

SAN PEDRO RIVER BASIN AQUIFER TEST
SIERRA VISTA, ARIZONA

FIGURE
17

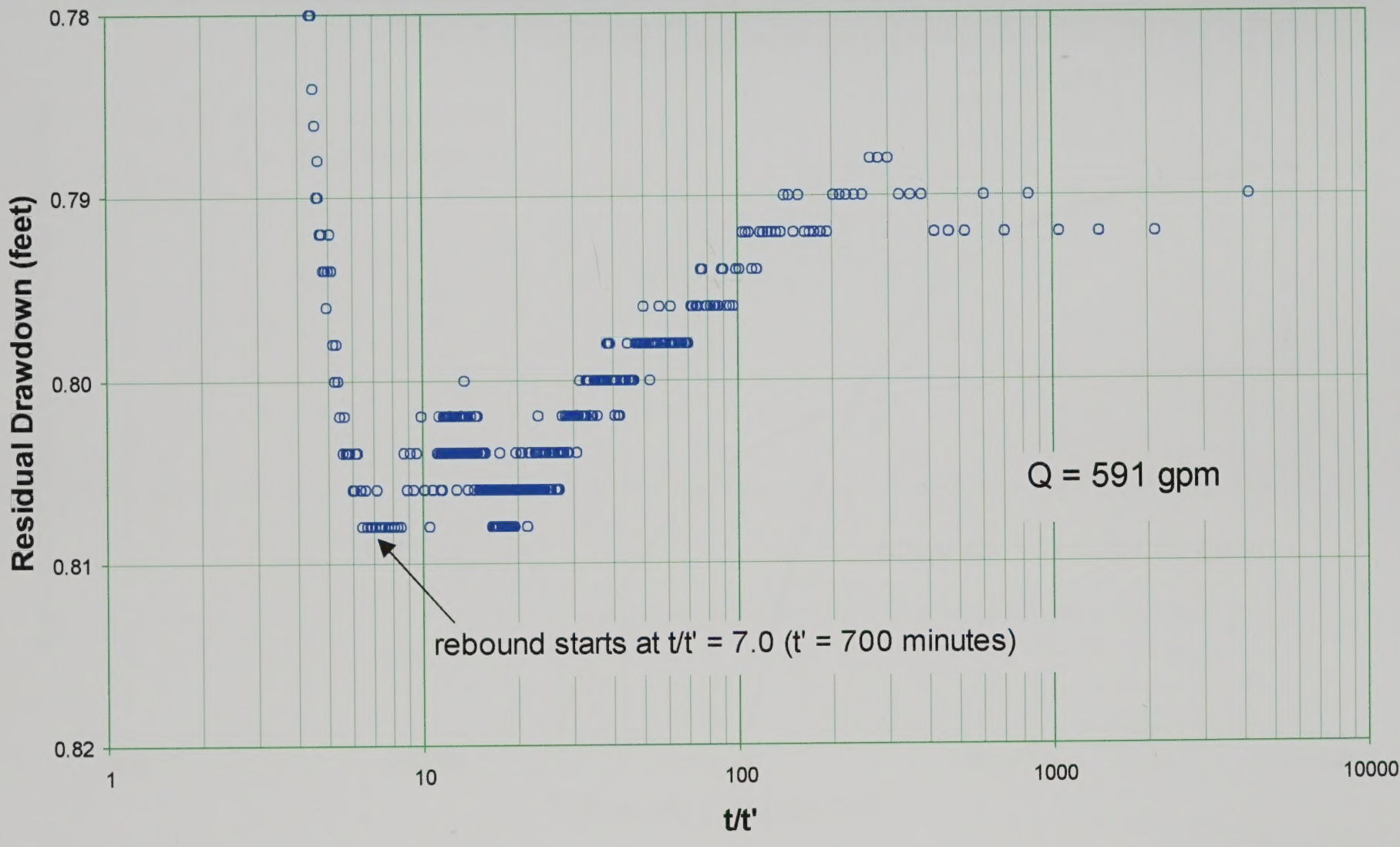

DS&A
David Schafer & Associates

NORTH WELL RESIDUAL DRAWDOWN - EXPANDED VIEW

SAN PEDRO RIVER BASIN AQUIFER TEST
SIERRA VISTA, ARIZONA

FIGURE
18

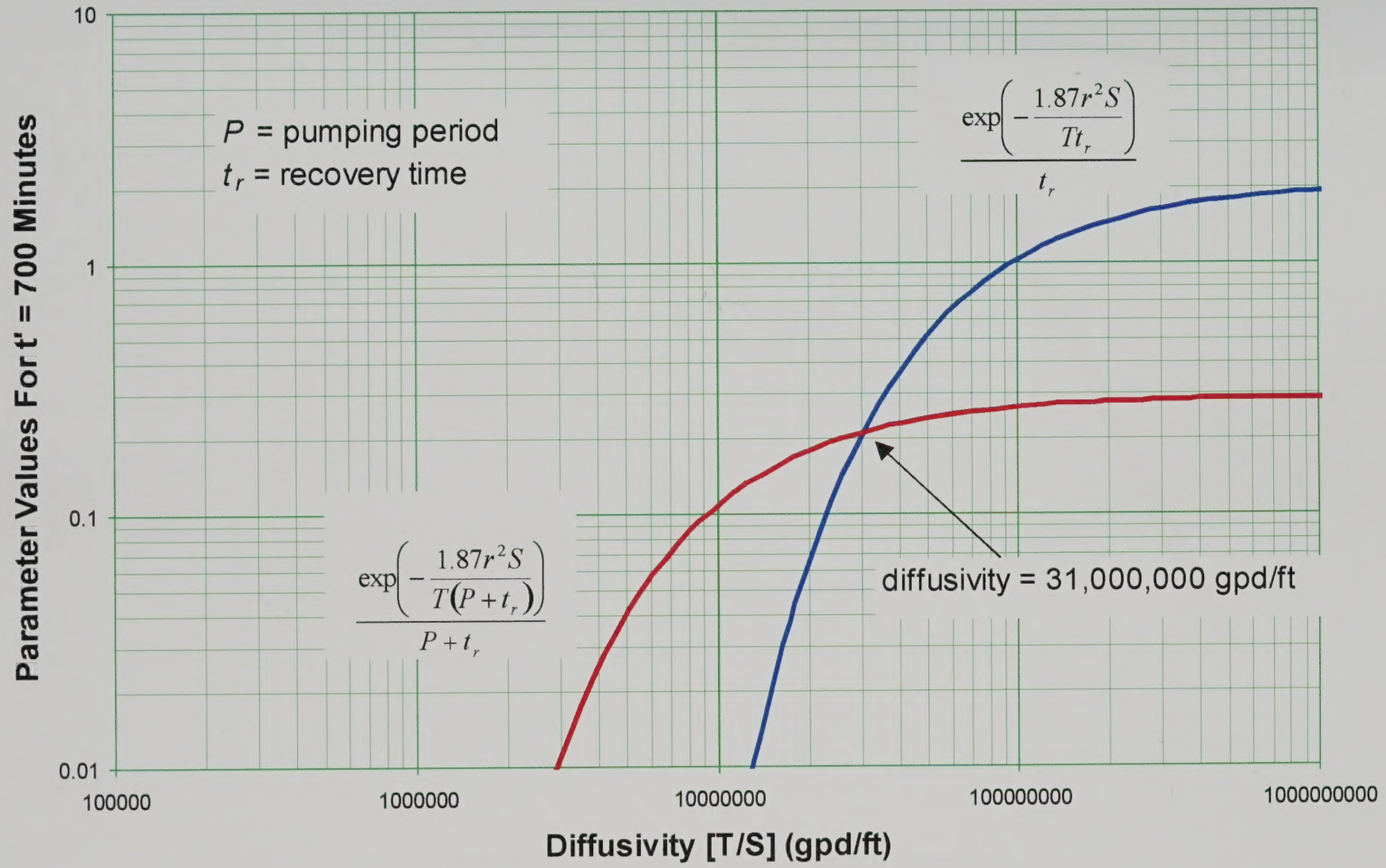

DS&A
David Schafer & Associates

DRAWDOWN DERIVATIVES FOR NORTH WELL

SAN PEDRO RIVER BASIN AQUIFER TEST
SIERRA VISTA, ARIZONA

FIGURE
19

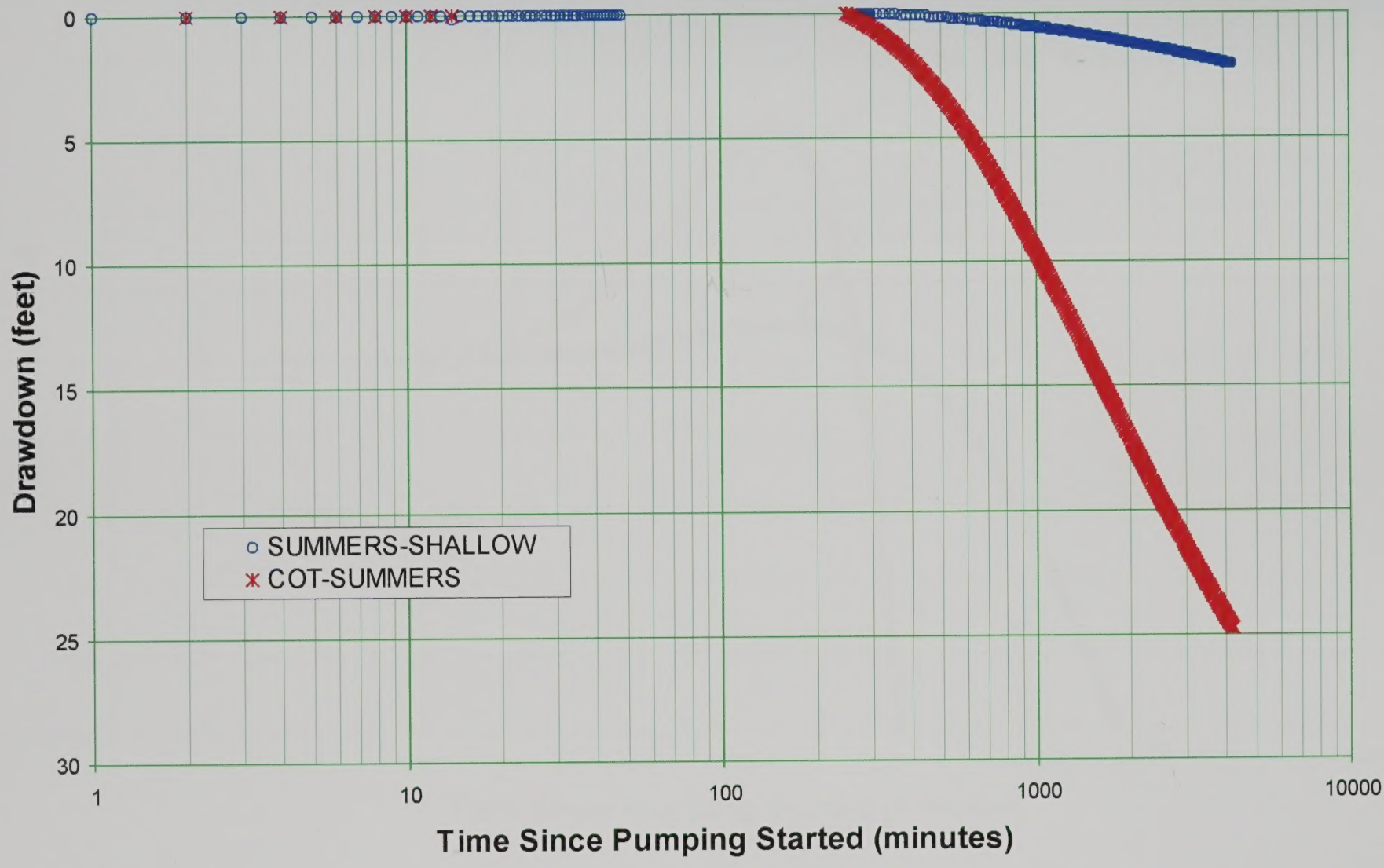

David Schafer & Associates

DRAWDOWN FOR SUMMERS WELL PAIR

SAN PEDRO RIVER BASIN AQUIFER TEST
SIERRA VISTA, ARIZONA

FIGURE
20

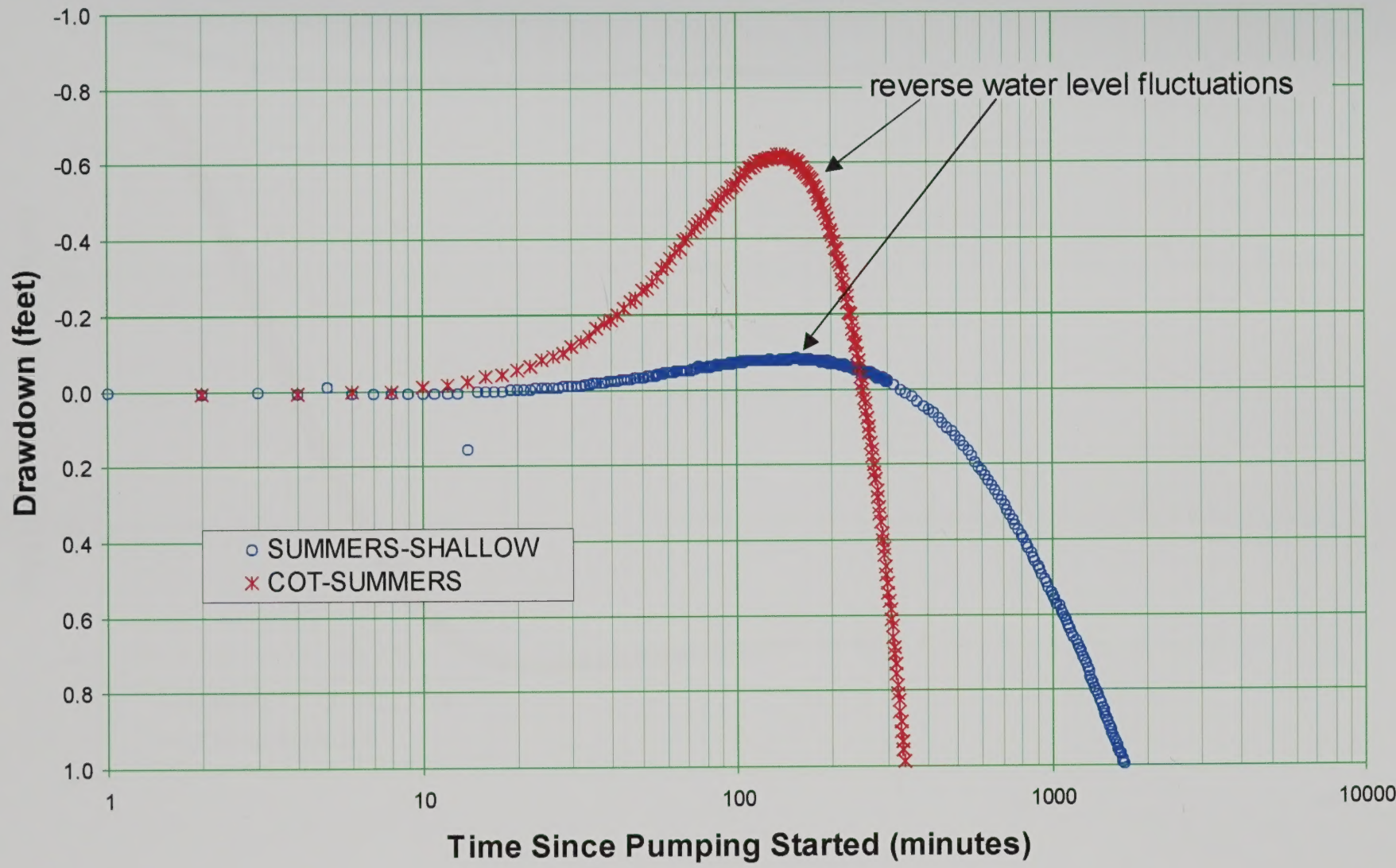

DS&A
David Schafer & Associates

DRAWDOWN FOR SUMMERS WELL PAIR - EXPANDED VIEW

SAN PEDRO RIVER BASIN AQUIFER TEST
SIERRA VISTA, ARIZONA

FIGURE
21

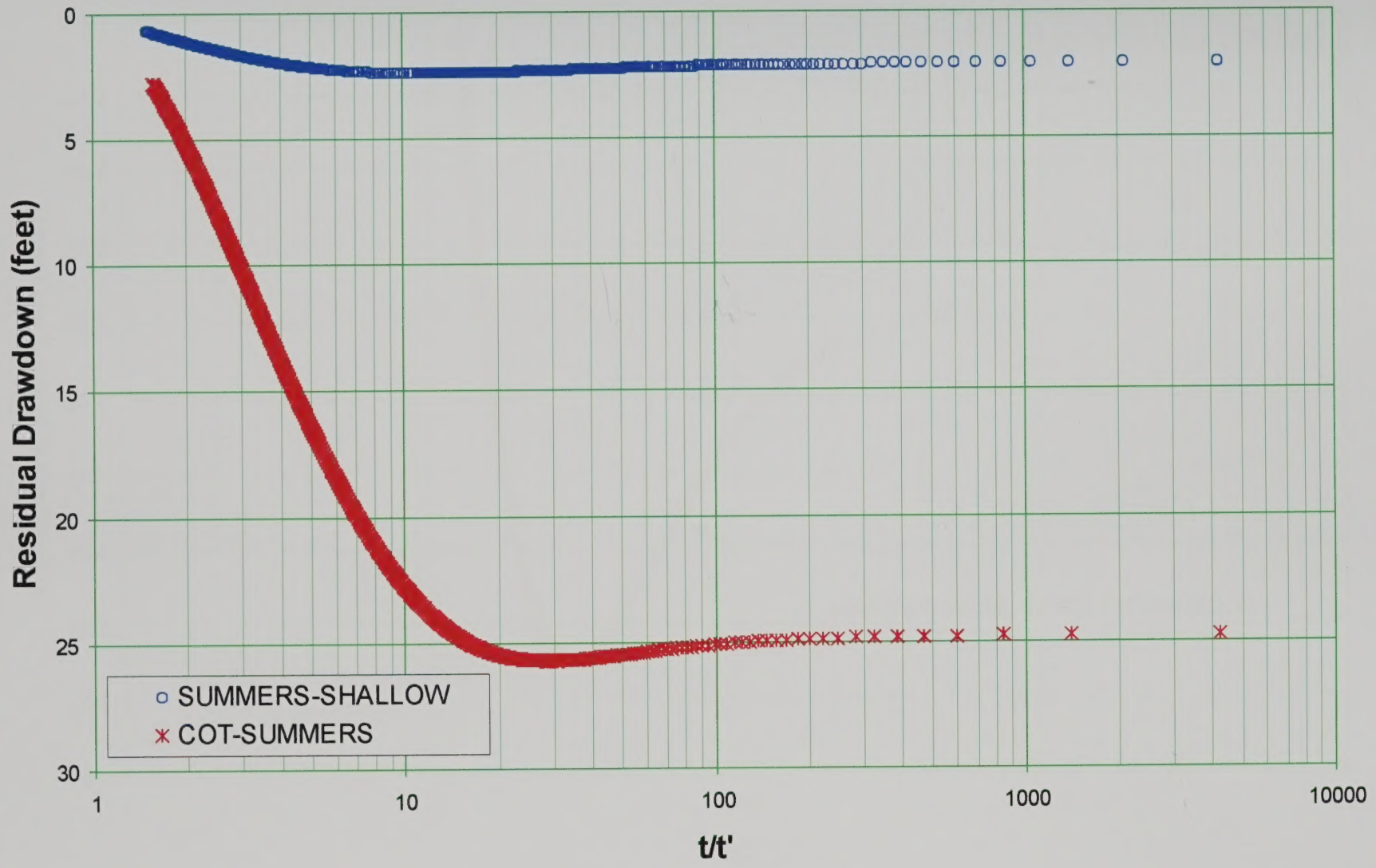

David Schafer & Associates

RECOVERY FOR SUMMERS WELL PAIR

SAN PEDRO RIVER BASIN AQUIFER TEST
SIERRA VISTA, ARIZONA

FIGURE
22

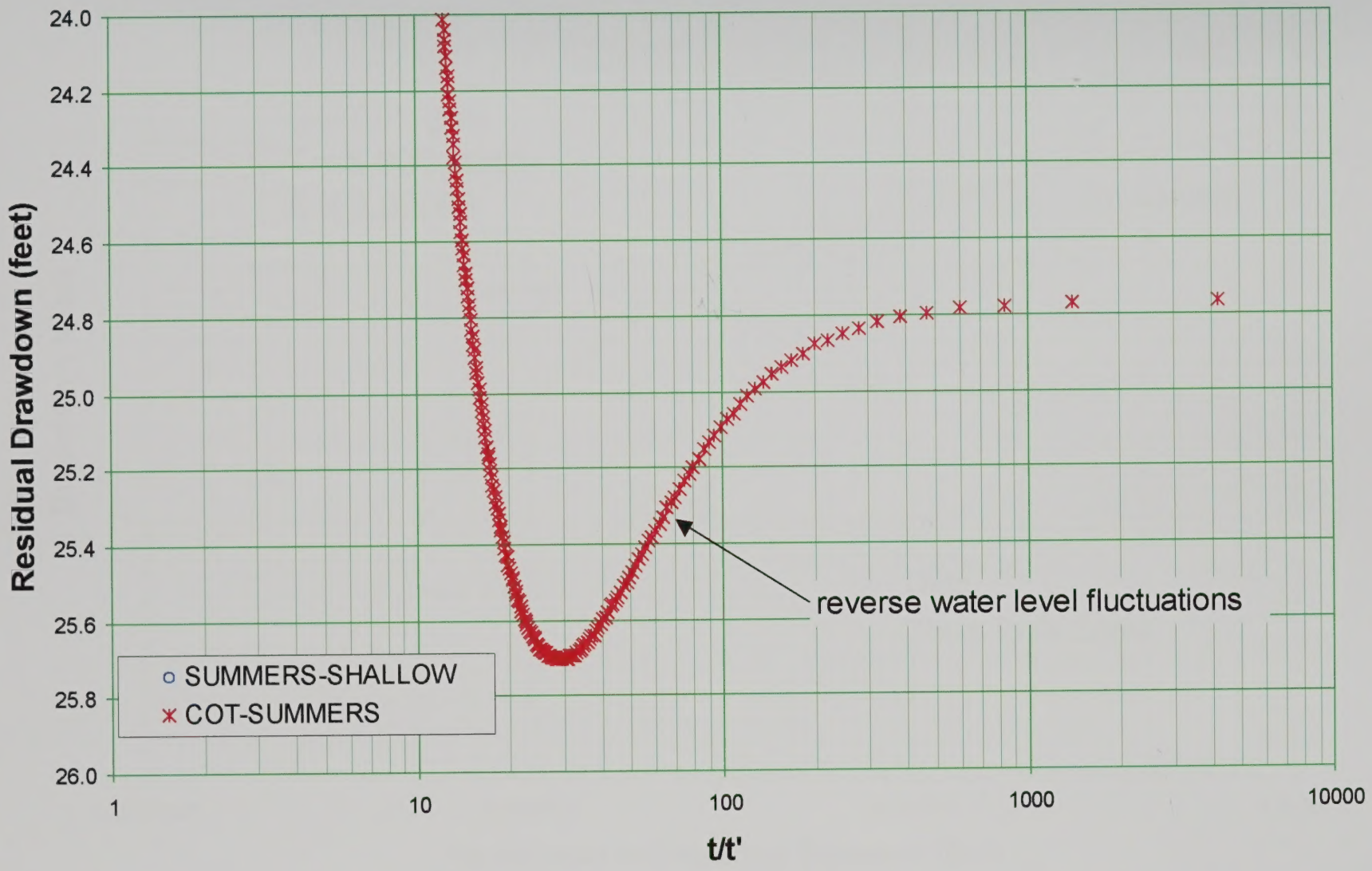

DS&A
David Schafer & Associates

RECOVERY FOR SUMMERS WELL PAIR - EXPANDED VIEW

SAN PEDRO RIVER BASIN AQUIFER TEST
SIERRA VISTA, ARIZONA

FIGURE
23

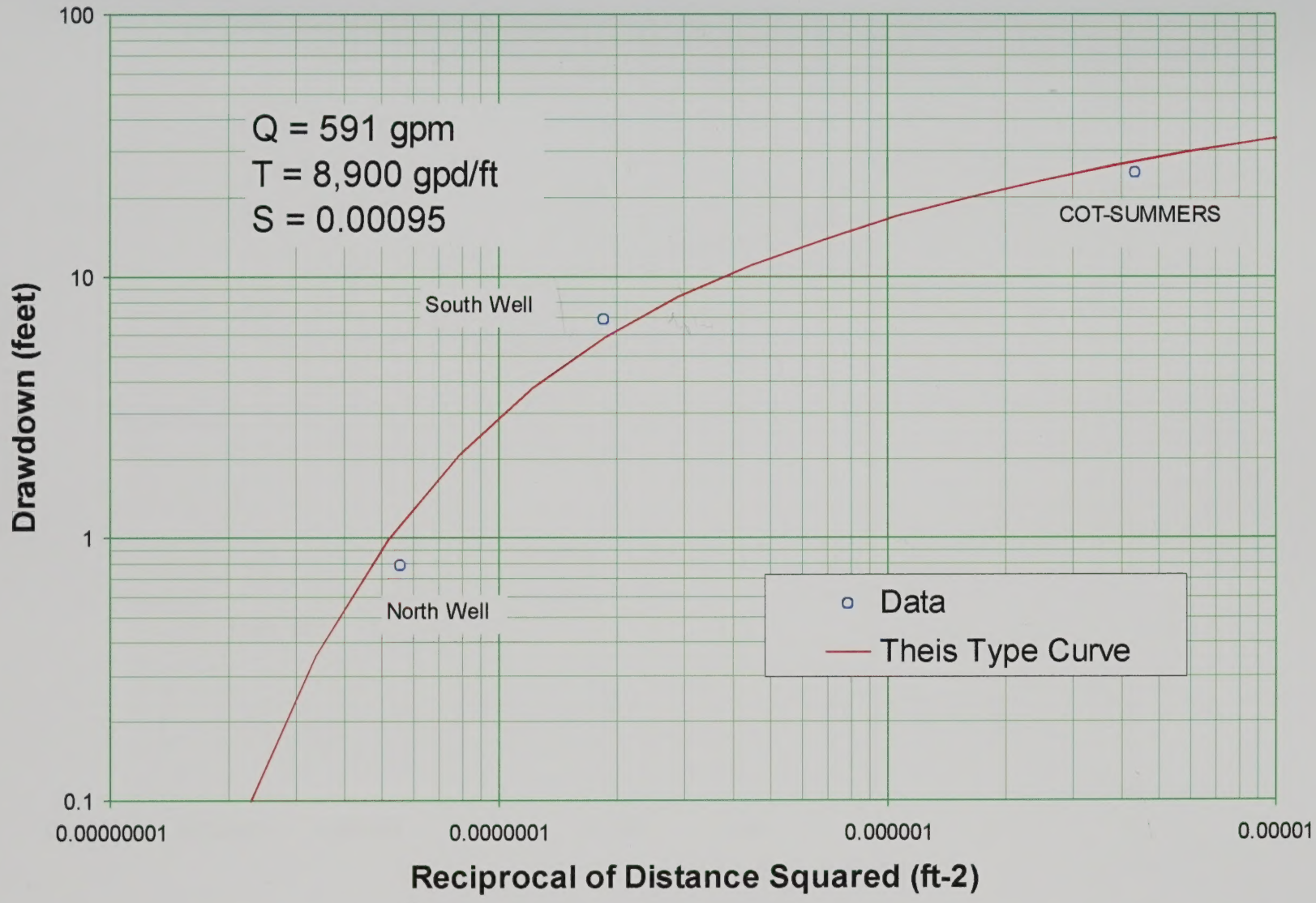

David Schafer & Associates

DISTANCE-DRAWDOWN GRAPH AT 4205 MINUTES

SAN PEDRO RIVER BASIN AQUIFER TEST
SIERRA VISTA, ARIZONA

FIGURE
24

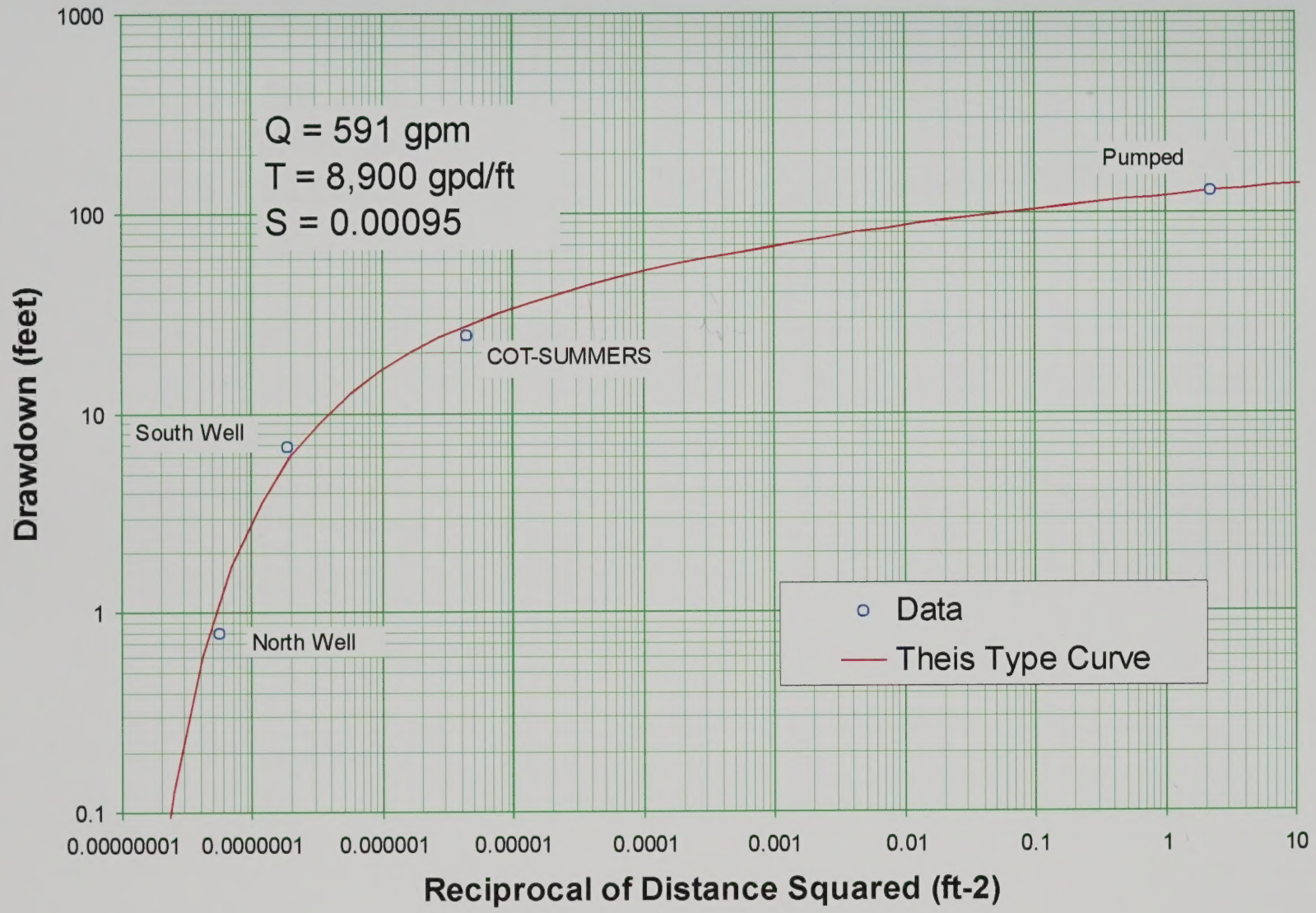

David Schafer & Associates

DISTANCE-DRAWDOWN GRAPH - EXPANDED SCALE

SAN PEDRO RIVER BASIN AQUIFER TEST
SIERRA VISTA, ARIZONA

FIGURE
25

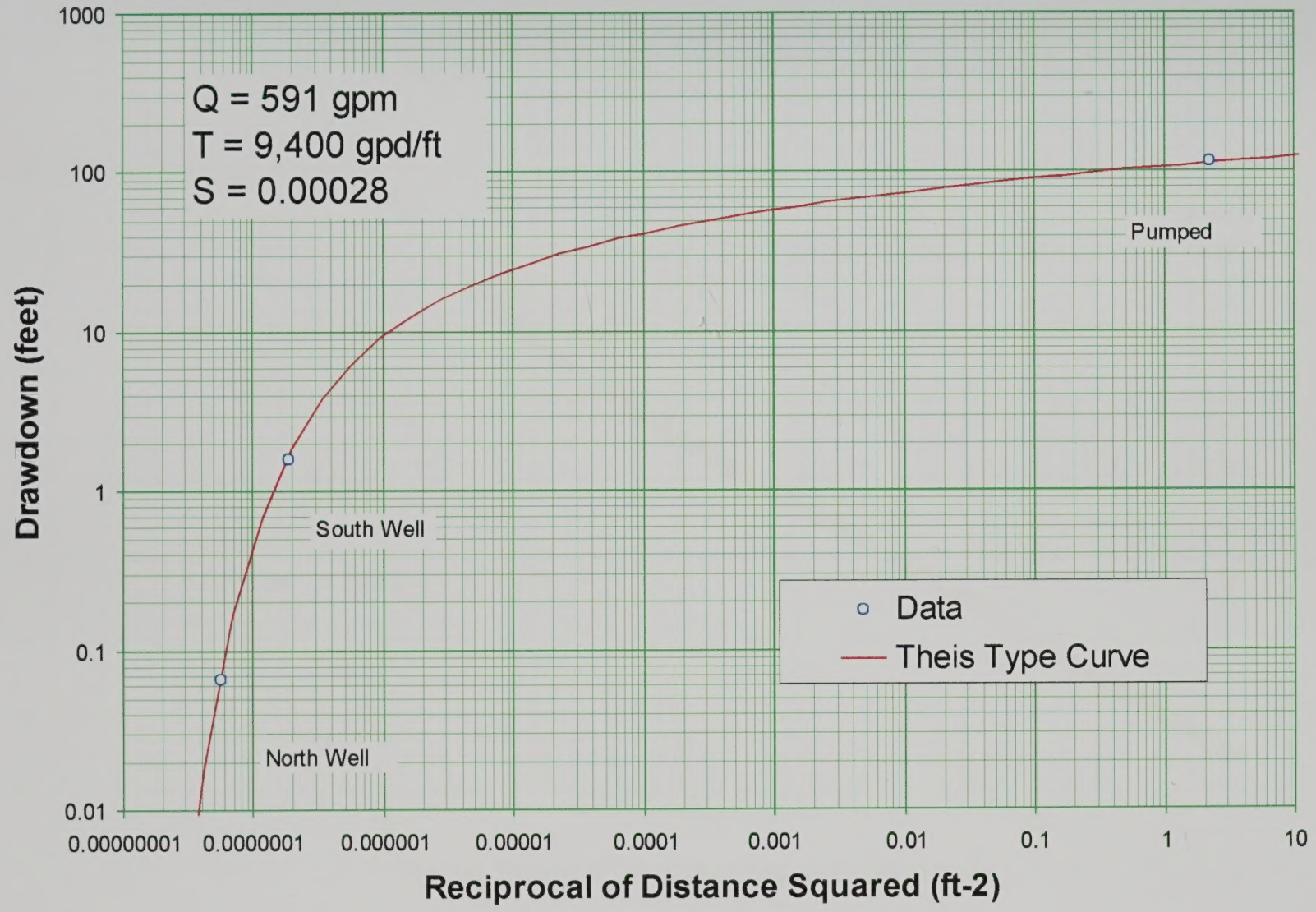

DS&A
David Schafer & Associates

DISTANCE-DRAWDOWN GRAPH AT 700 MINUTES

SAN PEDRO RIVER BASIN AQUIFER TEST
SIERRA VISTA, ARIZONA

FIGURE
26

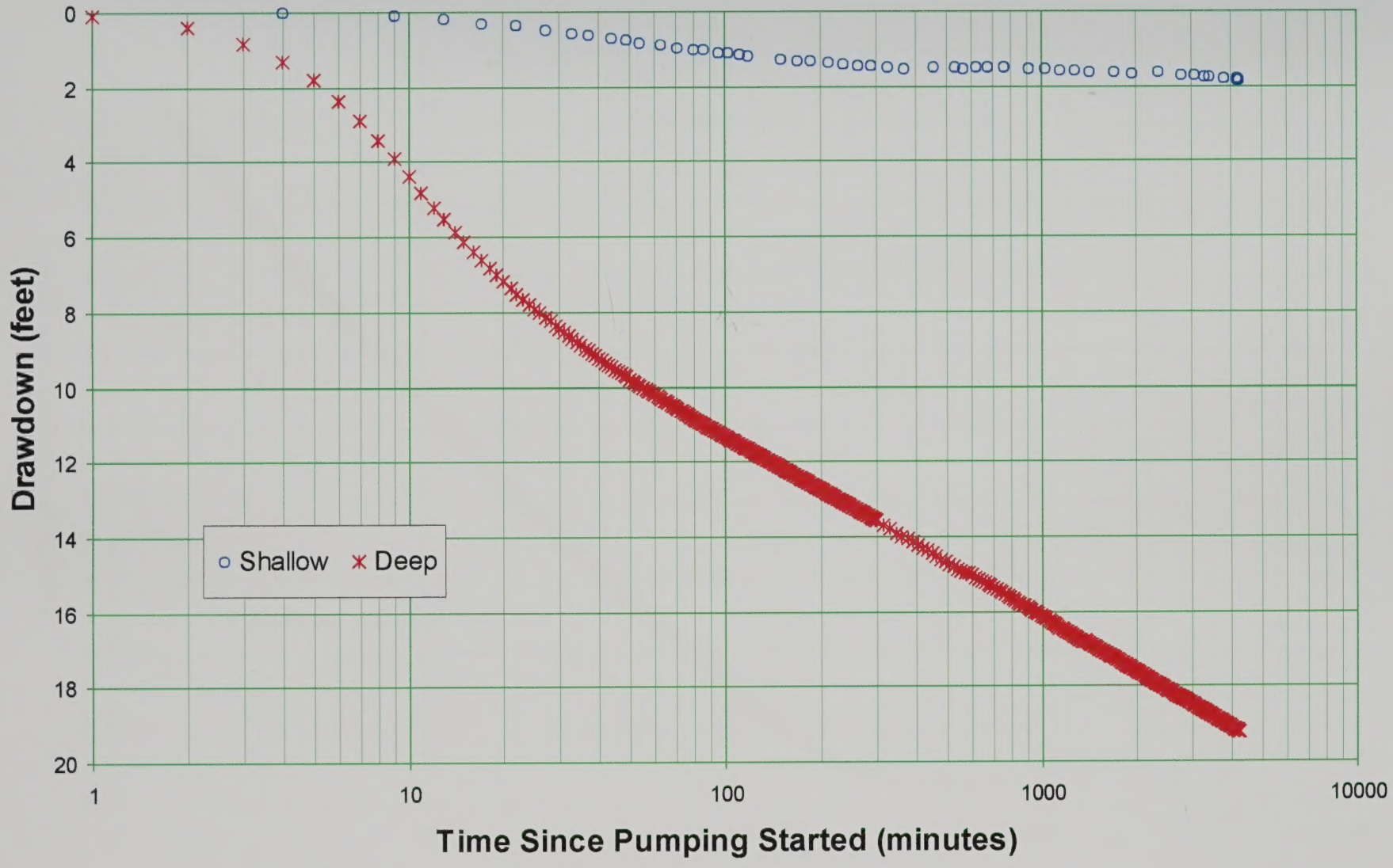

David Schafer & Associates

DRAWDOWN FOR SOUTH-20 WELL PAIR

SAN PEDRO RIVER BASIN AQUIFER TEST
SIERRA VISTA, ARIZONA

FIGURE
27

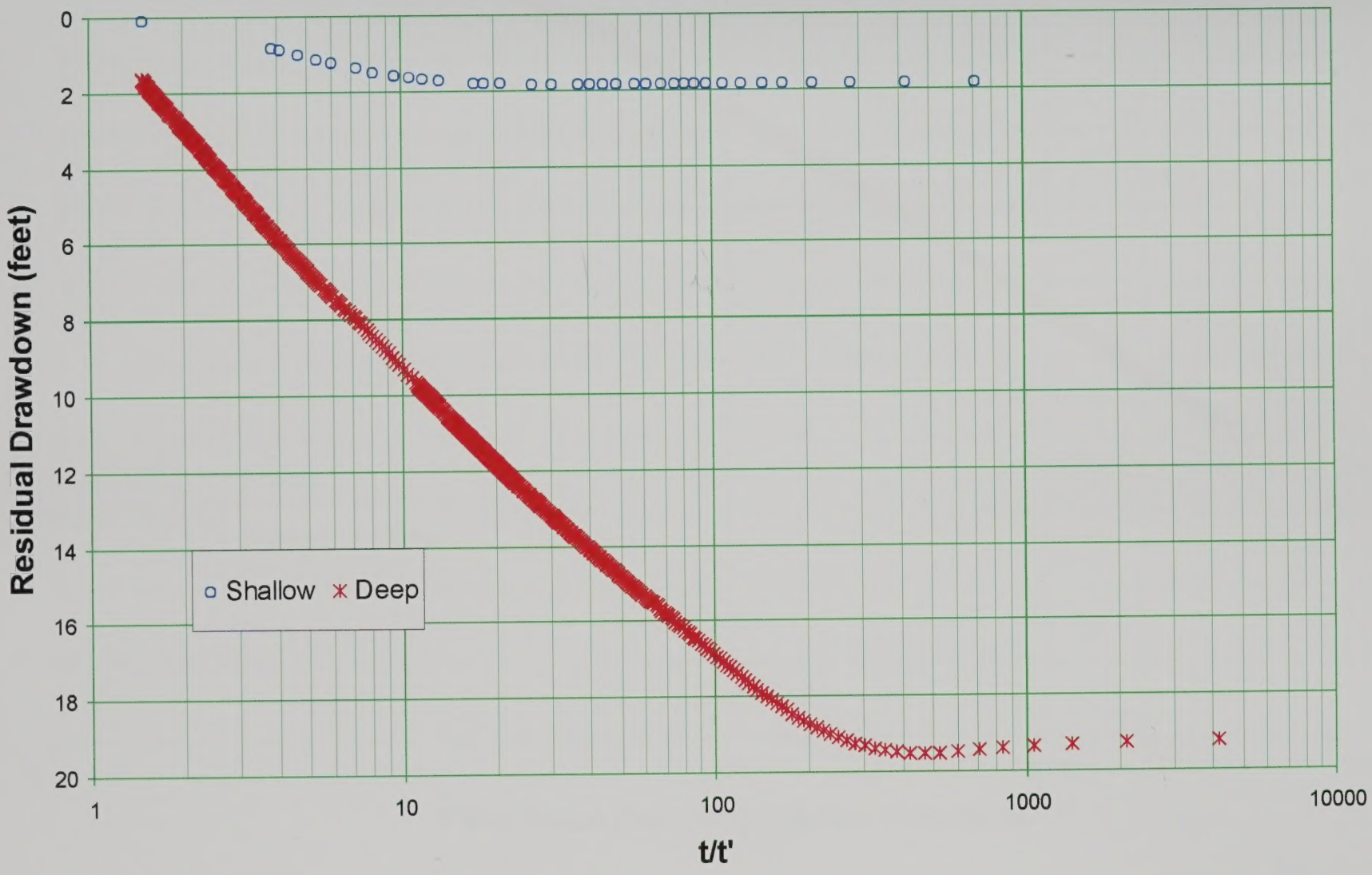

DS&A
David Schafer & Associates

RECOVERY FOR SOUTH-20 WELL PAIR

SAN PEDRO RIVER BASIN AQUIFER TEST
SIERRA VISTA, ARIZONA

FIGURE
28

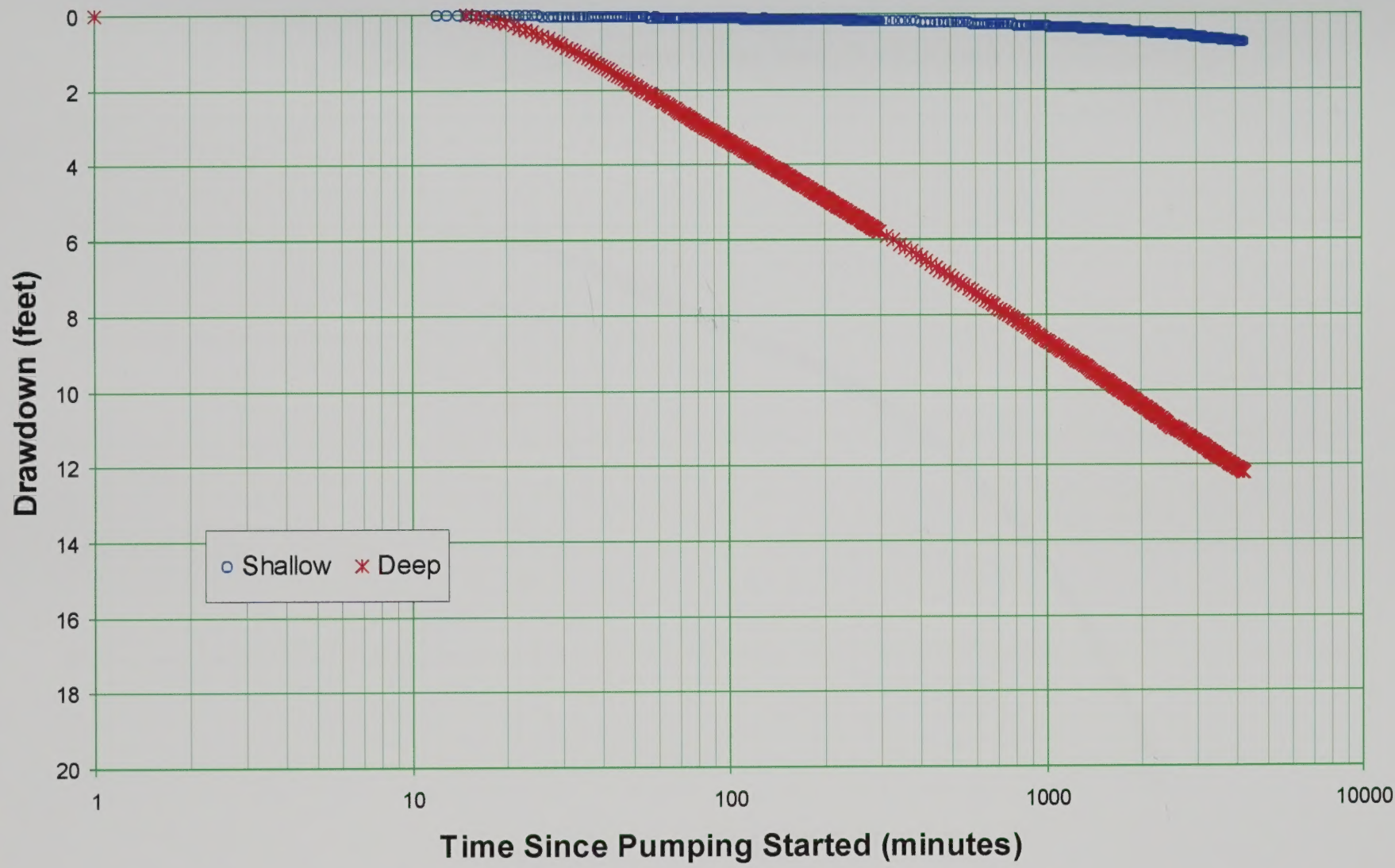

David Schafer & Associates

DRAWDOWN FOR SOUTH-50 WELL PAIR

SAN PEDRO RIVER BASIN AQUIFER TEST
SIERRA VISTA, ARIZONA

FIGURE
29

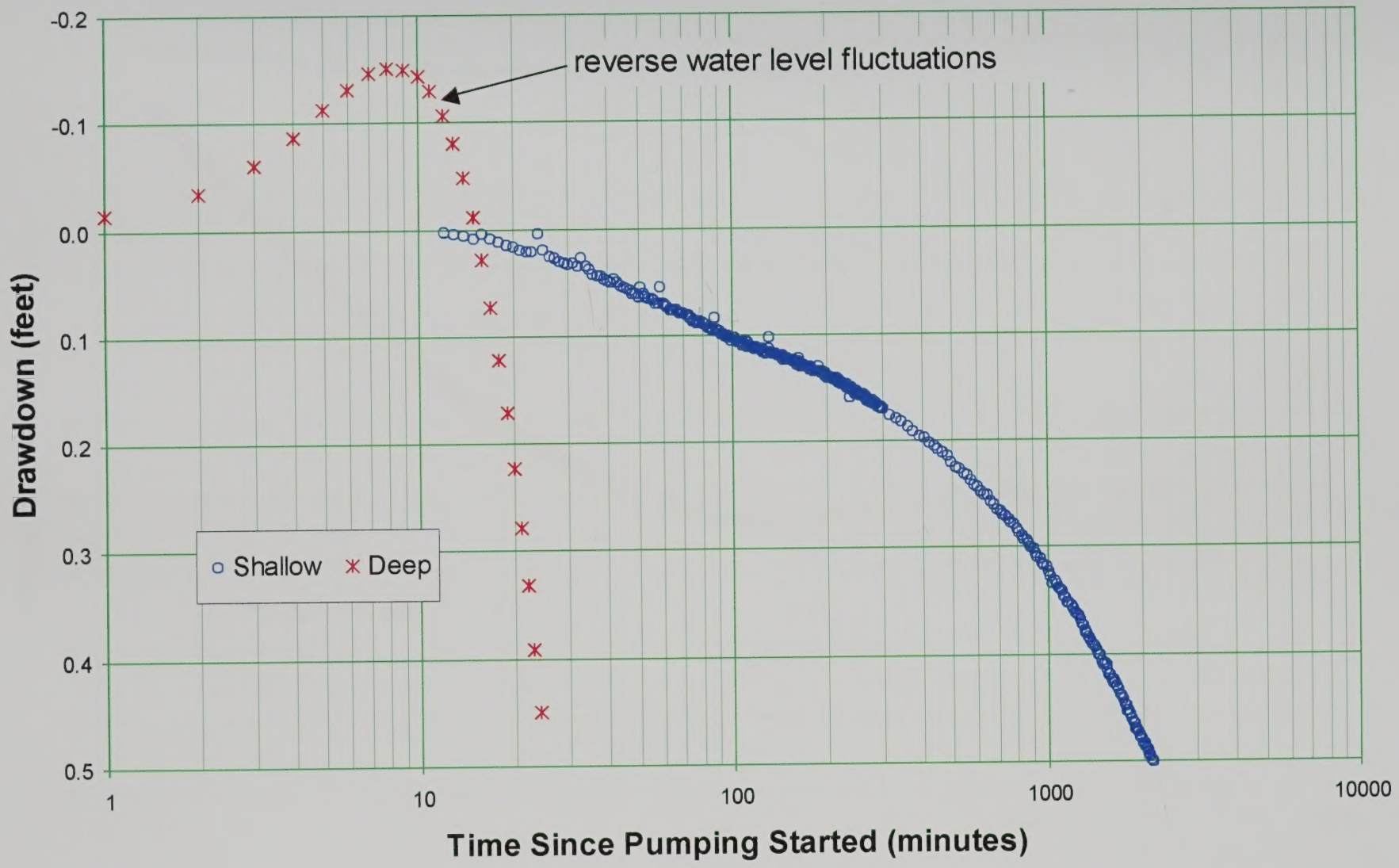

DS&A
David Schafer & Associates

DRAWDOWN FOR SOUTH-50 WELL PAIR - EXPANDED VIEW

SAN PEDRO RIVER BASIN AQUIFER TEST
SIERRA VISTA, ARIZONA

FIGURE
30

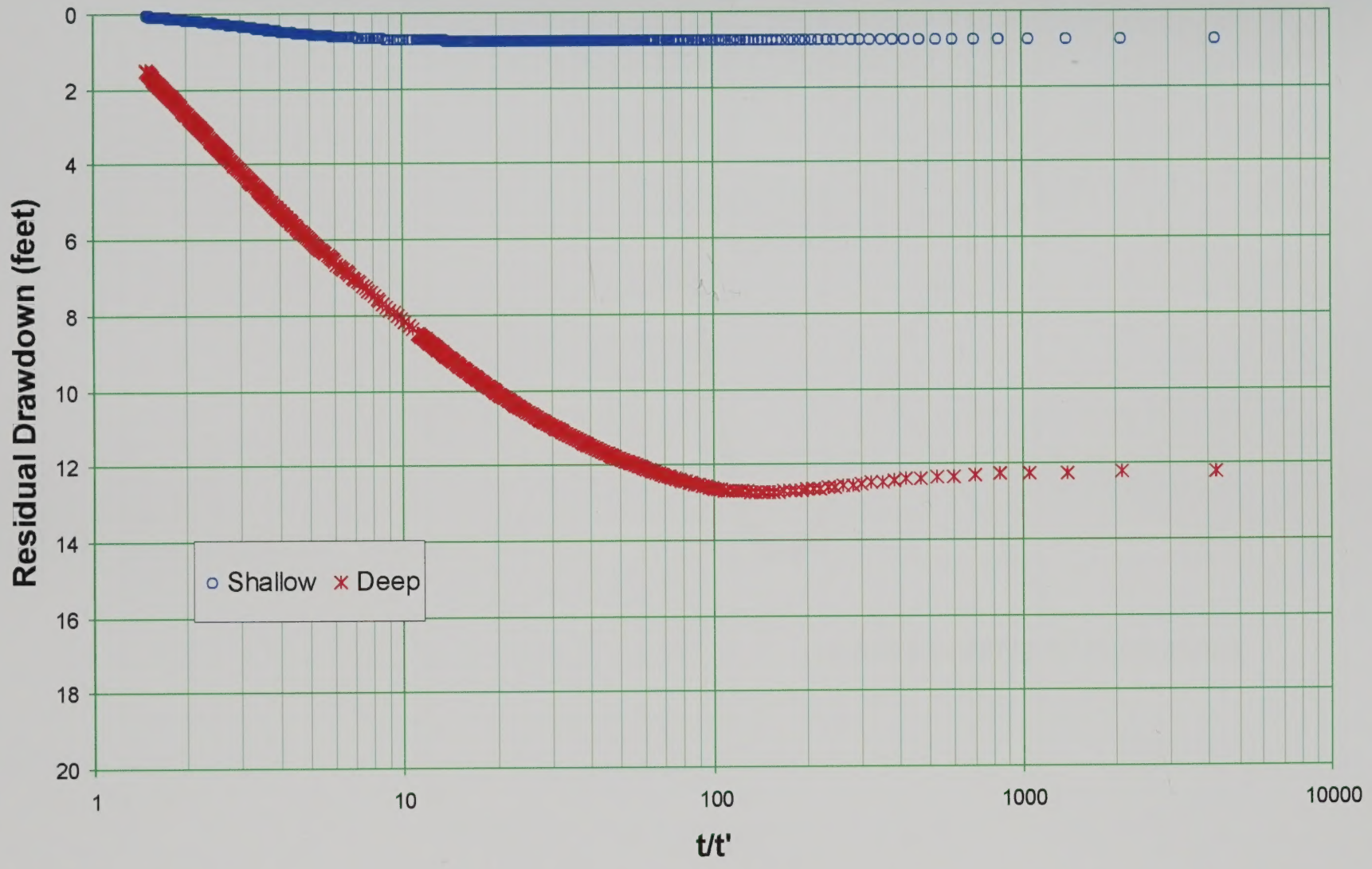

DS&A
David Schafer & Associates

RECOVERY FOR SOUTH-50 WELL PAIR

SAN PEDRO RIVER BASIN AQUIFER TEST
SIERRA VISTA, ARIZONA

FIGURE
31

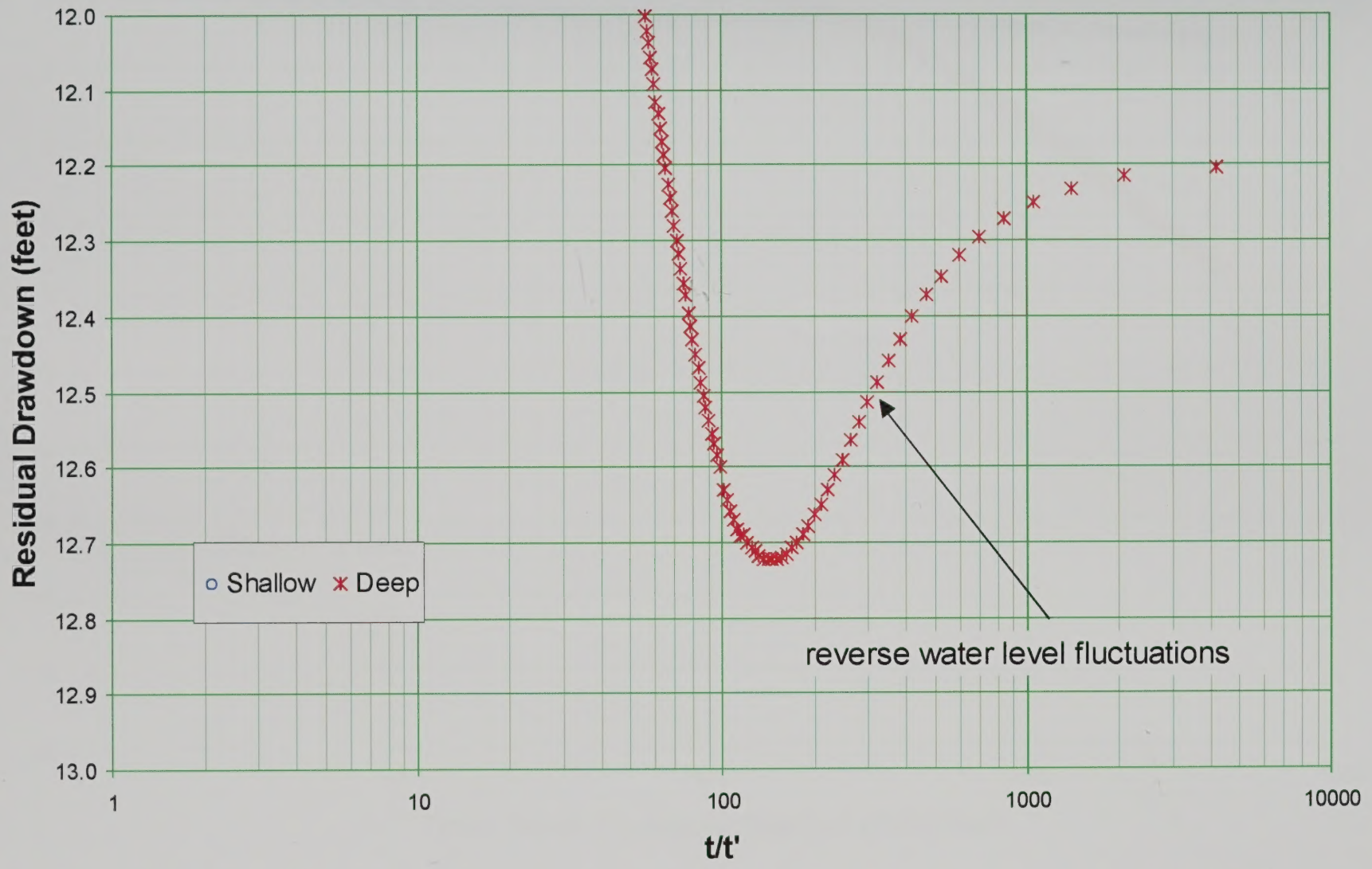

DS&A
David Schafer & Associates

RECOVERY FOR SOUTH-50 WELL PAIR - EXPANDED VIEW

SAN PEDRO RIVER BASIN AQUIFER TEST
SIERRA VISTA, ARIZONA

FIGURE
32

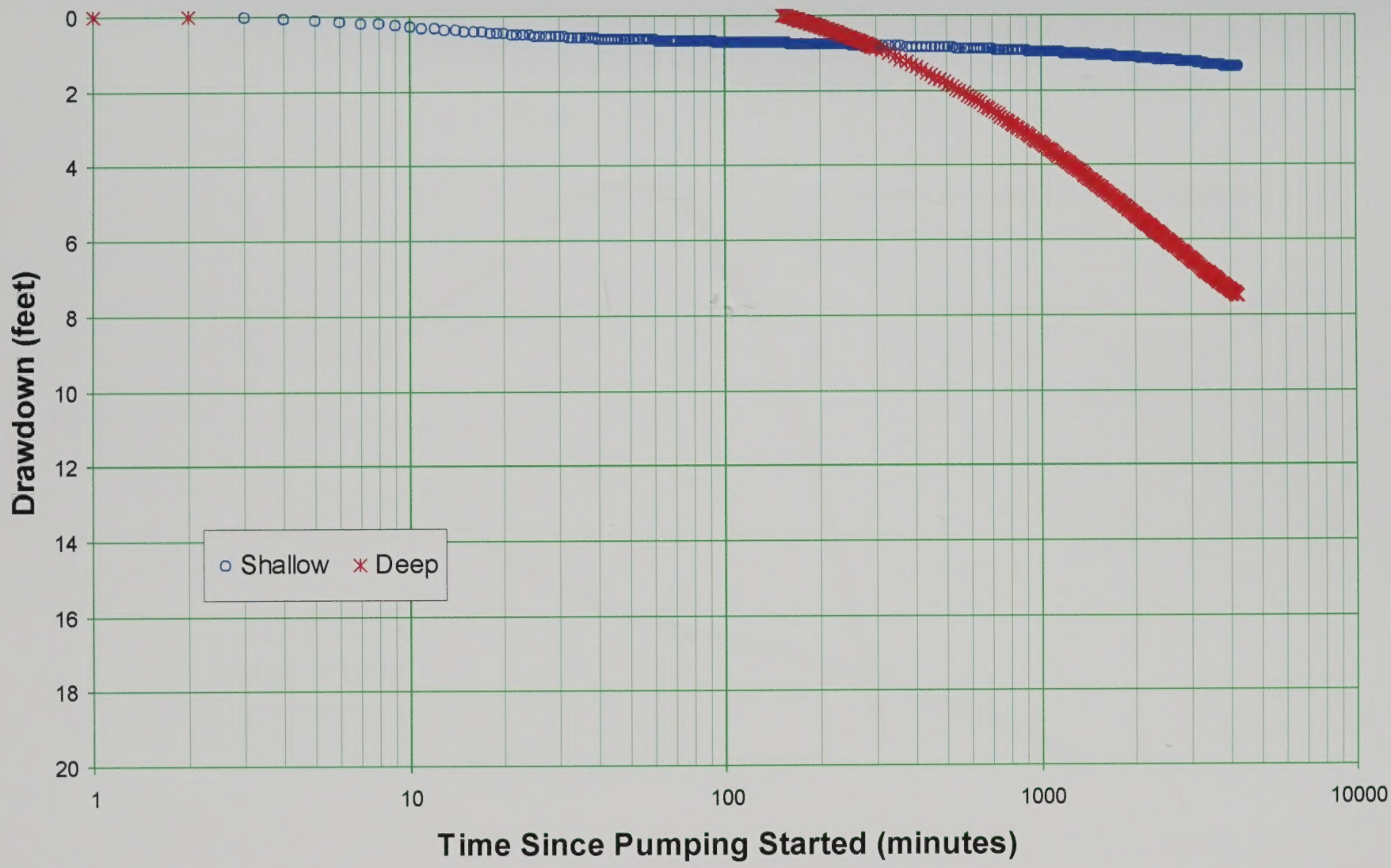

DS&A
David Schafer & Associates

DRAWDOWN FOR SOUTH-200 WELL PAIR

SAN PEDRO RIVER BASIN AQUIFER TEST
SIERRA VISTA, ARIZONA

FIGURE
33

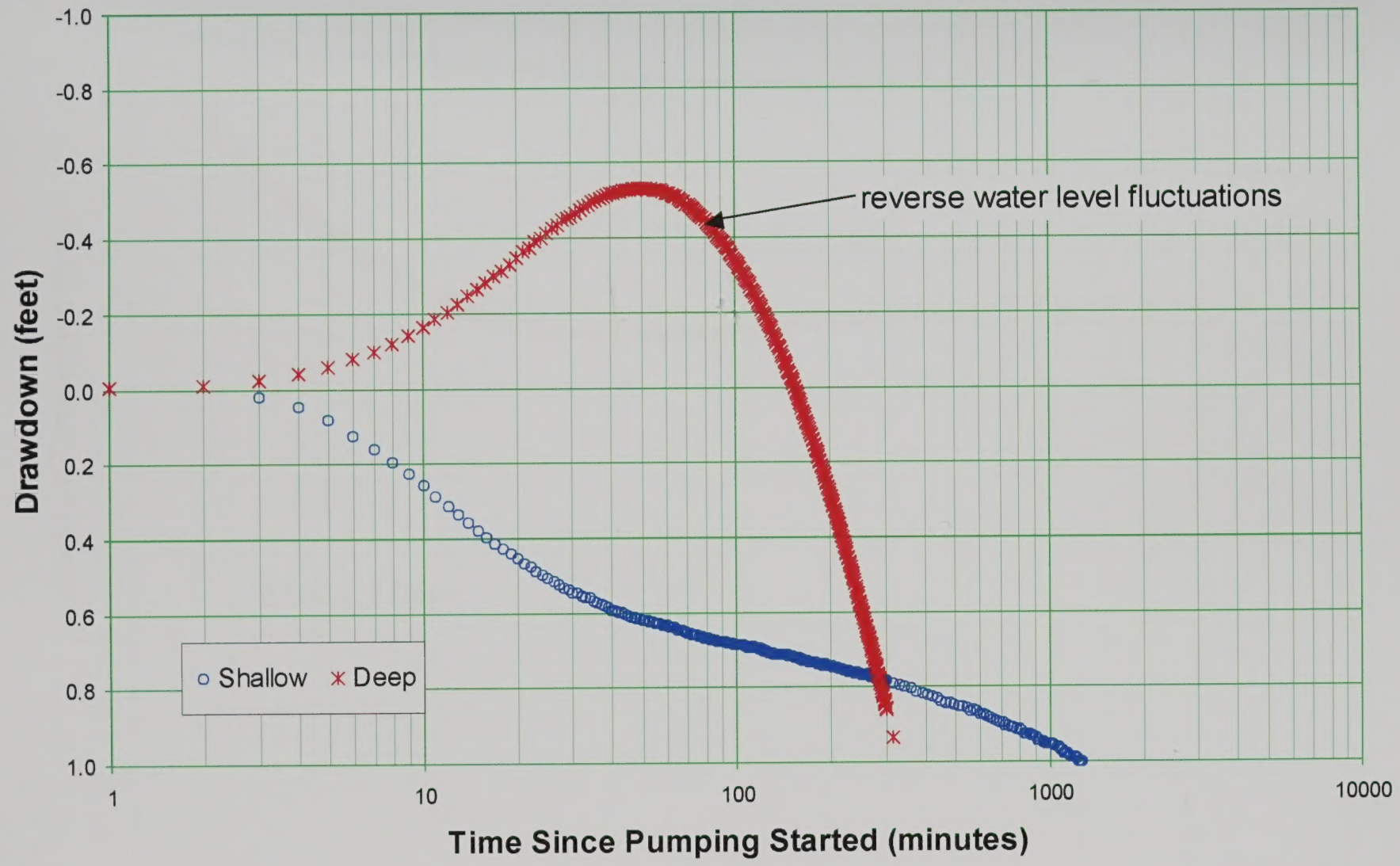

DS&A
David Schafer & Associates

DRAWDOWN FOR SOUTH-200 WELL PAIR - EXPANDED VIEW

SAN PEDRO RIVER BASIN AQUIFER TEST
SIERRA VISTA, ARIZONA

FIGURE
34

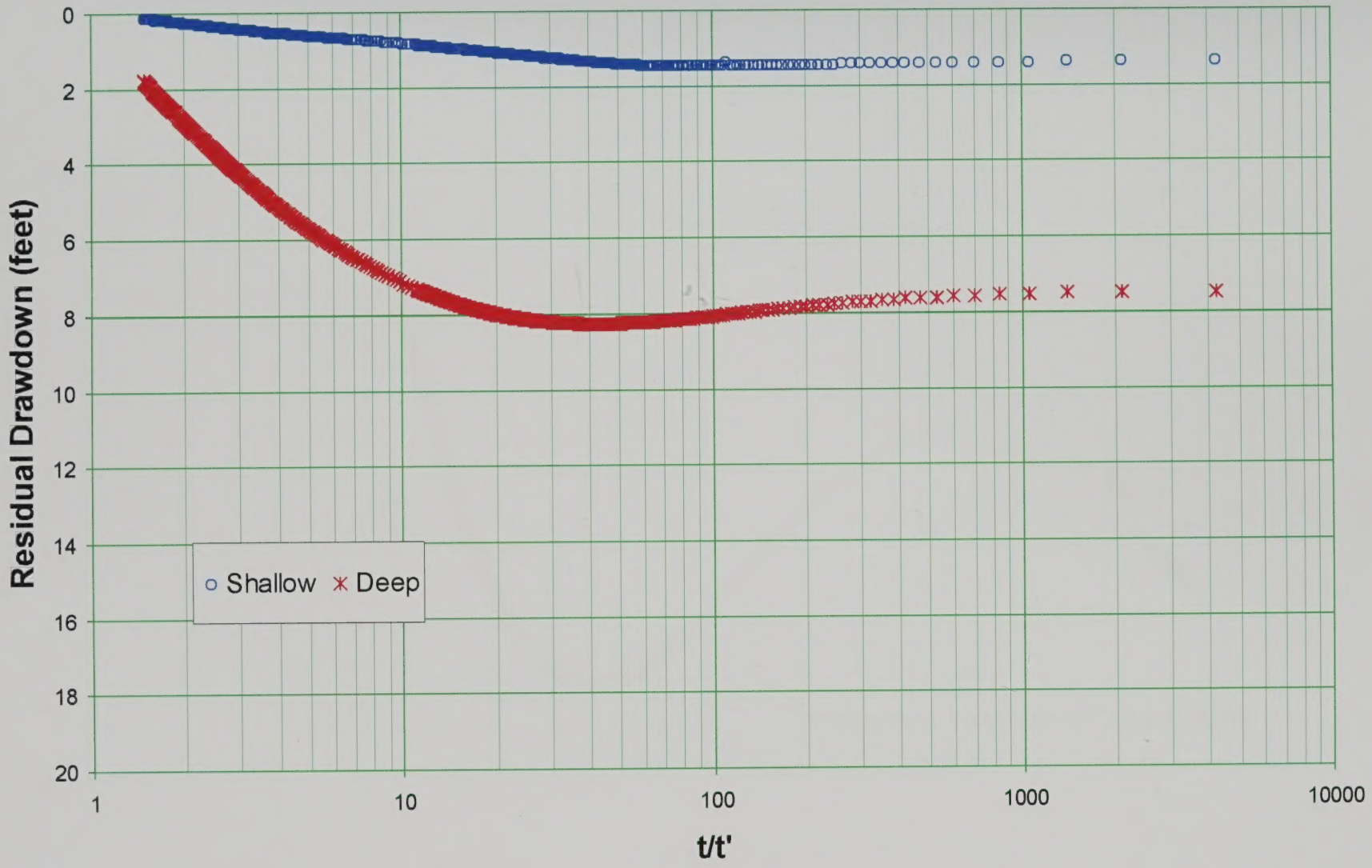

DS&A
David Schafer & Associates

RECOVERY FOR SOUTH-200 WELL PAIR

SAN PEDRO RIVER BASIN AQUIFER TEST
SIERRA VISTA, ARIZONA

FIGURE
35

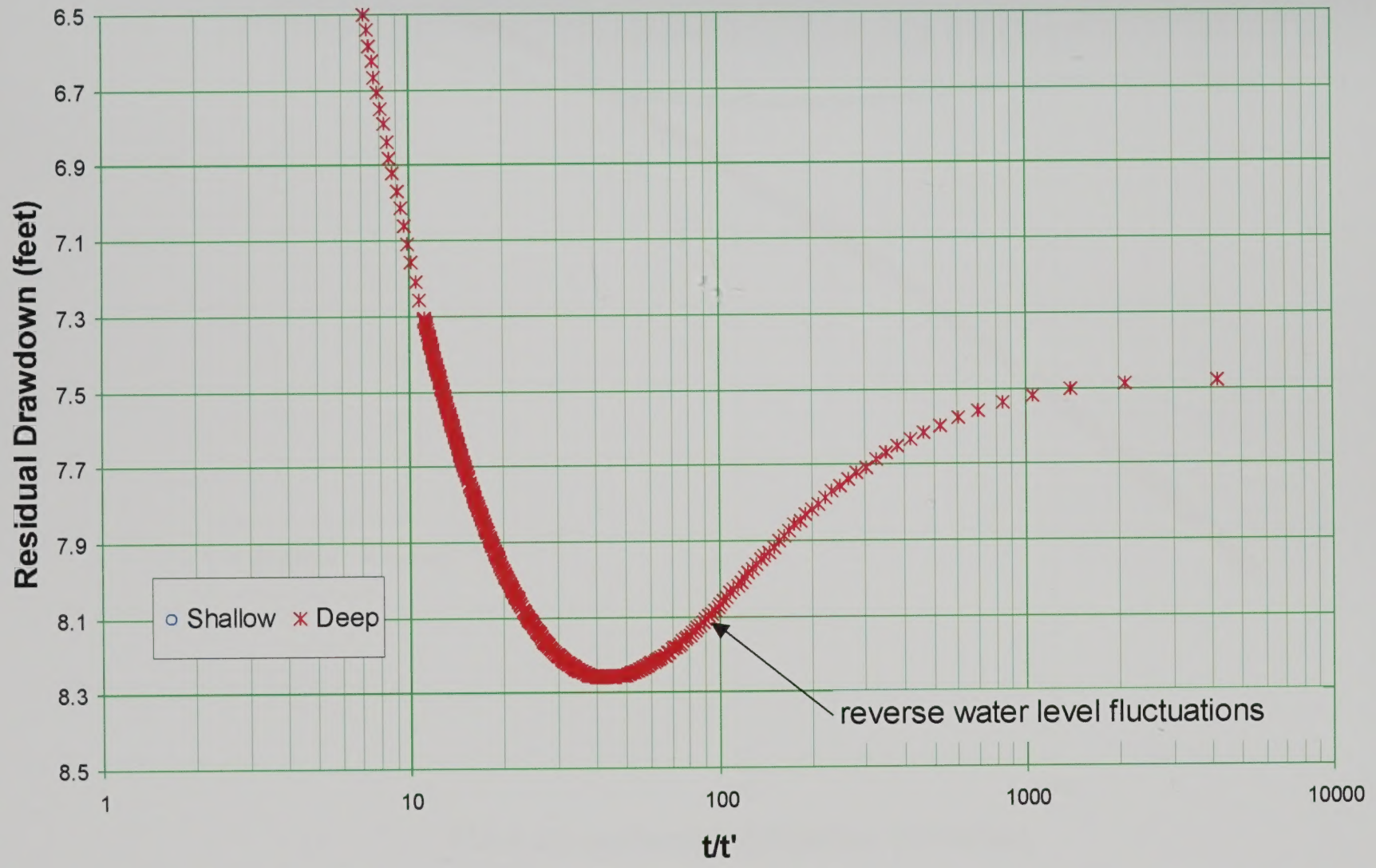

DS&A
David Schafer & Associates

RECOVERY FOR SOUTH-200 WELL PAIR - EXPANDED VIEW

SAN PEDRO RIVER BASIN AQUIFER TEST
SIERRA VISTA, ARIZONA

FIGURE
36

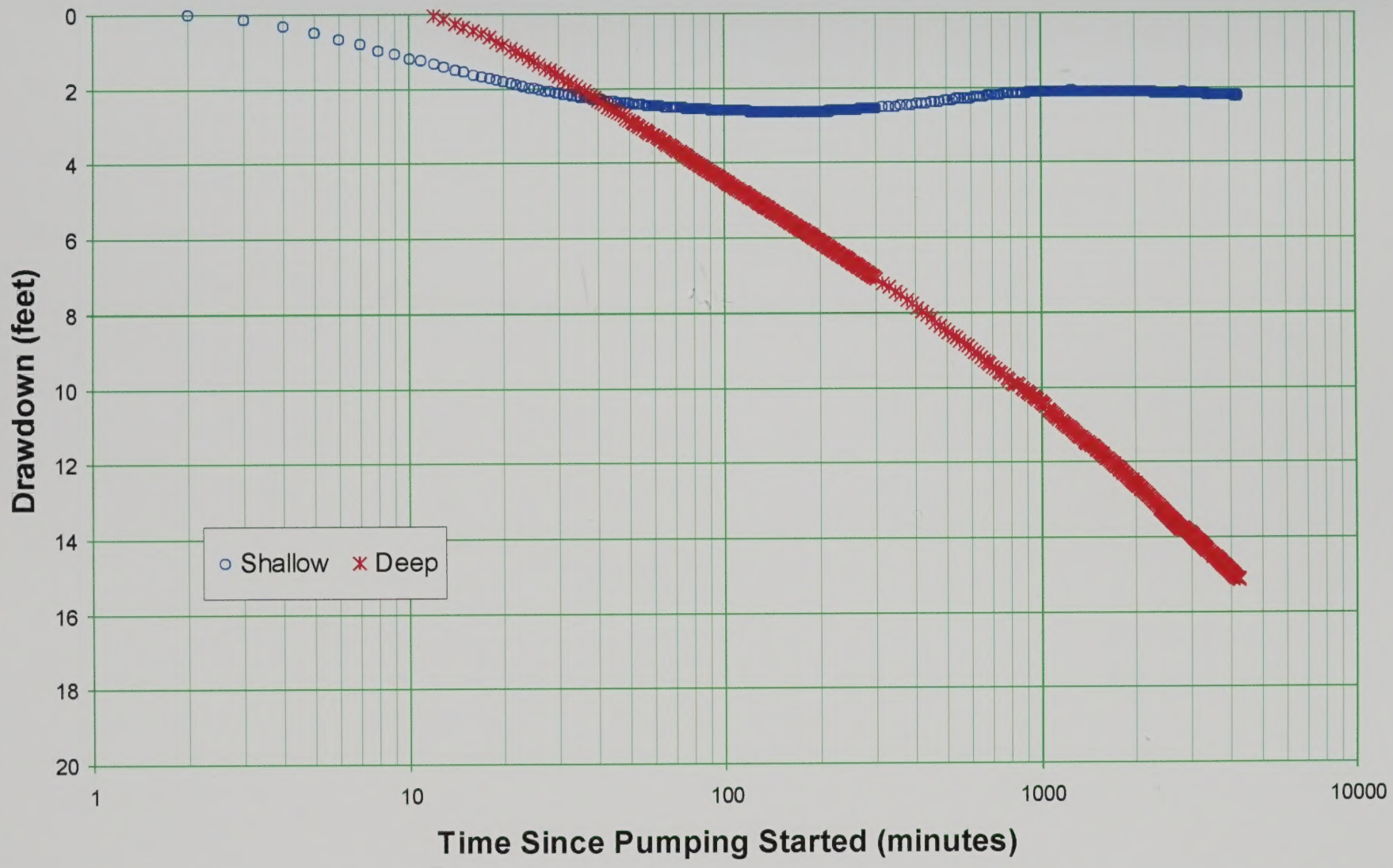

David Schafer & Associates

DRAWDOWN FOR EAST-50 WELL PAIR

SAN PEDRO RIVER BASIN AQUIFER TEST
SIERRA VISTA, ARIZONA

FIGURE
37

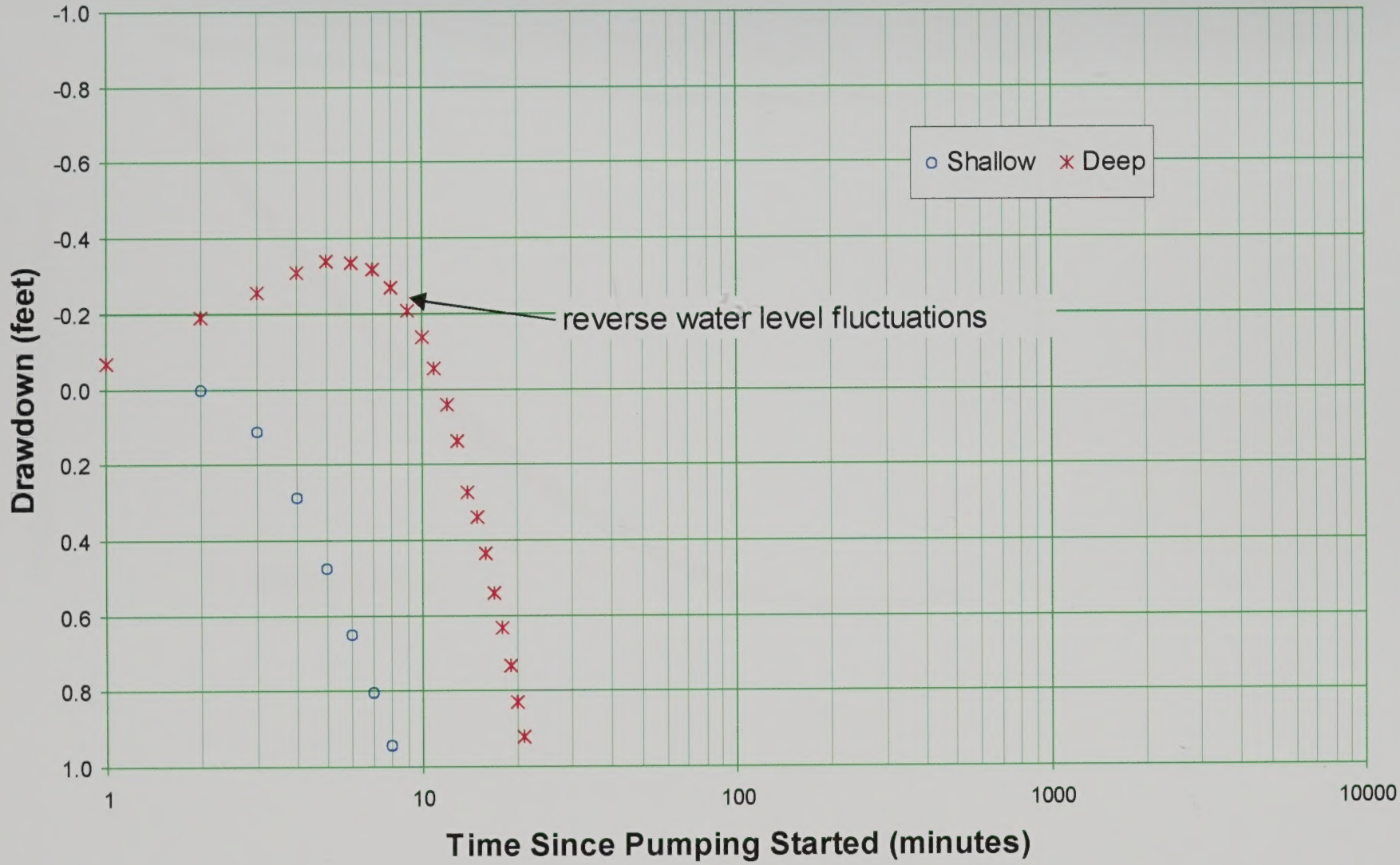

DS&A
David Schafer & Associates

DRAWDOWN FOR EAST-50 WELL PAIR - EXPANDED VIEW

SAN PEDRO RIVER BASIN AQUIFER TEST
SIERRA VISTA, ARIZONA

FIGURE
38

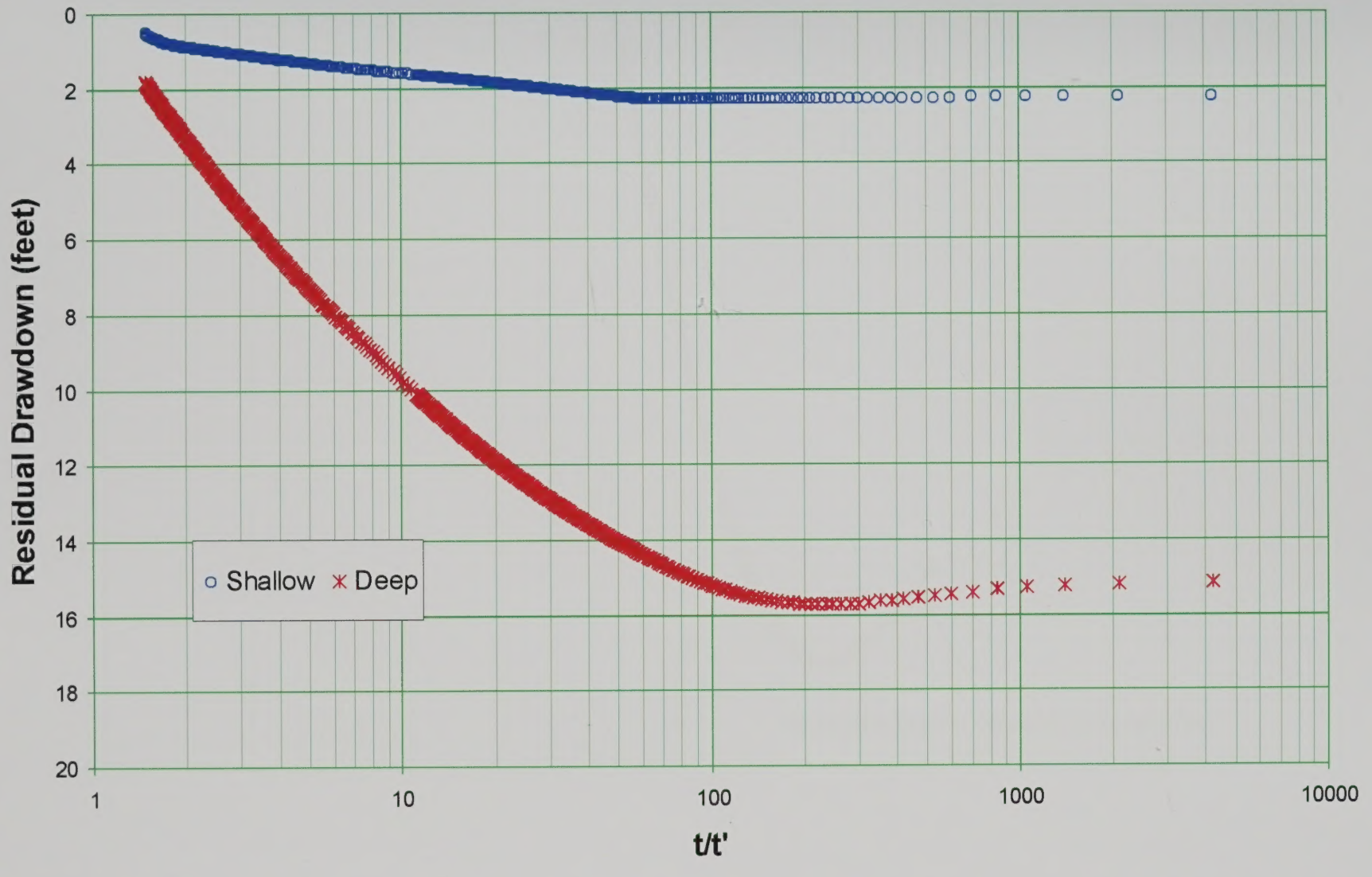

DS&A
David Schafer & Associates

RECOVERY FOR EAST-50 WELL PAIR

SAN PEDRO RIVER BASIN AQUIFER TEST
SIERRA VISTA, ARIZONA

FIGURE
39

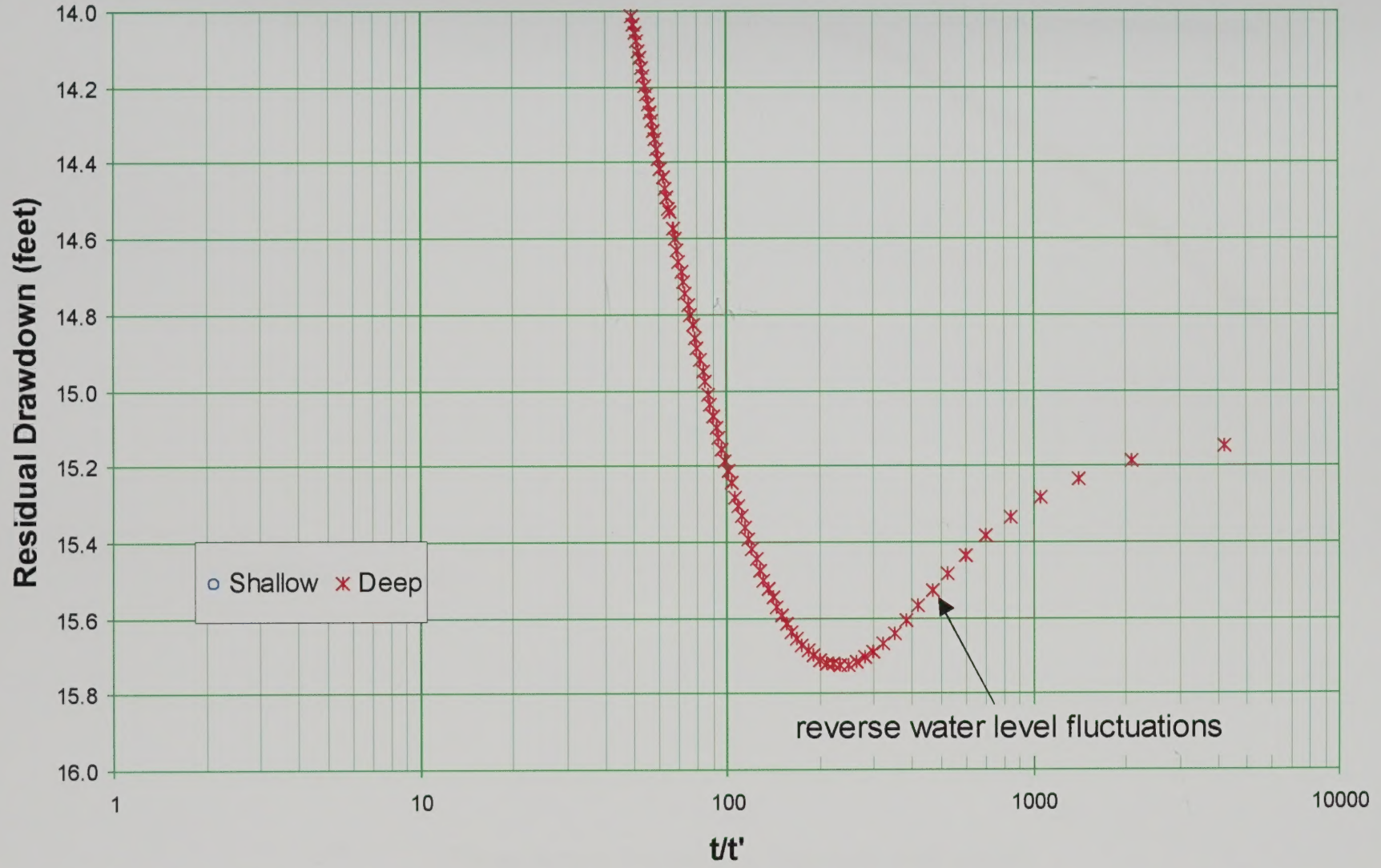

DS&A
David Schafer & Associates

RECOVERY FOR EAST-50 WELL PAIR - EXPANDED VIEW

SAN PEDRO RIVER BASIN AQUIFER TEST
SIERRA VISTA, ARIZONA

FIGURE
40

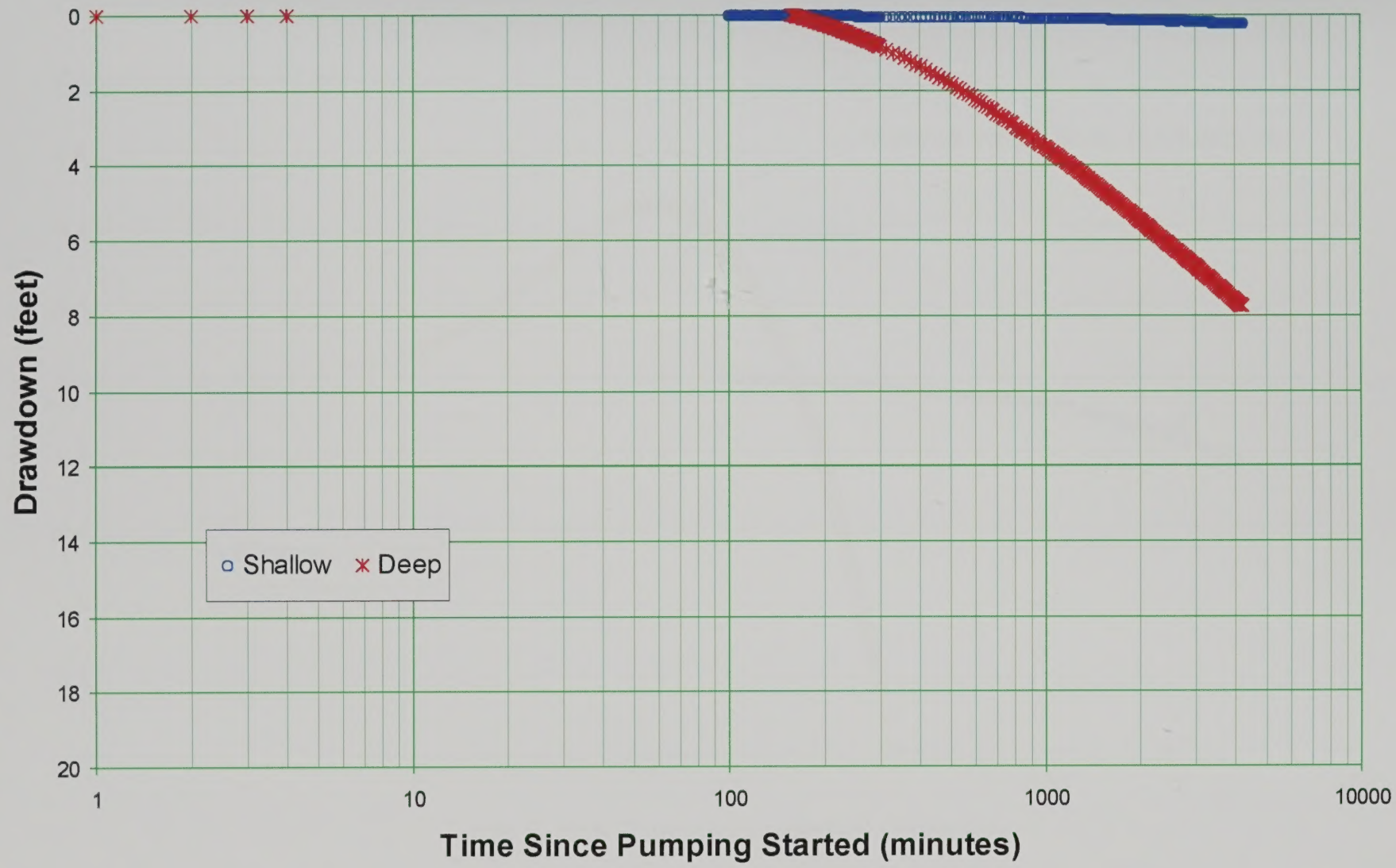

David Schafer & Associates

DRAWDOWN FOR EAST-200 WELL PAIR

SAN PEDRO RIVER BASIN AQUIFER TEST
SIERRA VISTA, ARIZONA

FIGURE
41

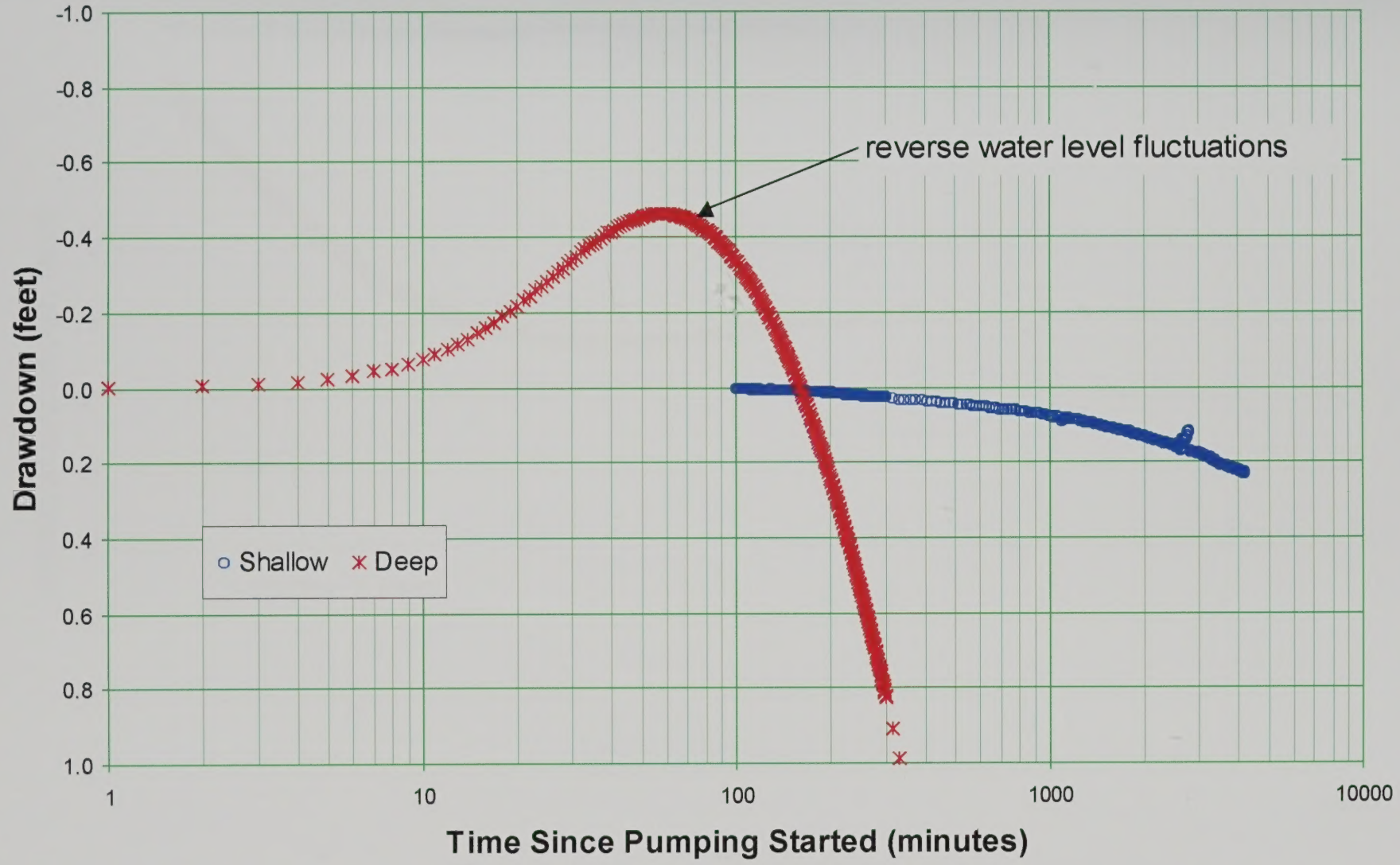

David Schafer & Associates

DRAWDOWN FOR EAST-200 WELL PAIR - EXPANDED VIEW

SAN PEDRO RIVER BASIN AQUIFER TEST
SIERRA VISTA, ARIZONA

FIGURE
42

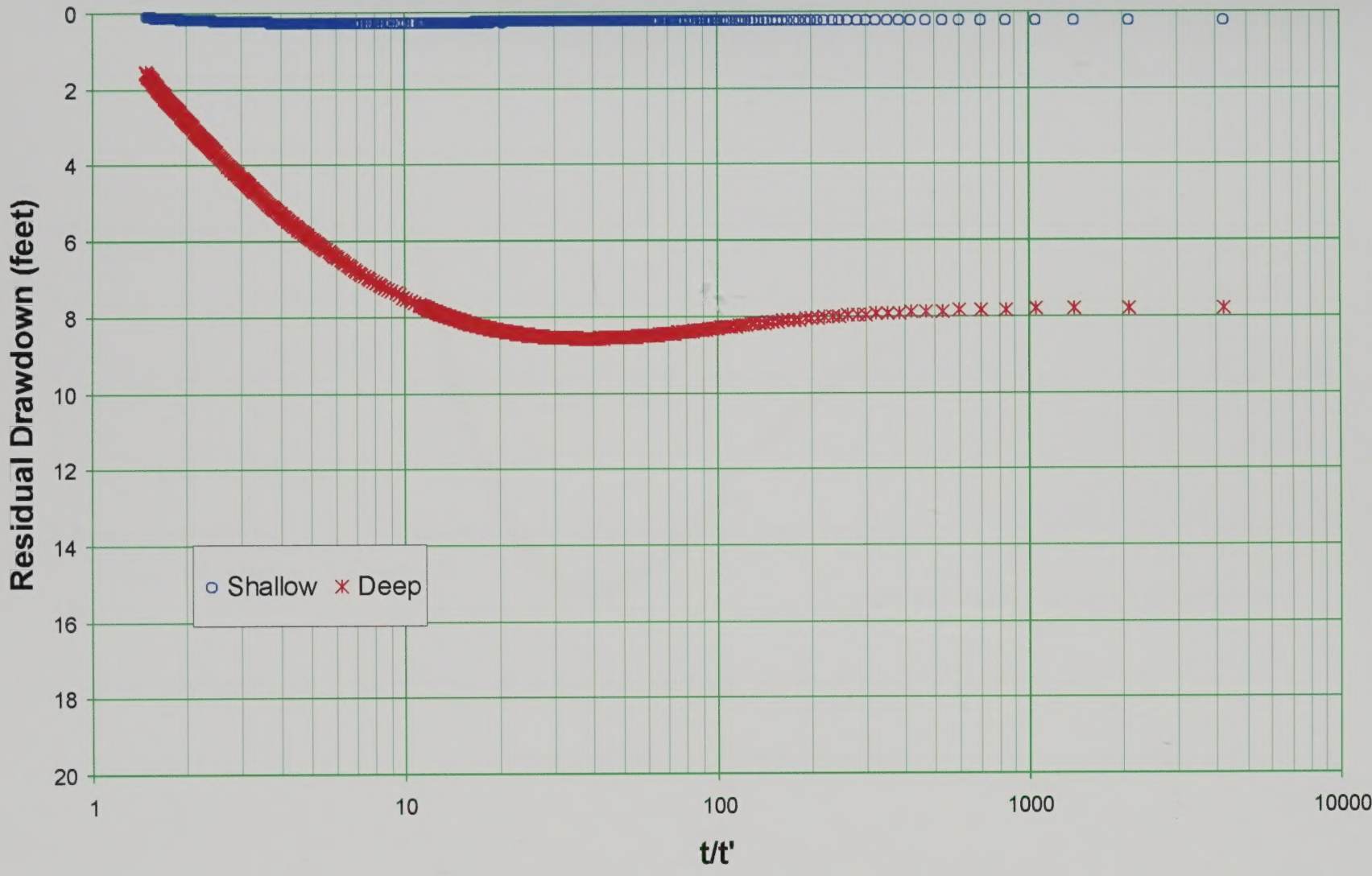

DS&A
David Schafer & Associates

RECOVERY FOR EAST-200 WELL PAIR

SAN PEDRO RIVER BASIN AQUIFER TEST
SIERRA VISTA, ARIZONA

FIGURE
43

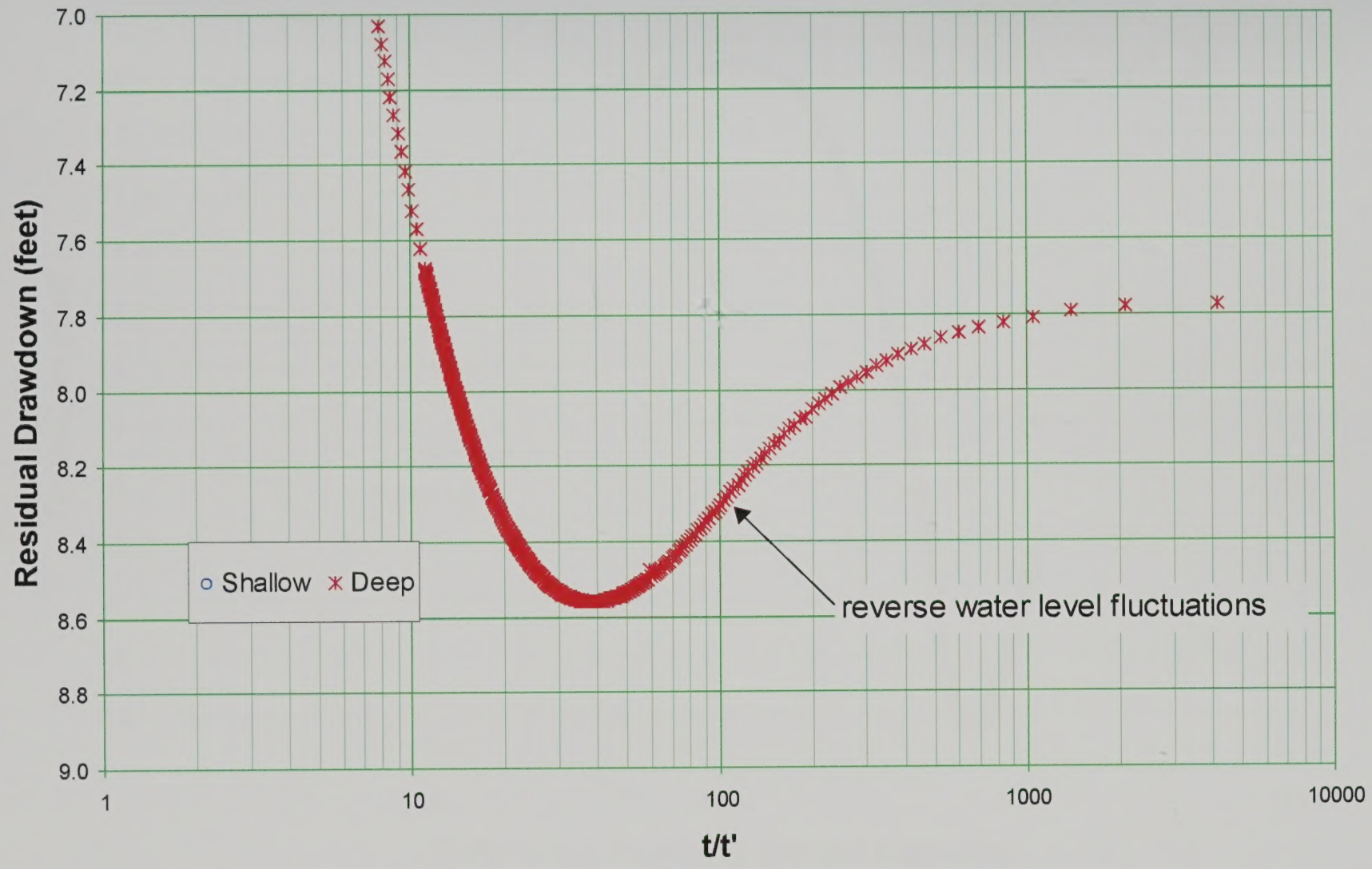

DS&A
David Schafer & Associates

RECOVERY FOR EAST-200 WELL PAIR - EXPANDED VIEW

SAN PEDRO RIVER BASIN AQUIFER TEST
SIERRA VISTA, ARIZONA

FIGURE
44

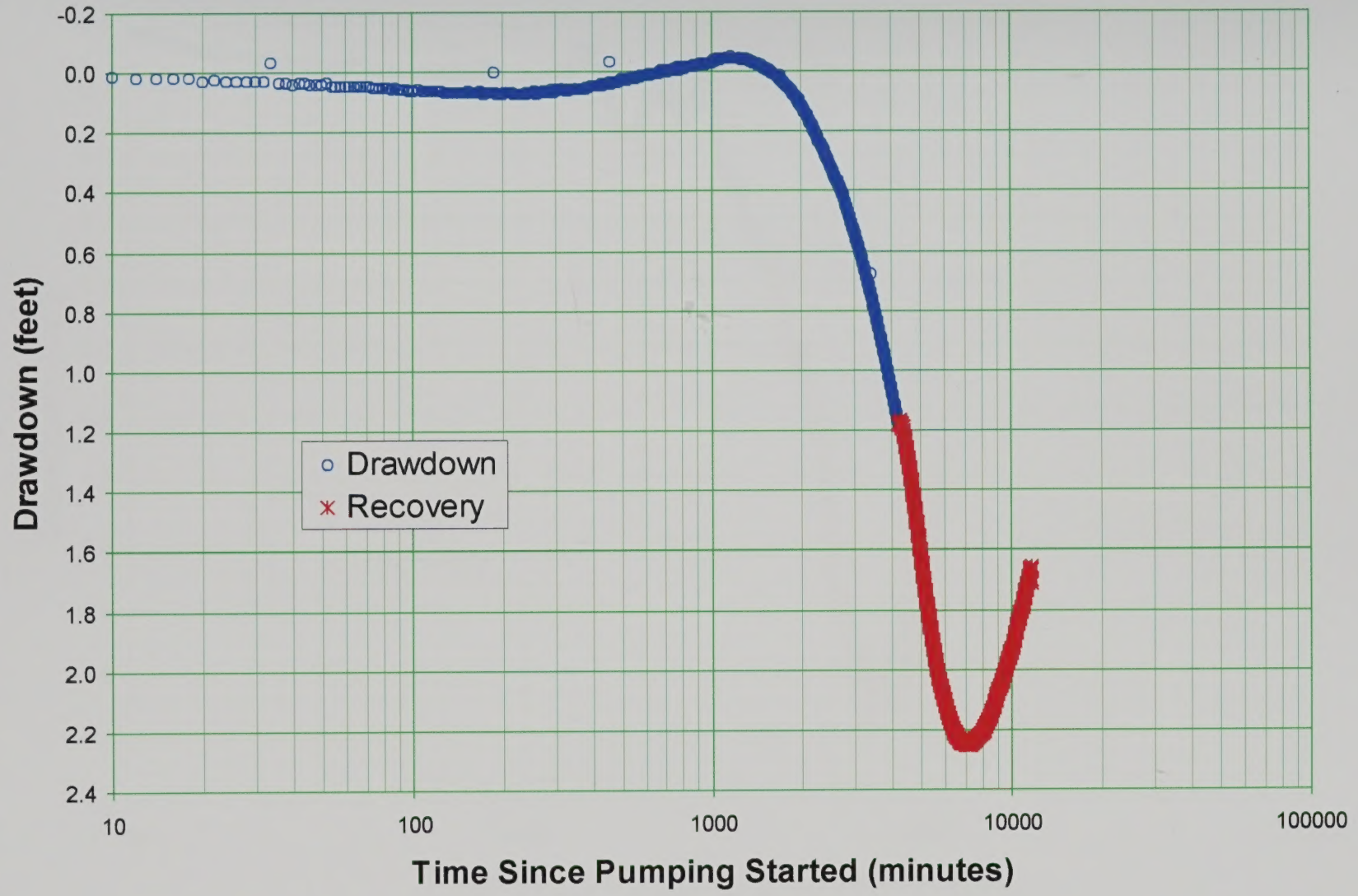

DS&A
David Schafer & Associates

DRAWDOWN AND RECOVERY FOR COT-UWD

SAN PEDRO RIVER BASIN AQUIFER TEST
SIERRA VISTA, ARIZONA

FIGURE
45

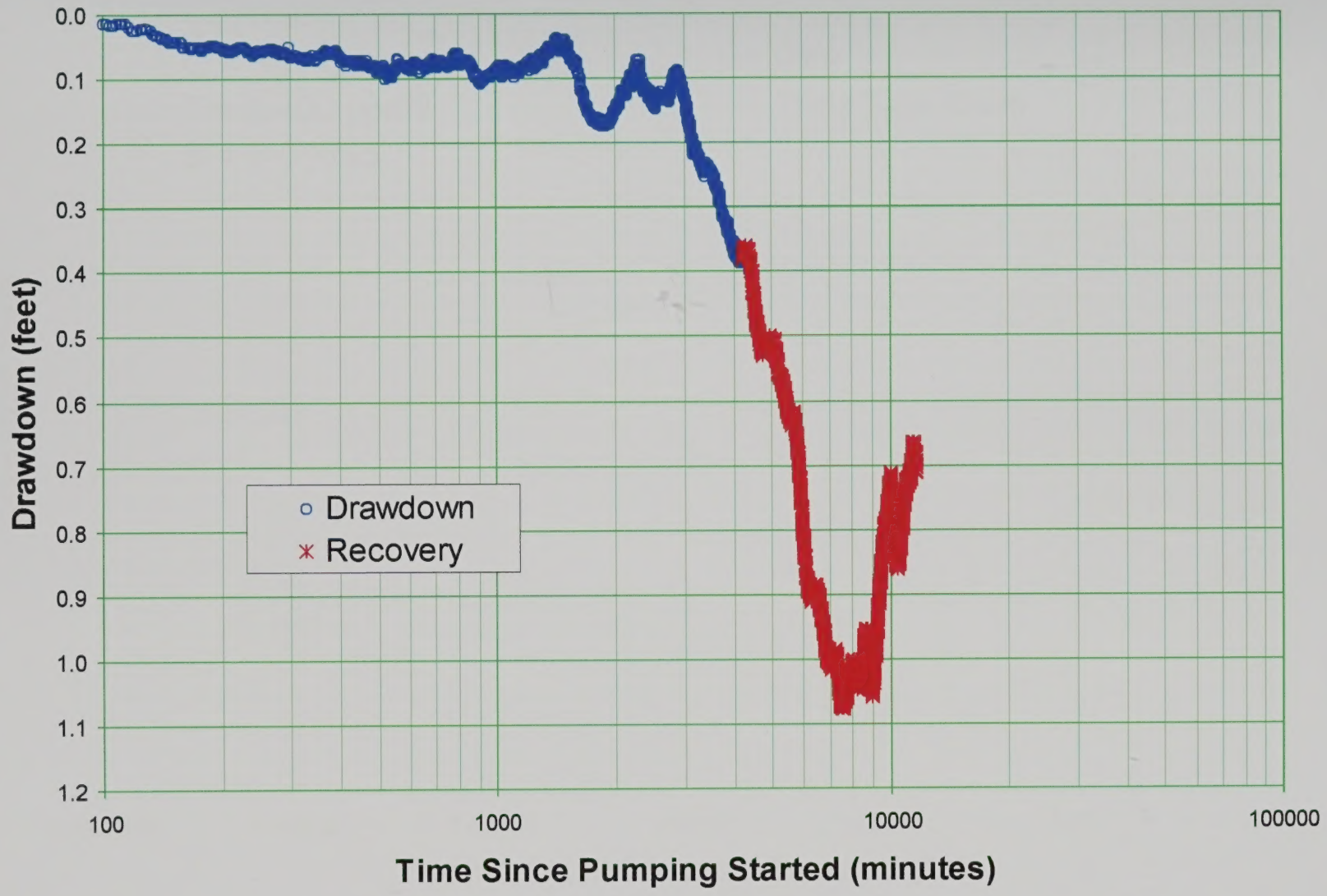

David Schafer & Associates

DRAWDOWN AND RECOVERY FOR COT-UCD

SAN PEDRO RIVER BASIN AQUIFER TEST
SIERRA VISTA, ARIZONA

FIGURE
46

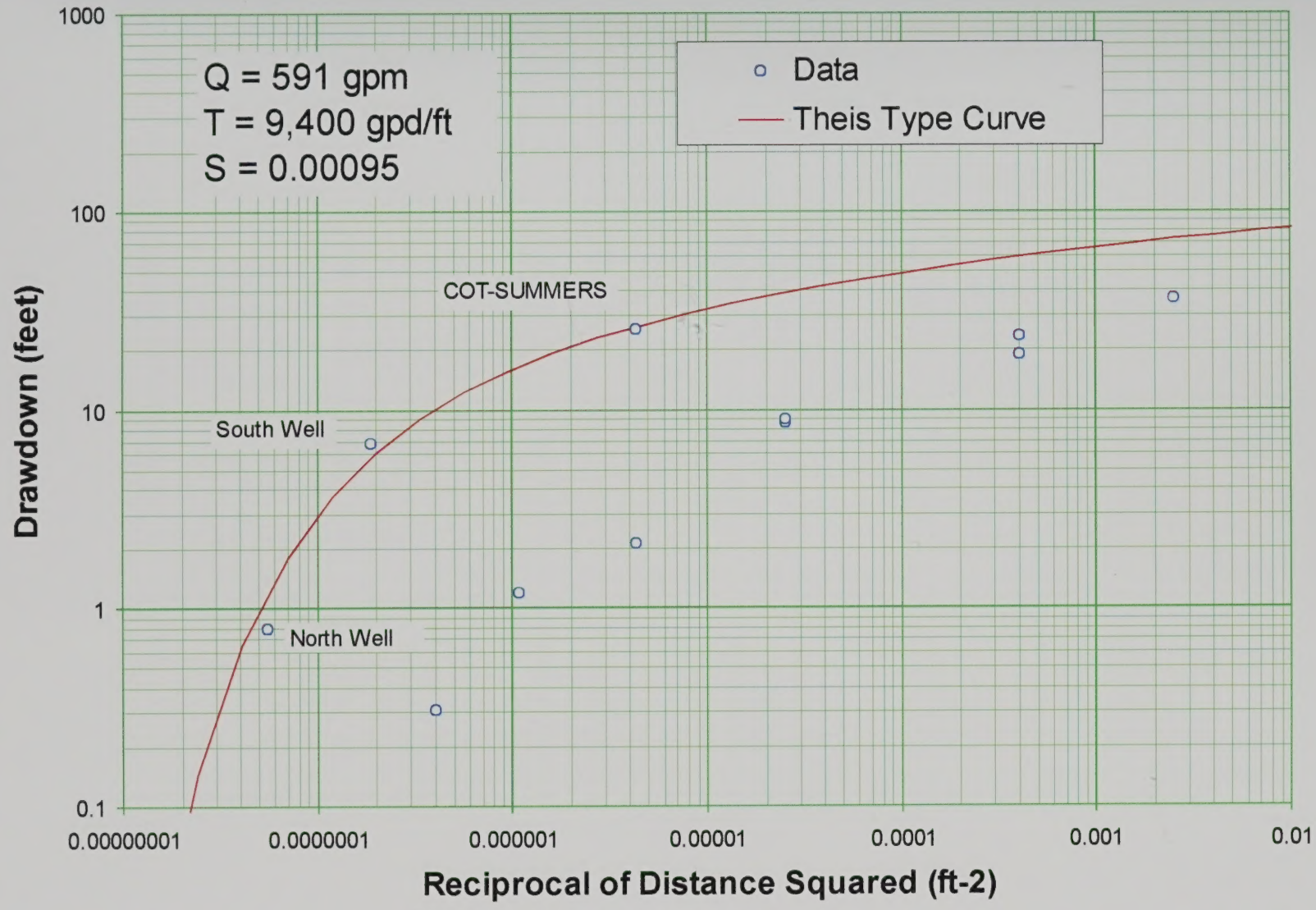

DS&A
David Schafer & Associates

DISTANCE-DRAWDOWN DATA FOR 60-FOOT ZONE CORRECTED FOR A=1

SAN PEDRO RIVER BASIN AQUIFER TEST
SIERRA VISTA, ARIZONA

FIGURE
47

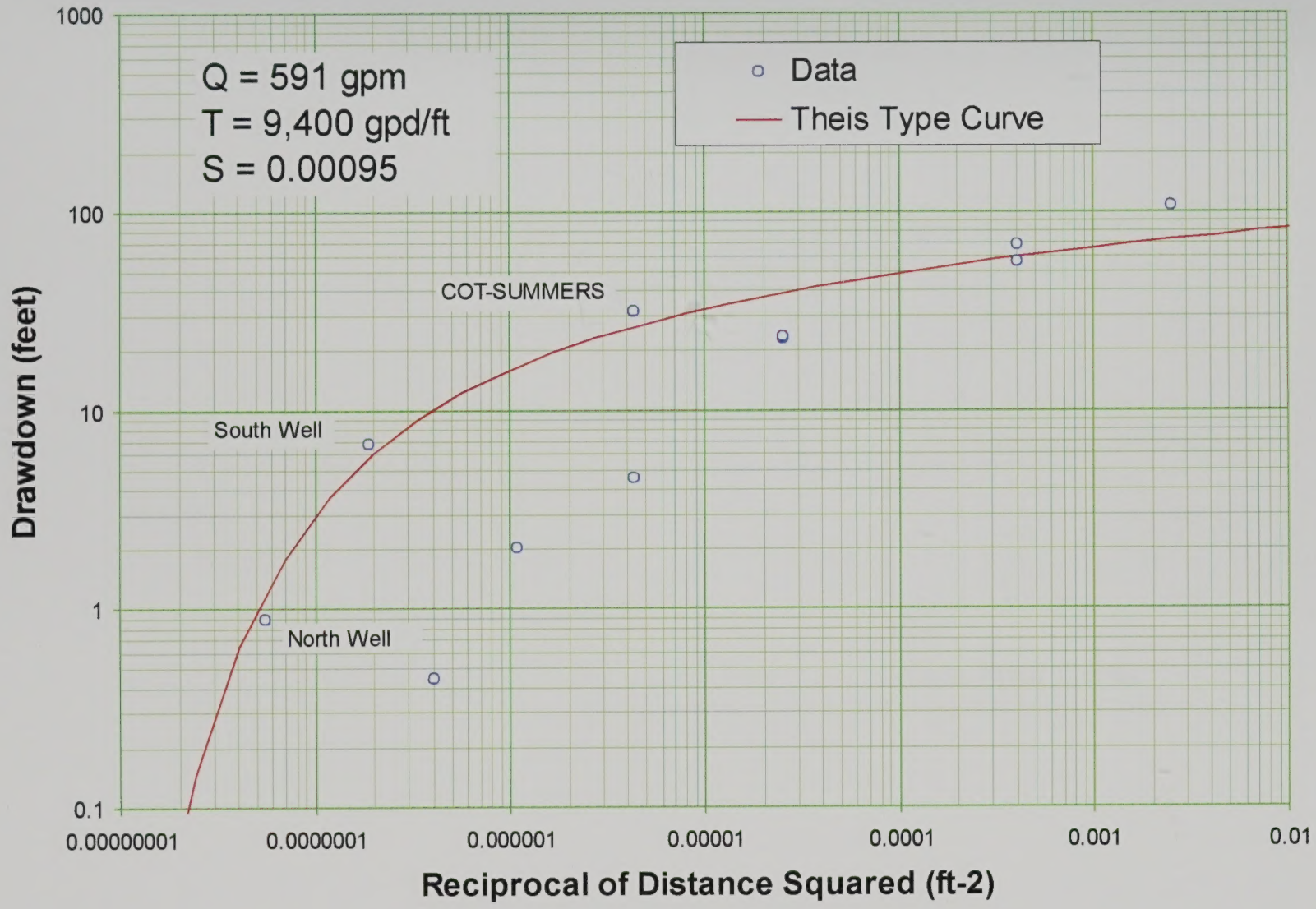

DS&A
David Schafer & Associates

DISTANCE-DRAWDOWN DATA FOR 60-FOOT ZONE CORRECTED FOR A=0.03

SAN PEDRO RIVER BASIN AQUIFER TEST
SIERRA VISTA, ARIZONA

FIGURE
48

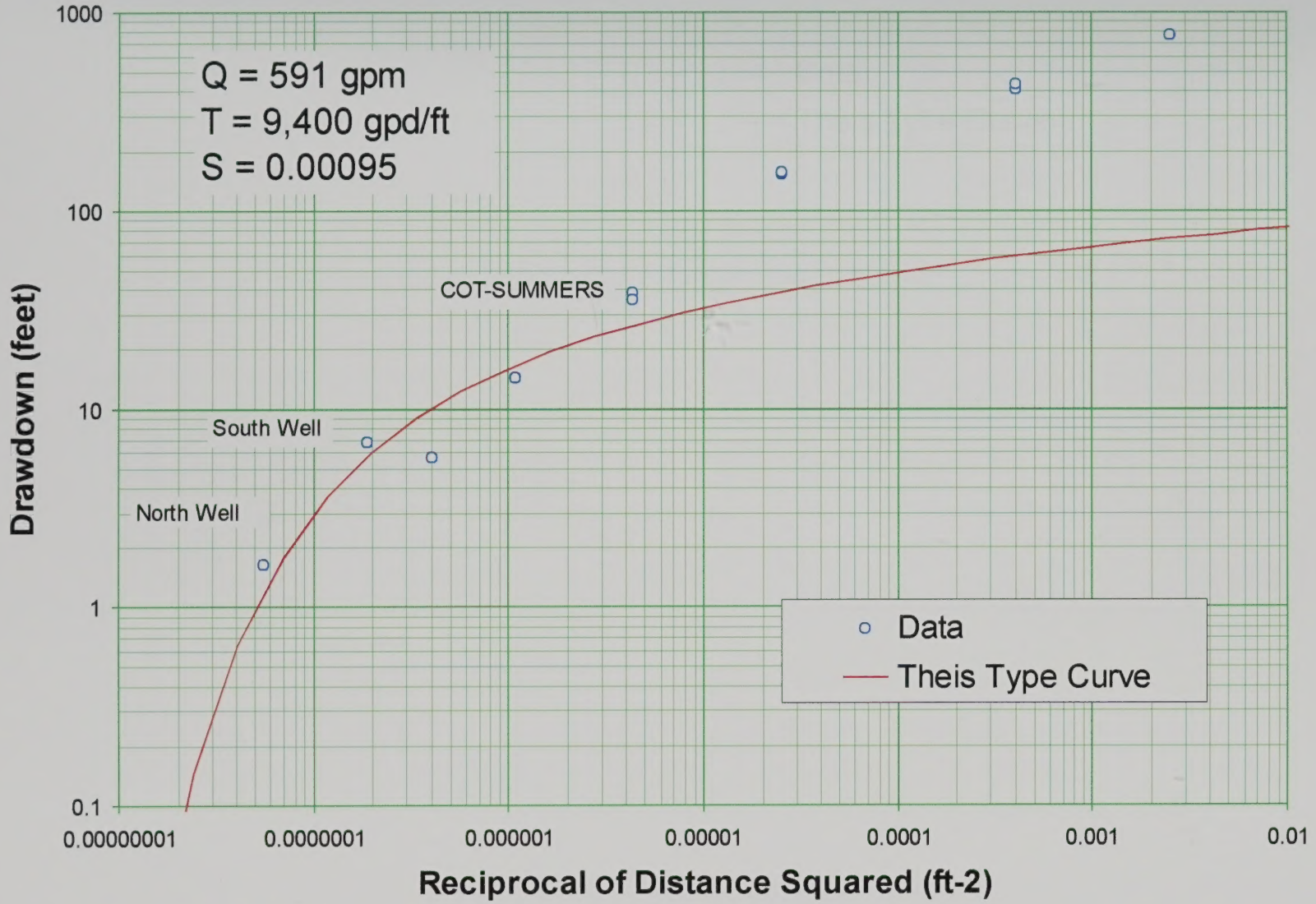

David Schafer & Associates

DISTANCE-DRAWDOWN DATA FOR 60-FOOT ZONE CORRECTED FOR A=0.0066

SAN PEDRO RIVER BASIN AQUIFER TEST
SIERRA VISTA, ARIZONA

FIGURE
49

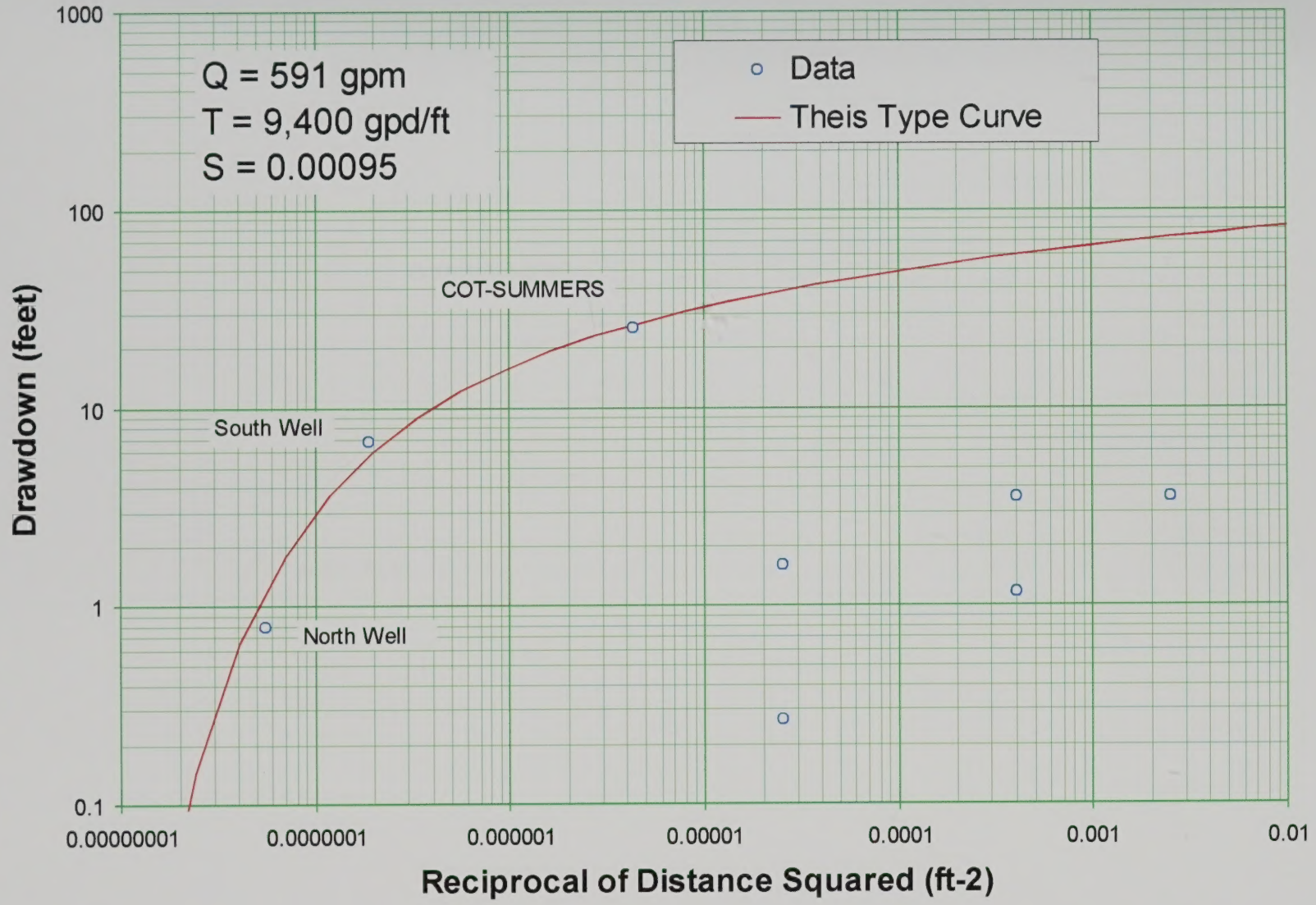

DS&A
David Schafer & Associates

DISTANCE-DRAWDOWN DATA FOR 20-FOOT ZONE CORRECTED FOR A=1

SAN PEDRO RIVER BASIN AQUIFER TEST
SIERRA VISTA, ARIZONA

FIGURE
50

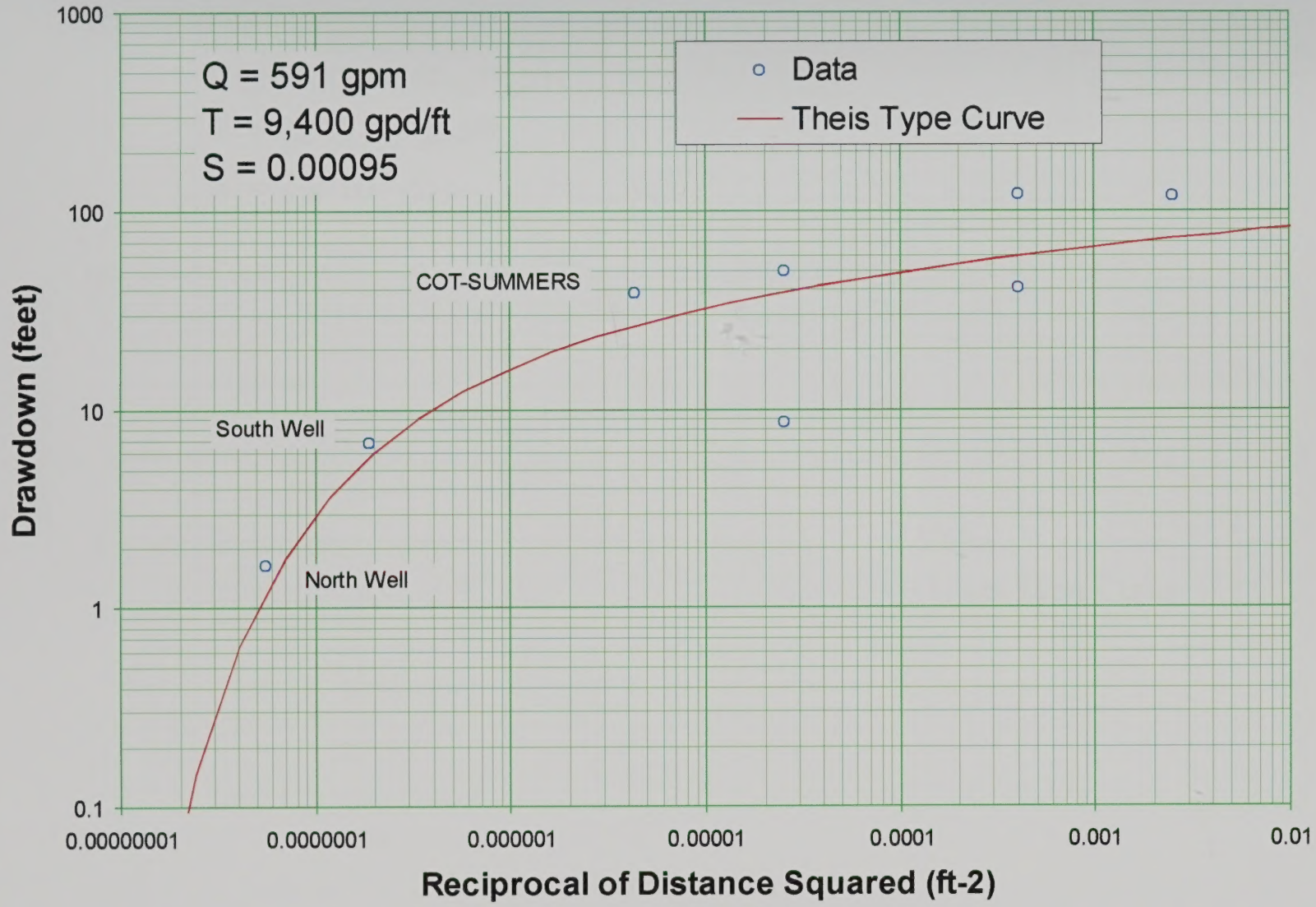

DS&A
David Schafer & Associates

DISTANCE-DRAWDOWN DATA FOR 20-FOOT ZONE CORRECTED FOR A=0.0066

SAN PEDRO RIVER BASIN AQUIFER TEST
SIERRA VISTA, ARIZONA

FIGURE
51

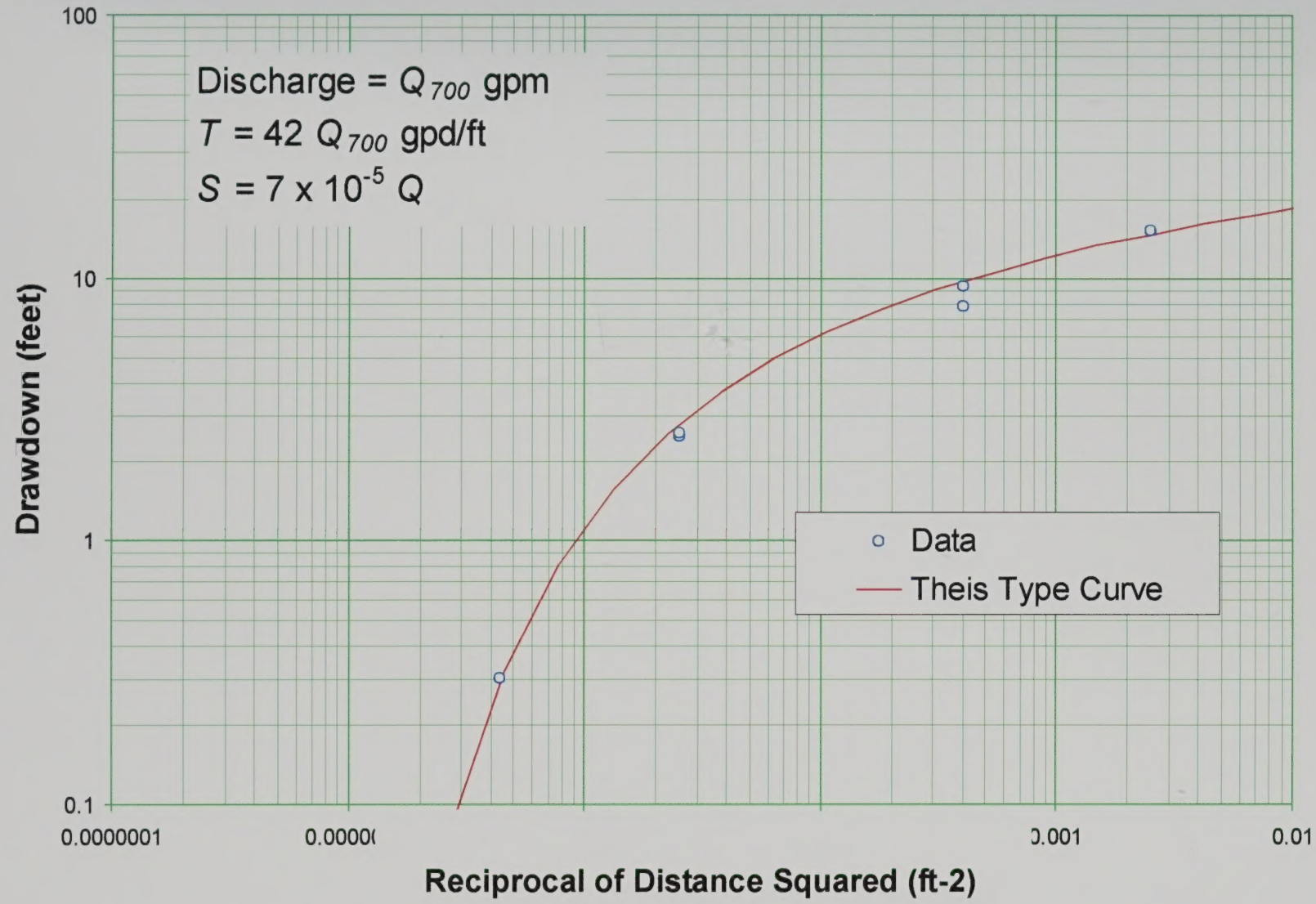

DS&A
David Schafer & Associates

UNCORRECTED DISTANCE-DRAWDOWN DATA AT 700 MINUTES FOR 60-FOOT ZONE

SAN PEDRO RIVER BASIN AQUIFER TEST
SIERRA VISTA, ARIZONA

FIGURE
52

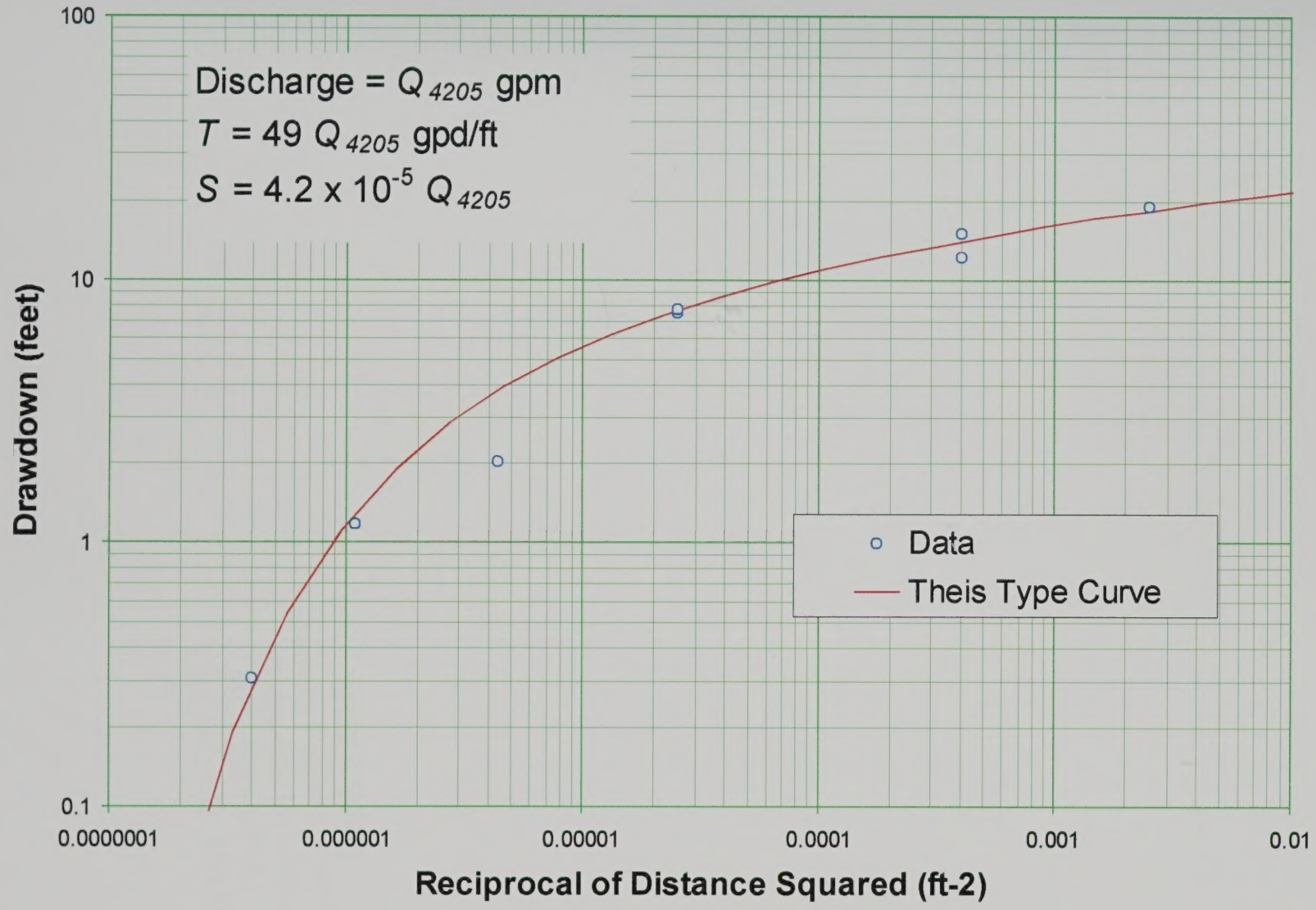

DS&A
David Schafer & Associates

UNCORRECTED DISTANCE-DRAWDOWN DATA AT 4205 MINUTES FOR 60-FOOT ZONE

SAN PEDRO RIVER BASIN AQUIFER TEST
SIERRA VISTA, ARIZONA

FIGURE
53